THE MINERALOGY OF THE HATRURIM FORMATION, ISRAEL

ABSTRACT

The Hatrurim Formation, (formerly known as the "Mottled Zone") is a unique rock complex, exposed mainly in the Judean Desert. It was apparently deposited as a normal marine, chalky-marly sequence of Campanian to Neogene age, but is today largely composed of high-temperature metamorphic minerals corresponding to the sanidinite and pyroxene-hornfels facies. No indication of contact metamorphism is, however, found in the area. One hundred fourteen minerals are described. Eight of them were previously known only as synthetic products and five others were reported from only one locality.

Optical data, X-ray diffraction data, thermal analyses, chemical analyses and crystal morphology (by SEM) of the minerals were obtained. Chemical analyses of naturally occurring tricalcium silicate (hatrurite), nagelschmidtite, portlandite and $6CaO.2Fe_2O_3.Al_2O_3$ (unnamed) are reported for the first time.

Most of the minerals were formed during one of the following stages: low to high-grade metamorphism, retrograde metamorphism, hydrothermal alteration and weathering processes.

INTRODUCTION

A. The Hatrurim Formation: description and occurrence

The present mineralogical investigation of the Hatrurim Formation (Gvirtzman and Buchbinder, 1966), formerly described as the Mottled Zone Complex (Picard 1931; Bentor 1960), is a part of a larger research program carried out by the author since 1963 as a project at the Geological Survey of Israel. The study is based on an examination of about 1,000 samples, collected from the various outcrops of the Hatrurim Formation.

In many parts of Israel a sequence of slightly phosphatic chalks and marls of the Ghareb Formation (Upper Campanian to Maastrichtian age), and clays and marls of the Taqiye Formation (Dano-Paleocene Age), are found overlying flint and phosphorite beds of the Mishash Formation (Campanian age). In many outcrops and in subsurface sections, these rocks are bituminous. The lower part of the Ghareb Formation may contain up to 26% organic matter and can be classified as oil shales (Shahar and Würzburger, 1967).

In a number of areas an entirely different, thermally metamorphosed facies, the so-called Hatrurim Formation ("Mottled Zone") appears instead of the normal sequence. These rocks in the Jerusalem-Jericho area attracted the attention of numerous geologists as early as the middle of the nineteenth century (see for review: Avnimelech, 1965). The name "Mottled Zone" was proposed by Picard (1931), who

Geol. Surv. Israel, Bull.	No. 70	pp.1–80; 18 figs.; 25 pls.	Jerusalem, February 1977

described its outcrops at Ma'ale Adumim and at Nebi Musa. The term "mottled" refers to the vivid, variegated colours of the rocks in all shades of brown, green, yellow, pink, red, violet, grey, and black.

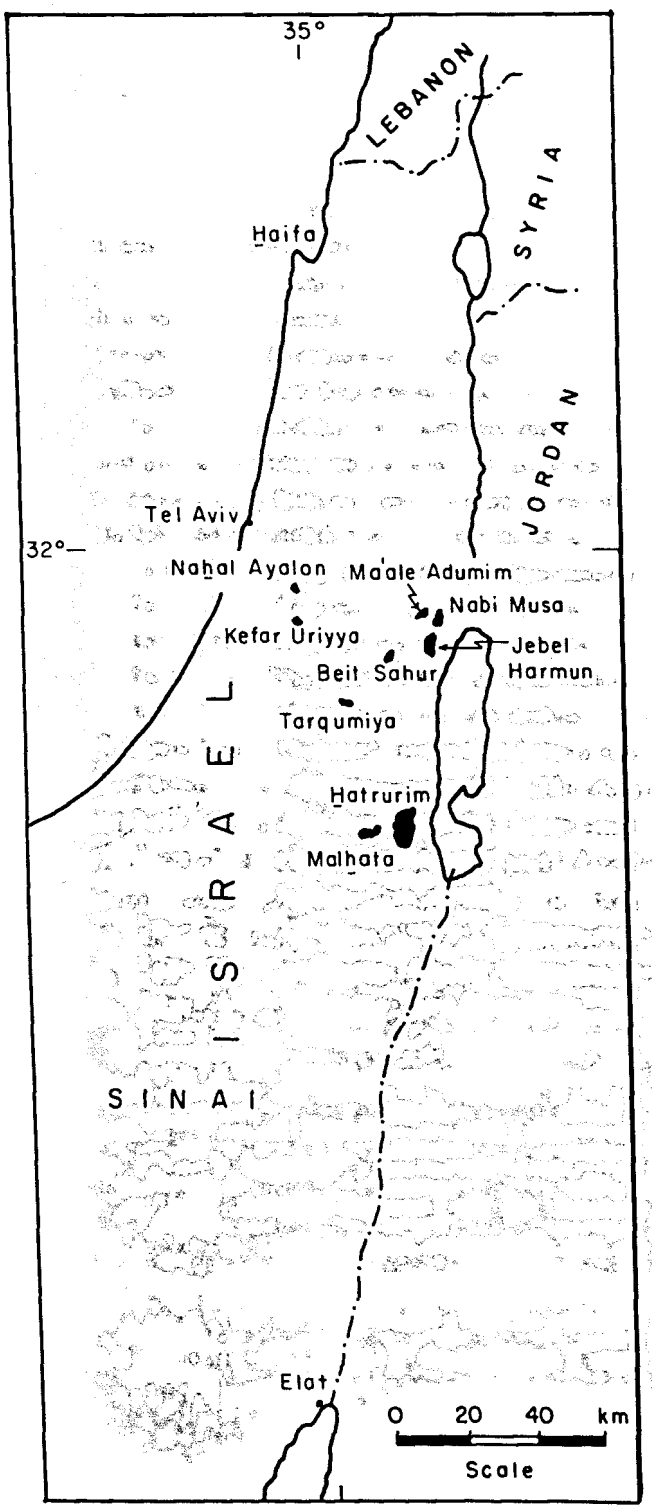

Figure 1. Outcrops of the Hatrurim Formation.

The known outcrops of the Hatrurim Formation are shown in Fig. 1. At least nine, widely separate outcrops are known: the Hatrurim syncline west of the Dead Sea, Ma'aleh Adumim, Beit Sahur, Nebi Musa, and Jebel Harmun in the Judean Desert, Nahal Ayalon in the Coastal Plain, Kefar Uriyya and Tarqumiye in the Shefela region (western foothills), and Nahal Malhata in the Be'er Sheva' Valley, in the northern Negev.

In its fully developed occurrence in the Hatrurim syncline the complex has a preserved thickness of more than 220 m and covers an area of 50 km.^{2} These outcrops have been described by Bentor and Vroman (1960). The complex includes the rock-time equivalents of the Ghareb, Taqiye and possibly Zor'a formations and relicts of the Hazeva Formation (Fig. 2). Maastrichtian, Danian and Landenian ages were confirmed on the basis of microfaunal relicts determined by Z. Reiss. Rare microfossils have been preserved also in outcrops of Nahal Ayalon (Gross *et al.*, 1967). Their study by Z. Reiss confirmed the Campanian age of the rocks. All other outcrops seem to be time equivalents of the Ghareb Formation, as determined by their stratigraphic position.

The Hatrurim Formation, which has been found only in synclinal areas, has a very complex mineralogy and is composed largely of uncommon high-temperature minerals. Elsewhere, these minerals are characteristic of contact-metamorphic rocks of the sanidinite and pyroxene hornfels facies. In all other known localities, these assemblages were found in narrow aureoles immediately adjacent to basaltic necks or other near-surface intrusions, or in limestone xenoliths within basalts. They were formed at very high temperatures (600–1000°C) and very low pressure. These localities include: Velardena and Coahuila, Mexico (Wright, 1908 ; Temple and Heinrich, 1964); Crestmore, Cali-

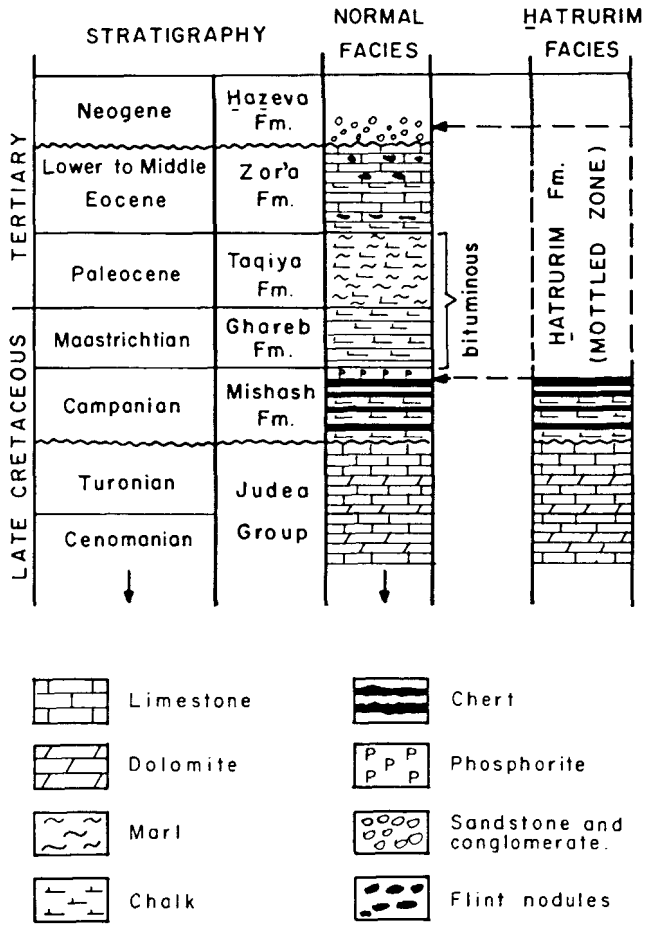

Figure 2. Schematic stratigraphic position of the Hatrurim Formation.

fornia (Eakle, 1917; Murdoch, 1955, 1961; Burnham, 1959); Little Belt Mountains, Montana (Taylor, 1935); Christmas Mountains, Texas (Clabaugh, 1953); Tres Hermanas Mountains, New Mexico (Homme and Rosenzweig, 1958); Scawt Hill, N. Ireland (Tilley, 1929, 1933, 1942; Tilley and Harwood, 1931); Carlingford, N. Ireland (Nockolds and Vincent, 1947; Osborne, 1932 a, b); Ballycraigy, N. Ireland (McConnell, 1954, 1955, 1960); Isles of Skye, Muck, and Rhum, Scotland (Wyatt, 1953; Tilley, 1947; Hughes, 1960); Kilchoan, Ardnamurchan, Scotland (Agrell, 1965); Mayen in Laacher See region, Germany (Jasmund and Hentschel, 1964); Tokatoka, New Zealand (Mason, 1957); Lower Tunguska, Siberia (Sobolev, 1935; Reverdatto, 1964); Mysore State, India (Naidu and Covidarajulu, 1954); Sinai (Gross *et al.*, in preparation).

Assemblages similar to those of the Hatrurim minerals are also recorded from portland cement clinker (Lea, 1956; Taylor, 1964) and blast furnace slags (Lapin, 1946; Nurse and Midgley, 1955; Kariakin, 1962).

The Hatrurim Formation is unique in the fact that it quite definitely could not have been formed by contact metamorphism. No igneous rocks have been found associated with it except for a small dike reported at Tarqumiye (Y. Bartov, personal communication) with hardly any contact zone. The rocks underlying the Hatrurim Formation are normal marine sediments without any sign of metamorphism. A different mechanism has to be invoked to explain the origin of the high-temperature mineral assemblage.

B. Genesis of the Hatrurim Formation

The ideas of earlier authors, based mainly on field evidence, have been summarized by Avnimelech (1965). These explanations range from volcanic (Tristram 1865, Hull 1886) to tectonic (Blanckenhorn, 1912). Picard (1931) thought the Mottled Zone rocks to have been formed by euxinic sedimentation and diagenesis. Avnimelech (1936) suggested in the case of Nahal Ayalon a local hydrothermal origin connected with Neogene volcanism. He later rejected this hypothesis in favour of a "diagenetic, or rather epigenetic process developed subaerially on an old "Danian" land surface" due to a period of strong insolation. Bentor and Vroman (1960) assumed that the rocks of the Mottled Zone were originally similar in composition to the bituminous Ghareb and Taqiye formations. Some time after burial of these strata under marine sediments of Eocene age, ground water rich in oxygen caused oxidation of the sulphide minerals and of the organic matter. "Owing to

the low thermal conductivity of the overlying sediments, the temperature of the ground water rose through the heat of oxidation and its geochemical activity was thereby enhanced." The result was a general redistribution of major and minor elements and the crystallization of new minerals. For processes of this kind the term "sedimentary hydrothermal" activity was proposed.

First evidence for a high-temperature origin of the "Mottled Zone" assemblage was presented by Bentor *et al.* (1963a, b), who showed that it contained high-temperature minerals such as spurrite, gehlenite and brownmillerite. They reiterated the previous view of Bentor and Vroman (1960) concerning spontaneous combustion of bituminous matter in the original rocks as a source of heat. Gross *et al.* (1967) advocated a penecontemporaneous origin in a reducing and alkaline environment and doubted the development of very high (above 640° C) temperatures during the formation of the mineral assemblage of Nahal Ayalon. Isotopic studies of carbon and oxygen (Bentor *et al.*, 1972, Kolodny and Gross, 1974) seem to confirm the concept of either induced or spontaneous combustion of organic matter that caused the thermal event. The carbon contained in spurrite, one of the most widespread high-temperature minerals in the Mottled Zone complex, is strongly enriched in C^{12}, pointing to an organic source for this element.

Decarbonation led to an enrichment of the metamorphic rocks both in C^{12} and O^{16}. Rocks later recarbonated are, on the contrary, enriched in O^{18} in comparison with the metamorphic rocks. The degree of enrichment correlates well with temperature zoning in the complex, as established independently by mineralogical criteria.

Brady and Greig (1939) already found that temperatures produced by combustion of coal seams may exceed 1,000° C, and according to Reverdatto (1970), who reviewed the literature on the subject, thermal metamorphism is common in burning coal seams and oil-bearing rocks.

C. Metamorphic model for the Hatrurim Formation

Kolodny *et al.* (1973), by using fission-track dating, found that the latest thermal event affecting the Hatrurim Formation in the Hatrurim syncline took place 13.6 or 16.8 ± 2 million years B.P. in Miocene times. The sandstone of the Hazeva Formation, considered to be of Neogene age and overlying the Hatrurim Formation unconformably, is also partly metamorphosed and mineralized in this area.

The Hazeva and subsequent formations never reached great thicknesses. The metamorphism could therefore not be significantly influenced by pressure. On the other hand it was shown, both by total analysis and by artificial thermal synthesis, that the mineral assemblage of the Hatrurim Formation was formed isochemically from the Taqiye and Ghareb formations, i.e. without addition of foreign elements (Bentor *et al.*, 1972). Thus, differences in mineral composition must be due to differences in the chemistry of the parent rock and to the degree of local heating, as well as subsequent events. The former chalky sediments are richer in Ca-bearing minerals than the former shaly sediments, which contain more silica and alumina. (The entire assemblage is characteristically Si-deficient, because after dissociation of the carbonates, calcium started to compete with aluminium for the available silica).

The mechanisms that caused ignition of the bitumen in the original rock are not known. Both the combustion and the necessary supply of oxygen may be connected with tectonic uplifting known from the Neogene (Bentor and Vroman, 1960; Reiss, 1966; Gvirtzman and Buchbinder, 1969.) The oxygen supply was evidently a chief controlling factor, since some

bituminous parts of the Ghareb-Taqiye formations remain unaltered. The mineral assemblages and their spatial and textural characters indicate rapid heating, with only a short time at the maximum temperature. Decarbonation and dehydration were the major chemical changes at this high-temperature stage of metamorphism. The metamorphic grade of these rocks are the sanidinite and pyroxene hornfels facies. With the cooling began the stage of the retrograde metamorphism in which aqueous fluids containing some CO_2 participitated. The progressive hydration caused development of zeolitic rocks rich in hydrogarnets and calc-silicate hydrated rocks.

The metamorphic pattern is complicated by younger, still active, weathering processes, with extensive hydration and recarbonation by atmospheric CO_2. In some instances sulfatization occurs, resulting in the formation of gypsum and ettringite. The results of these three stages (high-temperature, low-pressure metamorphism, hydrothermal mineralization, and weathering) are often superimposed, and in a single outcrop different facies, obtained during separate episodes, may be represented together.

In the course of the present study various rock types were discerned and defined. Altogether, more than 40 rock types are distinguished. They are mentioned in the description of mineral distribution and paragenesis, but will be fully described in a separate study dealing with the petrography of the Hatrurim Formation (S. Gross, in preparation).

METHODS OF INVESTIGATION

The choice of methods applied in the present work was dictated by the exceedingly fine grain size (1–10 μ) of many minerals, and the difficulty or impossibility of isolating them in a pure state. Under these circumstances, identification had to rely chiefly on methods suitable for small quantities but which do not require complete isolation.

All samples were studied in thin sections for mineral identification, structure and textural relationship. Most of the minerals were investigated also in immersion liquids. In the petrographical examination of some calc-silicate and calc-silicate-hydrate rocks, techniques of cement microscopy were used. Thin sections about 15–20 μ thick (instead of the standard petrographic thin sections) were prepared by grinding the specimens on emery papers and then on a chamois wheel, sprinkled with 5 μ alumina powder in alcohol (in order to prevent hydration). Polished sections prepared in the same manner were etched by different reagents (Terrier and Hornain, 1967) and examined in reflected light. Such sections are very useful in the determination of such minerals as tricalcium-silicate, larnite, and others, and in the study of the relationships between them.

As the samples were very heterogeneous in composition, it was often necessary to remove some major constituents before further investigation. This was important especially when monomineralic fractions were needed for chemical analyses.

Separation techniques were adjusted to each sample, according to the results of thin-section or X-ray studies. Usually a combination of several methods, both chemical and physical, was used. The separation techniques included comminution, dissolution in dilute acids (mcstly in 5% acetic acid), heating to various temperatures, sieving, decantation, separation by a Franz isodynamic magnetic separator, centrifuguing in heavy liquids, ultrasonic vibration, and hydration of some calcsilicates and Ca-aluminates using differences in their hydraulic properties. Hand-picking could be employed only in the case of relatively well crystallized minerals.

X-ray examination was carried out with a General Electric diffractometer (XRD–6) with

Ni-filtered Cu Kα radiation. The intensity of reflections was estimated by peak height. Powder photographs were also taken on a quadruple semi-focusing Nonius camera and the intensity of reflections estimated visually.

The clays were fractionated by differential sedimentation in water to separate the $< 2\ \mu$ fraction. Oriented samples were prepared by pipetting the suspension on glass slides and glazed porcelain tiles, and diffractometer patterns were obtained for untreated, glycolated, and heated (to 450°– 600°, according to the clay mineral present) samples. Separate portions were heated up to 800°– 1000° C and then X-rayed to examine the phases formed after dehydroxylation. Oriented aggregates of the tobermorite minerals were prepared in the same manner as the clay minerals, but alcohol or kerosene were used instead of water to prepare the suspensions. The particle size of clay minerals and tobermorite minerals was determined from peak broadening, according to the method of Klug and Alexander (1954).

DTA curves were recorded on a Robert Stone apparatus (model KA – 2H) with a heating rate of about 10° – 12° per minute.

TGA was carried out on a Stanton Thermobalance (model TR – 01) with a heating rate of 5° per minute.

The lattice parameters a_o of garnets and spinels were determined on the basis of all distinct reflections. Some knowledge of the microstructure and morphology, especially of tobermorites, was obtained by examining freshly fractured surfaces with a scanning electron microscope (Cambridge Stereoscan S–600).

Twenty two chemical analyses of minerals were carried out, mostly by classical methods and partly by atomic absorption spectroscopy. H_2O was determined by the Penfield method, and only in rare cases, where sample size was smaller than 0.5 g, was it computed from the loss of weight recorded by the thermobalance. SiO_2 was in all cases determined gravimetrically.

All the wet chemical analyses were carried out at the Geochemistry Division, G.S.I. Three microprobe analyses were performed on a Cameca MS 46 instrument at the mineralogical laboratory of CERILH (Paris) and two at the BRGM (Orleans, France). About 15 analyses were performed on the Jeol (model JAX5), microprobe of the Department of Geology, the Hebrew University, Jerusalem.

ACKNOWLEDGMENTS

The present work was carried out as a project of the Geological Survey of Israel. The results are a part of a Ph.D. thesis at the Hebrew University of Jerusalem under the guidance of Prof. Y. K. Bentor, whom I hereby thank for his constant involvement and encouragement. Special thanks are due to Prof. L. Heller for her help in the determination of some of the described minerals and her advice in the study of the calcium silicates.

Among the many people who assisted in this study, especially by providing field samples, are: Y. Arkin, M. Braun, M. Greenberg, Prof. Y. Kolodny, N. Lasman, Prof. E. Mazor, I. Rot, Dr. E. Sass, U. Würzburger, Dr. Y. Zak and several others.

The electron microprobe study of the Ca_2SiO_4 polymorphs and the study of polished sections was made possible through the courtesy of P. Terrier of the C.E.R.I.L.H (Paris).

Thanks are due to Dr. M. Fleischer of the U.S. Geological Survey, Washington, and to Dr. G. Gvirtzman, of the G.S.I, for their critical reading of the manuscript and for their valuable suggestions. The writer is grateful to H. Foner and I. Perath of the G.S.I. for their comprehensive editing of the final manuscript.

Thanks are also due to A. Barzilay, E. Daniels, Y. Deutsch, M. Dvorachek, S. Goelman, H. Lavi, I. Levi, A. Peleg, Z. Salman and others at the Geological Survey of Israel for their technical assistance.

MINERALOGY

CLASSIFICATION

Most of the minerals are described on the basis of the Strunz (1971) classification. The calcium-silicate-hydrates are classified according to Taylor (1961).

Some minerals, having structures not yet known, are assigned to appropriate groups on the basis of approximate composition.

I. NATIVE ELEMENTS

Sulfur – S

The mineral was identified microscopically in two samples of gypsum rock. It occurs as minute light yellow scales or radiating clusters, up to 10 μ in length. The refringence and birefringence are strong, the elongation positive; biaxial positive, with $r < v$. The sulfur is a secondary mineral and was formed by the reduction of gypsum, probably with the participation of sulfur bacteria.

II. SULFIDES

Greigite – Fe_3S_4

Polushkina and Sidorenko (1963, 1968) and Kramm and Sukhitskaya (1965) found a sedimentary mineral which they described as melnikovite. This cubic mineral is today known under the name greigite (The Commission of New Minerals and Mineral Names, I.M.A., Fleischer, 1968). Sedimentary occurrences of greigite were described by Skinner *et al.* (1964), Stashchuk and Kropacheva (1969), Garavelli and Nuovo (1971), Akhlestina (1972) and Dell (1972). Hydrothermal greigite has been described by Radusinovic (1966), Gruzdev *et al.* (1972), and by Williams (1968). Many successful syntheses of a phase which is obviously greigite have been reported by Lepp (1957), Berner (1964), Yamaguchi *et al.* (1960) and others. A hydrothermal greigite connected with ore deposits has been described recently by Gruzdev *et al.* (1972).

Greigite occurs in black rocks of the Mottled Zone, composed mainly of spurrite and calcite with some mayenite and brownmillerite. Greigite is a minor constituent and occurs as finely disseminated material accompanied by organic matter and chlorite. The mineral is black with a dull lustre and is strongly magnetic. It dissolves in warm dilute HCl. The strongest lines of the X-ray pattern are: 2.97 Å, 2.49 Å, and 1.74 Å. As greigite occurs in otherwise well-crystallized metamorphic rock it seems to be of later origin. It may have been hydrothermally formed by the action of H_2S or sulfide ion on brownmillerite under reducing and slightly alkaline conditions.

The source of the H_2S or sulfide ion is the residual organic matter. The high sulfur content of the hydrocarbons – one of the highest known – is generally characteristic of hydrocarbons in Israel (Shahar and Würzburger, 1967).

III. HALIDES

Halite – NaCl

Halite occurs as efflorescent, hair-like aggregates, or as stalactites in fissures and cavities of exposed rocks at the base of the Mottled Zone. The hair-like aggregates are often curved and form occasionally loops. Every hair is a thin pipe with a diameter up to 40 μ, partly filled with calcite or aragonite. The mineral is white or colourless, $n = 1.542 \pm 0.002$.

Halite is a mineral formed under the present arid conditions of the area. The hair-like curved

Table 1. Chemical analysis of halite

	Wt. %
Na	36.50
K	0.001
Ca	0.05
SO_3	0.03
Cl	58.20
Br	0.003
Insoluble residue	1.55
Total	96.33
Cl:Br	19400

Analyst, I. Grudniewicz

aggregates are formed by solutions rising by capillary force, feeding the "pipes" from the inside. At the end of their growth the bigger pipes became curved by the influence of their own weight.

IV. OXIDES AND HYDROXIDES

a. Oxides

Periclase – MgO

Small idiomorphic and isotropic crystals of periclase were identified during examination of a polished section of a larnite marble, etched with HF vapor. In reflected light the mineral is light pink and of high reflectivity. Its main X-ray spacings are 2.10 Å and 1.49 Å. Periclase is a high-temperature metamorphic mineral formed by dissociation of dolomite.

Spinel – $(Mg, Fe)Al_2O_4$

Spinel occurs in melilite and larnite rocks, metamorphosed phosphorites, and in gypsum-carbonate rocks. It occurs as small octahedral crystals (Plate I – 2, 7) or as anhedral grains. The colour in thin sections varies from yellow to brown and green. The mineral is isotropic. Crystal size ranges from 1 to 10 μ. The index of refraction varies from 1.740 to 1.795 and a_o is in the range 8.10 Å – 8.14 Å. The higher values correspond to the iron-rich variety, hercynite.

Spinel is a high-temperature mineral. It was formed in the phosphorites during the thermal event, at the expense of montmorillonite. Being more resistant to weathering than other minerals of the high-grade metamorphic calc-silicate rocks, spinel is found as a relict mineral in weathering crusts.

Magnesioferrite – $MgFe_2^{3+}O_4$

The mineral was identified in larnite-melilite rocks associated with titanomagnetite. It occurs either as octahedral or as anhedral crystals (Plate I – 8). In transmitted light it is reddish-brown. The average size is about 30 μ but some large crystals reach 60 μ in diameter. In polished sections it is isotropic, gray with internal reddish reflections and high reflectivity. $a_o = 8.36$ Å. Electronscan pictures of magnesioferrite are shown in plates I – 8 and II. These show clearly the presence of Fe, Mg, and some Al. Electron probe analysis shows: Fe_2O_3 – 81.7% ; MgO – 8.8%; Al_2O_3 – 4.5%; TiO_2 – neg; (part of the iron may be present in the form of Fe^{2+}).

Magnesioferrite is a high-temperature mineral and is found chiefly in fumaroles, in regions of volcanic activity (Draper, 1935). The magnesioferrite of Hatrurim occurs in assemblages of the highest metamorphic grade (sanidinite facies), and was formed by metamorphism of marls.

Magnetite – Fe_3O_4

The occurrence of magnetite in the Mottled Zone was mentioned by Bentor and Vroman (1960). The mineral occurs as an accessory in melilite-larnite rocks, associated with andradite, perovskite and hematite. It is found also as very

small inclusions in fassaite crystals from a pyroxene-wollastonite-anorthite fels. The crystals are commonly anhedral, rarely of octahedral habit (Plate I – 1, 6). The mineral is opaque in thin sections and gray in polished section.

Titanomagnetite

Occurs in a melilite-larnite rock in the form of octahedral crystals up to 30 μ across. Electron probe analyses show 20 – 23% TiO_2, 35% TiO_2 in several crystals. The latter crystals may be exsolved ulvöspinel (Fe_2TiO_4); this assumption, however, needs verification. Magnetite and titanomagnetite were formed at high temperatures characteristic of the sanidinite facies.

Hematite – Fe_2O_3

The appearance of hematite in the Mottled Zone is mentioned by Bentor and Vroman (1960). This mineral occurs in small amounts in nearly every sample. In the Hatrurim area, concretions of hematite are widely distributed. They occur only in metamorphosed sediments of the Taqiye Formation. The concretions are rounded or ellipsoid to platy in shape and up to 8 cm in diameter. The analysis of a hematite concretion on a dry basis is given in Table 2.

Table 2. Analysis of a hematite concretion

Oxide	Wt. %
Fe_2O_3	87.80
Al_2O_3	4.24
CaO	4.75
MnO	0.85
MgO	0.28
SiO_2	2.35
Total	100.27

Analyst, I. Grudniewicz.

The mineral is steel gray to iron black, with a red streak. In thin section it is blood red, with a high dispersion. The crystals are usually anhedral and occasionally vermicular. In small concretions each grain is often surrounded by a rim of hydrogarnet (Plates XI – 3 and XIV – 2). These concretions were probably formed by the oxidation of marcasite or pyrite concretions, known to occur in the non-metamorphosed Taqiye Formation.

Ilmenite – $FeTiO_3$

Ilmenite is found as a detrital mineral in the Hazeva sandstone. Black, opaque with a submetallic luster. Microchemical tests performed on single grains indicate the presence of Fe and Ti.

Maghemite – γ-Fe_2O_3

Maghemite occurs in maghemite-hematite nodules and is an accessory mineral in most of the rock types. It occurs as brown octahedral crystals or as small anhedral grains about 10 μ in diameter. Isotropic. Colour in thin section brown to yellow, in polished section bluish-grey. On heating to 400° C it changes to hematite. Identification of maghemite was made on the basis of its X-ray diffraction pattern which agrees with ASTM card 4-0755. The maghemite was probably formed as an alteration product of magnetite.

Perovskite – $CaTiO_3$

Perovskite is found as a rare accessory mineral in highly metamorphosed gehlenite-larnite rocks. It occurs as small cubic or octahedral crystals. In thin section it is brown, isotropic, with extremely high index of refraction. In reflected light, light grey. The strongest X-ray lines are: 2.69 (vvs); 1.91 (s); and 2.30 Å (m). The mineral was formed by high-temperature metamorphism, characteristic of the sanidinite facies. The mineral is resistant to weathering and is therefore preserved in the weathering crusts, together with alteration products of calc-silicate rocks.

Perovskite (?) – ferrian

Crystals of a mineral penetrated by iron-gehlenite were observed in a polished section of a gehlenite rock (Plate XVII – 5, 6). In reflected light the mineral is light-grey with high reflectivity. In thin section it occurs as reddish-brown, isotropic, anhedral crystals, 30 μ to 60 μ in diameter. The mineral is weakly magnetic. For electron probe analysis a fairly large crystal (50 μ in diameter) was selected; the results are given in Table 3.

Table 3. Electron microprobe analysis of "perovskite ferrian"

Oxide	Wt. %	Cations per 3 oxygens	
CaO	39.50	Ca	1.00
TiO_2	45.23	Ti	0.80
Fe_2O_3	11.78	Fe^{3+}	0.21
Al_2O_3	1.19	Al	0.03
SiO_2	0.53	Si	0.01
Cr_2O_3	0.12		
Total	98.35		

Analyst, G. Socroun (H.U.)

Distribution pictures for Ca, Ti, Fe, Al are given in Plate III. The mineral appears to belong to the perovskite group.

The mineral was formed by high-temperature metamorphism of shales and belongs to the sanidine facies.

Pyrolusite – MnO_2

Found in two samples of lizarditic limestones as dendritic growths on fracture surfaces. The mineral seems to be a late weathering product.

Rutile – TiO_2

Occurs as a rare detrital mineral in metamorphosed sandstone, as reddish brown and prismatic crystals.

Mayenite – $Ca_{12}Al_{14}O_{33}$

The compound was previously known as a constituent of cement clinker. It was identified as a natural mineral by means of X-ray diffraction by L. Heller (1963, personal communication) in a spurrite rock from the Nahal Ayalon outcrop. It was described by Hentschel (1964) in limestone xenoliths in a lava from Mayen (Germany). It is a common mineral in the spurrite and larnite rocks from Hatrurim, Nahal Ayalon, Tarqumiye and Ma'aleh Adumim. It occurs as rounded, colourless isotropic grains, dark-grey in reflected light, usually 7 to 15 μ in diameter. Rarely, crystals reach 35 μ. Index of refraction: n = 1.614 ± 0.002. The X-ray powder pattern is identical with the data of ASTM Card 9–413. The mineral is cubic with a_0 = 11.97 Å.

X-ray scanning images for Ca, Si, Al, and Fe are presented in Plate IV. The dark-grey rounded areas in the micrograph represent the mayenite. In Table 4, two analyses of mayenite are given.

Table 4. Chemical analyses of mayenite

	1	2
CaO	47.0	45.7
Al_2O_3	49.5	45.2
Fe_2O_3	1.5	2.0
MnO	1.4	
SiO_2	0.4	
TiO_2	traces	
Loss on ignition	–	2.2
Total	99.8	95.1

1. Mayenite from Hatrurim, electron microprobe analysis by G. Socroun. 2. Mayenite from Mayen (Hentschel, 1964).

The composition of the mayenite from Hatrurim, calculated on the basis of 0 = 33, is: $(Ca_{11.7}Mg_{0.5})(Al_{13.5}Fe^{3+}_{0.25}Si_{0.10})O_{33}$.

SEM pictures (Plate I – 3) of a freshly fractured surface of a larnite rock rich in mayenite reveal the spherical morphology of mayenite. The mineral, though not attacked by cold dilute acids, is observed microscopically to hydrate immediately in the presence of water and to form platy hexagonal crystals of calcium aluminate hydrates. Plate I – 4 are SEM micrographs of a fresh surface of a larnite-mayenite rock when autoclaved at 110° C. Spherical holes represent the spaces occupied by mayenite before autoclaving. Micrograph 4 shows hollow shells of an unidentified phase that surrounded the mayenite grains.

Mayenite is a mineral of the sanidinite facies, occurring always in association with brownmillerite. It was obtained by heating Ghareb calcareous rocks at 600° C. (Bentor *et al.*, 1972).

Calcium-dialuminate – $CaAl_4O_7$

Rankin and Wright (1915) reported the existence of a compound of the composition $3CaO.5Al_2O_3$, and Tavasci (1937) concluded that the formula is $CaAl_4O_7$. This view is now generally accepted. This phase was found as an accessory mineral in three samples of larnite rock, associated with brownmillerite and mayenite. Identification was possible because of the close correspondence of the X-ray data with those of the synthetic phase. It occurs as laths or rounded grains up to 30 μ across. Extinction is parallel, elongation negative, biaxial positive, 2V small. Birefringence is low and the index of refraction is lower than that of larnite. The X-ray powder diffraction data of the calcium dialuminate are given in Table 5.

The mineral does not hydrate with water. It was obtained by heating Ghareb limestones at 1000° C. The $CaAl_4O_7$ is characteristic of high-grade metamorphosed argillaceous limestones of the Hatrurim Formation.

Table 5. Diffraction data for $CaAl_4O_7$

1		2	
d(meas) Å	I	d(calc)Å	I
4.44	s	4.439	s
3.59	vw	3.609	vw
3.49	vvs	3.52	vvs
3.37	vvw	3.372	vvw
3.08	m	3.079	m
2.53	vw	2.53	vw

1. Ma'ale Adumim Sample SG, 598. 2. ASTM Card 7-82. (Lines not overlapped by larnite, mayenite, or brownmilerite).

Brownmillerite – $Ca_2(Al, Fe)_2O_5$

Brownmillerite is an important constituent of Portland cement. For many years it was thought that this compound has a definite composition – $4\,CaO.Al_2O_3.Fe_2O_3$. Later it was shown that a series of solid solutions exist, ranging between the end members $Ca_2Fe_2O_5$ and $Ca_2Al_2O_5$. This series was investigated by Toropov *et al.* (1937), Yamauchi (1937), Toropov and Boikova (1956), and others. The system was reinvestigated recently by Lister and Glasser (1967) and by Majumdar (1965). The crystal structure of brownmillerite has been determined by Colville and Geller (1971). It was shown that a complete solid solution series of $Ca_2Fe_2O_5$ – $Ca_2Al_2O_5$ exists, up to a composition $2CaO.O.31Fe_2O_3.O.69Al_2O_3$ (Smith, 1962), and that a slight discontinuity exists near the composition $6CaO.Al_2O_3.2Fe_2O_3$ (Newkirk and Thwaite, 1958; Smith, 1962).

X-ray powder data for the solid solution series show a change in the lattice spacings with composition. The relationship between spacing and composition has been studied by Copeland *et al.*, (1959), Midgley (1958), and Smith (1962).

Table 6. Chemical analyses of brownmillerite.

Oxide	1	2	3	4	5	6
CaO	44.8	46.6	47.7	46.8	43.7	46.2
MgO	n.d.	n.d.	1.6	1.4	n.d.	n.d.
Al_2O_3	22.3	19.8	19.7	22.7	13.1	17.2
Fe_2O_3	27.6	32.5	28.6	25.5	41.9	30.5
TiO_2	1.5	2.8	1.9	3.0	1.9	
Cr_2O_3	0.1	0.3	n.d.	0.3	n.d	
ins. res.	4.0					
Total	100.3	102.0	99.5	99.7	100.6	93.9

Cations per five oxygens

Ca	1.99	1.99	2.00	2.00	2.07	2.16	1.99	2.07	1.95	1.95	2.16	
Mg	neg.		n.d.		0.09		0.08		n.d.		n.d.	
Al	1.09	2.00	0.91	1.98	0.99	1.92	1.06	1.92	0.64	2.01	0.89	
Fe	0.86		0.98		0.87		0.76		1.31		1.00	
Ti	0.05		0.08		0.06		0.09		0.06			
Cr	0.003		0.01		n.d.		0.01		n.d.			

1. Brownmillerite from a calcite-gypsum rock, Nebi Musa. Atomic absorption spectroscopy by S. Erlich on grains separated by magnetic separation. 2. Brownmillerite from a weathered rock, consisting mostly of calcite, gypsum, portlandite and jennite. Analysis by Holoye and Gross, BRGM (France). 3. Brownmillerite from an altered larnite rock. Analyst, G. Socroun. 4. Brownmillerite from a larnite rock rich in mayenite. Analyst, G. Socroun. 5. Brownmillerite from a spurrite-marble. Analyst, S. Gross. 6. Brownmillerite from Mayen (Hentschel, 1964).

Brownmillerite in nature was first discovered in Nahal Ayalon and Hatrurim (Bentor *et al.*, 1963) and a year later it was reported by Hentschel from Mayen in Germany (Hentschel, 1964). It is one of the most widely distributed minerals in the spurrite and larnite rocks of the Mottled Zone, in association with mayenite. As a relict mineral it occurs also in weathering crusts derived from larnite rocks. The common variety has the composition $4CaO.Al_2O_3.Fe_2O_3$. A compound with an approximate composition of $6CaO.Al_2O_3.2Fe_2O_3$ was recorded in a few samples.

Analyses 1 – 5 show that the composition of the ferrite phase is close to $4CaO.Al_2O_3$-Fe_2O_3; the mol percent of $2CaO.Fe_2O_3$ ranges from 44 to 54%. The mol percent of $2CaO.Fe_2O_3$ of analysis 5 is about 67%, and is identical with the phase described as $6CaO.2Fe_2O_3.Al_2O_3$. The data from the chemical analyses are in good agreement with the X-ray diffraction data. (Table 7).

The natural brownmillerite is much more resistant to hydration and acid attack than the synthetic mineral (see page 19). Brownmillerite was synthesized by the author by firing stoi-

Table 7. Diffraction data for brownmillerites.

	1		2		3		4		5	
hkl	I	d(Å)	I	d(Å)	I	d(Å)	I	d(Å)	I	d(Å)
020	50	7.24	vs	7.20	s	7.255	s	7.248	m	7.28
040	30	3.63	m	3.62	w	3.648	w	3.64	w	3.66
121	10	3.39	vw	3.39			vw	3.38	vw	3.39
200	80	2.77	m	2.77	m	2.775	m	2.77	m	2.778
002	70	2.67	m	2.66	m	2.675	s	2.67	s	2.683
141,012	100	2.63	vs	2.63	vs	2.642	vs	2.63	vs	2.652
150	20	2.57	m	2.56			w	2.569		
211,060	10	2.43	vw	2.42					vw	2.44
240	30	2.20	vw	2.19					vw	2.21
042,132	30	2.15	vw	2.15	vw	2.15	m	2.149		
161	60	2.04	m	2.043			m	2.043	w	2.044
202	80	1.92	m	1.923	m	1.931	m	1.924	m	1.935
222	20	1.86	w	1.857			w	1.860		
080	40	1.81	m	1.81	w	1.81	w	1.806		
311,330	20	1.73	w	1.73			w	1.730		
242			w	1.697						
172,341	40	1.57	m	1.576	w	1.58	w	1.571	w	1.58
143	40	1.53	m	1.532			w	1.531		
312	10	1.51	w	1.513	w	1.51				
082	20	1.50	w	1.50						
			vw	1.48						
233			vw	1.46						
0100,332	10	1.45	w	1.451						
	10	1.42	w	1.416						
420			w	1.356					w	1.36
	20	1.39								
262	10	1.33	m	1.319			w	1.31	w	1.32
	20	1.32								
343			m	1.203						

1. ASTM 11–124. Synthetic $4CaO.Fe_2O_3.Al_2O_3$. 2. Brownmillerite (analysis 1, Table 6). 3. Brownmillerite (analysis 2, Table 6). 4. Brownmillerite (analysis 3, Table 6). 5. $6CaO.2Fe_2O_3.Al_2O_3$ (analysis 5, Table 6).

chiometric proportions of $CaCO_3$, Al_2O_3 and Fe_2O_3 at 900° C. Hydration of brownmillerite is discussed on page 18.

The brownmillerite of the Mottled Zone was formed during high-temperature metamorphism of impure limestones, by reaction between $CaCO_3$, clays and iron oxides.

Quartz – SiO_2

Most of the quartz occurring in the Hatrurim Formation is detritic and the amount present is negligible. The exceptions are the metamorphosed sandstones and conglomerates of the Hazeva Formation in the Hatrurim syncline (Kolodny *et al.*, 1973) and the siliceous rocks

at the base of the Hatrurim Formation outcrop at Nahal Ayalon (Gross *et al.*, 1967). The latter are composed of microquartz, chalcedony and opal, and their textures suggest a replacement origin. Quartz grains, partly or entirely replaced by calcite, apophyllite and tobermorite were observed. Chalcedony occurs in the form of spherulites, radiating aggregates, and incrustation rims surrounding quartz grains and filling voids.

α–Cristobalite – (low-temperature modification) – SiO_2

α– cristobalite occurs in the clay fraction of limestones and gypsum rocks at Hatrurim and as an essential constituent of the opaline-carbonate rocks of Nahal Ayalon. In thin sections thin fibres with negative elongation are observed. The strongest X-ray lines are: 4.04 (vvs), 2.49 (s), 2.84 (m). The α – cristobalite is a conversion product of earlier-formed opal.

Opal – $SiO_2 . nH_2O$

Opal is found only at Nahal Ayalon (Gross *et al.*, 1967). It occurs in the form of irregular concretions in the carbonate rocks, as crusts, enamel or hyalite-like coatings on cavities and fissures, and in botryoid shapes. The opal is colourless, white, grey, or black and is transparent to translucent. H = 5.5-6, sp. gr. – 2.00. Inclusions of calcite and organic matter are common. Globular texture may be observed in thin sections. n = 1.444 – 1.446. Water content is 4.1%. It is partly released below 100° C and fully released up to 300° C. On heating to 700° C the opal converts to cristobalite and quartz.

b. Hydroxides

Gibbsite – γ-$Al(OH)_3$

Gibbsite occurs at Hatrurim in lizardite limestones and calcite-zeolite rocks, occasionally associated with bayerite. The strongest reflections in the diffractogram are 4.8 – 4.9Å-(vs), 4.37Å(m) and 2.39Å(m). Fig. 3A shows the DTA curve of gibbsite with an endothermic peak at 325° C. Gibbsite is formed by the low-temperature alteration of calcium aluminates and aluminous silicates.

Bayerite – α-$Al(OH)_3$

Until recently bayerite was known only as synthetic compound. Gedeon (1956) reported a natural occurrence of bayerite in Hungary. Fleischer (1956) suggested the need of X-ray confirmation of this mineral. Sasvari and Zalai (1957) showed by X-ray study that the material described by Gedeon was actually gibbsite, but bayerite was later found in Hungarian clays by Naray-Szabo and Peter (1967). The first proven natural occurrence of bayerite was reported from Hatrurim (Gross and Heller, 1963).

Khorosheva (1968) reported recently a new occurrence of bayerite in weathering crusts on amphibolites and serpentines in Russia. The mineral at Hatrurim occurs in two distinct assemblages:

1. As vein and cavity filling in spurrite and larnite-gehlenite rocks, associated with calcite, gypsum, tobermorite and ettringite.
2. Associated with lizardites.

Bayerite occurs as very fine fibers or as lamellar, radiating, hemispherical crusts lining walls of a calcite-filled vein. n > 1.54, elongation of fibers is negative, birefringence very low. The mineral was identified by its powder pattern, which resembles that of the synthetic material. The natural mineral has a higher thermal stability than the synthetic material: after heating at 230° C its X-ray pattern is not affected, whereas synthetic bayerite is generally decomposed at about 160°. After heating at temperatures ranging from 320° to 700° the natural material is amorphous to X-rays. Heating at higher temperatures gave α – Al_2O_3. The DTA–curve (Fig. 3A) shows a symmetrical, strongly endothermic peak at 290° C.

The bayerite of the Mottled Zone was formed

by the aging of aluminium gels derived by hydration of such minerals as mayenite, and by weathering of the lizardites. The presence of portlandite and ettringite indicates a very high pH. According to Schoen *et al.* (1970), the bayerite from Hatrurim must be metastable and its slow rate of recrystallization to nordstrandite may be due to the extreme dryness of the region.

Boehmite – AlOOH

Boehmite occurs in carbonate rocks that have undergone low-grade metamorphism. The mineral was identified only by X-ray powder diffraction. The 6.1 Å spacing is relatively sharp and remains after treatment with acid. The mineral is formed probably by dehydration of gibbsite.

Brucite – $Mg(OH)_2$

The mineral occurs in veins of spurrite rocks with some monticellite, and in melilite rocks associated with afwillite, tobermorites, ettringite, jennite, calcite, aragonite, hydromagnesite, and a serpentine mineral. It is found in veins as aggregates of white and transparent hexagonal plates, with a perfect {0001} cleavage. The mineral is colourless in thin section. The elongation of the plates in negative. nO = 1.560, nE = 1.580, nE – nO = 0.020, (all ± 0.002), uniaxial positive, r > v. The DTA curve (Fig. 3D) shows an endothermic peak at 462° C. Brucite is a low-temperature hydrothermal mineral formed by the alteration of Mg-bearing minerals such as akermanite and monticellite.

Portlandite – $Ca(OH)_2$

Portlandite is very rare in nature. It has previously been described by Tilley (1933), Minguzzi (1937), Carobbi (1940), Hentschel (1961), Bentor *et al.* (1963), and Gross *et al.* (1967). It occurs as aggregates of large crystals up to 2 mm in diameter, occupying fractures and voids of hydrated calc-silicate rocks (Plate XXIII – 5, 6). Aggregates of anhedral crystals or hexagonal flakes line the walls of thin veins in spurrite-calcite rocks.

The mineral is mostly colourless, transparent, with pearly luster on cleavage planes. At Ma'ale Adumim yellow crystals stained by chromate were observed. Hardness is 2, with perfect cleavage on {0001}. The mineral is uniaxial negative with nE = 1.548 ± 0.002, nO = 1.576 ± 0.002, nO – nE = 0.028. Slowly soluble in water and easily in dilute acids. It alters to $CaCO_3$ at room temperature on exposure to moist air. The X-ray pattern is identical with that of synthetic $Ca(OH)_2$ after correction for preferred orientation. Analysis of portlandite from a vein in a spurrite rock is given in Table 8.

Table 8. Chemical analysis of portlandite.

Oxide	Wt. %
SiO_2	1.2
Al_2O_3	0.4
Fe_2O_3	
CaO	48.4
MgO	neg.
CO_2	6.1
$\pm H_2O$	43.1
Total	99.2

Portlandite from a vein in a spurrite rock, Hatrurim.
Analysis by M. Gaon performed on a 270 mg sample after storage of 2 years. The sample was slightly contaminated by tobermorite and partly recarbonated.

A DTA pattern of well-crystallized portlandite is presented in Fig. 3C. A small and broad endothermic effect registered below 150° C may be due to desorption of water. The prominent peak at 520° C is caused by the dehydration of the $Ca(OH)_2$. The small endo-

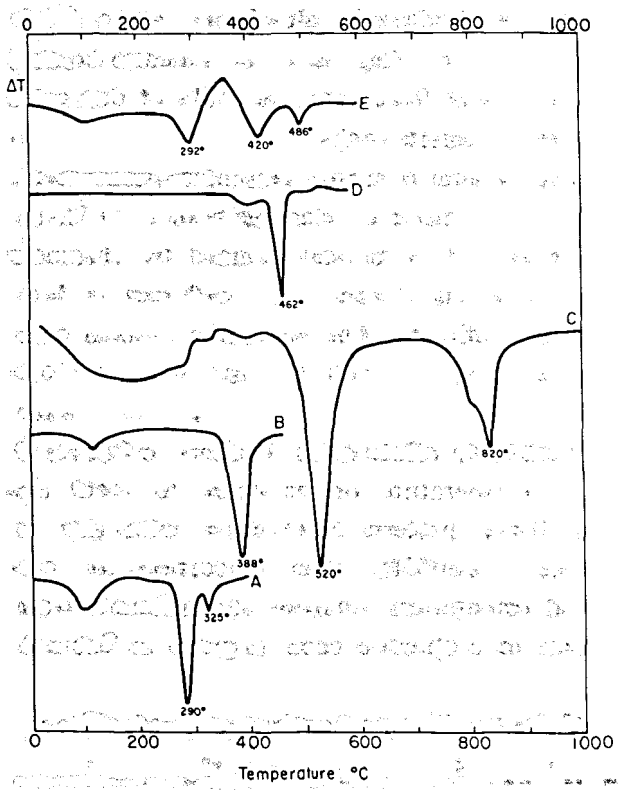

Figure 3. DTA curves of: A – bayerite and gibbsite (sample SG 523); B – goethite (sample SG 558); C - portlandite (sample SG 442); D – brucite (sample SG 281); E – hydrotalcite and hydromagnesite (sample R – 4b).

thermic effect at 820° is caused by decarbonation of $CaCO_3$ formed (by reaction with atmospheric CO_2) during two years' storage of the sample. Portlandite in a finely divided state is decomposed at slightly lower temperatures.

Portlandite is a secondary mineral, formed by hydration of calc-silicate rocks at low temperatures, in the absence of CO_2.

Goethite – α-FeOOH

Goethite occurs as scales or acicular crystals. In thin sections it is pleochroic: X-yellow, Z-orange-yellow. In the diffraction pattern a strong reflection at 4.17 Å is observed. On the DTA curve (Fig. 3B) there is an endothermic peak due to dehydration at about 390° for well-crystallized goethite, which is shifted to 260° – 320° C for poorly crystalline material. Goethite is a weathering product of ferriferous minerals, especially of the Fe-gehlenite.

Lepidocrocite – γ-FeOOH

Lepidocrocite is a common weathering product occurring in the form of disseminated small scales or aggregates in nearly every type of rock. It is reddish-brown or yellowish in thin section, and strongly pleochroic.

Hydrocalumite – $Ca_{16}Al_8(OH)_{54}.CO_3.21H_2O$

Hydrocalumite was discovered by Tilley *et al.* (1934) at Scawt Hill (N. Ireland) in cavities of larnite rocks. It was later found in porcellanites at Boissejour (France) by Grünhagen *et al.* (1963), and at Mayen (Jasmund and Hentschel, 1964). In those occurrences it is associated with ettringite, afwillite and portlandite.

Hydrocalumite is closely related to $4\,CaO.Al_2O_3.13H_2O$ from which it is derived by substitution of CO_3^{2-} for $2\,OH^- + 3H_2O$ once in every eight structural elements (Buttler *et al.*, 1959). It was found at Hatrurim in veins and cavities of spurrite and larnite rocks and as a crust about 1 cm thick surrounding a core of larnite-mayenite-brownmillerite rock. The crust is composed of bands of hydrocalumite, ettringite and afwillite (Plate XXII – 3). The mineral occurs as tabular crystals up to 0.2 mm across, or as aggregates. It is bluish-green in mass and colourless in thin section. Fair (001) cleavage. The optical properties are: Biaxial negative, 2V small, $r < v$, elongation positive, birefringence = 0.021. The X-ray data agree with those of Wells *et al.* (1943). The endothermic peak at 142° C on the DTA curve (Fig. 5A) corresponds to dehydration of the hydrocalumite. The X-ray reflections of a sample heated at 150° C become diffuse and the basal spacing 7.86 Å is shifted to 7.3 Å. The mineral was formed at Hatrurim by hydration of mayenite in the presence of CO_3^{2-} ions.

Dicalcium-aluminate-hydrate–
$Ca_2 Al_2 O_5 .n H_2 O$

This phase is common in the hydration products of portland cement. Optical and X-ray data are reported by Roberts (1957) and Midgley (1957). DTA data are reported by Kalousek *et al.* (1949). A brief review is given by Jones (1960). The dicalcium-aluminate-hydrate of Hatrurim occurs in veins, cavities and weathering crusts of calc-silicate rocks. In one vein, consisting predominantly of portlandite, numerous hexagonal plates up to 15 μ across were observed. The index of refraction is lower than that of portlandite. The plates gave a uniaxial negative interference figure.

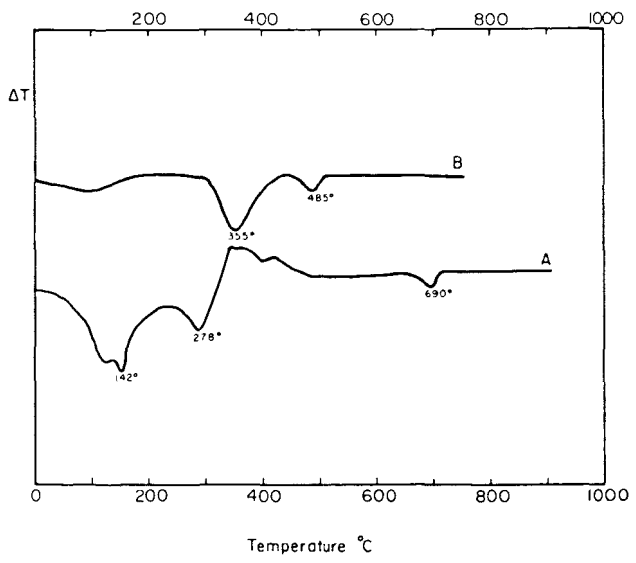

Figure 4. DTA curves of: A – calcium aluminate hydrates (sample SG 478); B – hydrogarnet with a_0 – 12.33 Å (sample SG 464).

The mineral was identified on the basis of its X-ray pattern. The basal spacing depends upon the hydration state. The 8 hydrate with basal spacing of 10.5 Å shrinks to 8.8 Å (6 hydrate) on heating to 110° C. During electron probe microanalysis of a vein of a spurrite-brownmillerite-mayenite rock a grain was detected giving the following analysis: $Al_2 O_3$ – 41.9% , CaO–45.7% , Fe and Ti traces, Mg neg. Assuming the deficit to be due to $H_2 O$, the following approximate composition is obtained: $Ca_2 Al_2 O_5 .1.8 H_2 O$. Schneider and Thorvaldson (1943) obtained the compound $Ca_2 Al_2 O_5 .3 H_2 O$ by autoclaving at 105° – 150° C. In the dehydrating conditions of the electron probe, further dehydration could have occurred. The DTA curve (Fig. 4A) shows an endothermic effect at about 280° C, corresponding to loss of molecular water.

On a SEM photomicrograph of a fresh surface of jennite rock (Plate I – 5) a hexagonal plate about 4 μ across can be seen. It is most likely to be a calcium-aluminate-hydrate, as the X-ray diffraction of this rock indicates the presence of both di- and tetra-calcium-aluminate-hydrates. Microscopic investigation of hydration products of a powdered spurrite-mayenite bearing rock (isolated to exclude atmospheric CO_2) shows growth of minute hexagonal scales. Their longest X-ray spacings are 10.7 Å, corresponding to the 8 hydrate.

The mineral, which may be metastable, is found predominantly in weathering crusts in close association with tetra-calcium-aluminate-hydrate, calcium-silicate-hydrates, ettringite, hydrogarnet, and portlandite. It is formed by hydration of mayenite.

Tetracalcium-aluminate-hydrate –
$Ca_4 Al_2 O_7 .n H_2 O$

According to Roberts (1957) there are at least six polytypes of crystalline modifications having the general formula $Ca_4 Al_2 O_7 .n H_2 O$. This compound is distinguished by the basal spacing which is in the range 8.2 – 7.9 Å, depending on the form. It crystallizes in thin hexagonal plates which are similar to those of the dicalcium-aluminate-hydrate. The main polymorph found in Hatrurim is characterized by the main spacings: 8.1 (vs), 3.95 (m) and 2.88 (s), corresponding to the 13 hydrate. It occurs in association with dicalcium-aluminate-hydrate, calcite, aragonite, vaterite, ettringite,

portlandite, and calcium-silicate-hydrates. The DTA curve shows an endothermic effect in the range 140° – 190° C, corresponding to loss of molecular water. This compound may be obtained from the dicalcium-aluminate hydrate by reaction with lime water.

Calcium-aluminate-ferrite-hydrate – $Ca(Al, Fe_2)O_4 .nH_2O$

In a number of specimens of weathered larnite rocks consisting predominantly of carbonates, calcium-silicate-hydrates, ettringite, and portlandite, the brownmillerite crystals were replaced partly or entirely by a brown isotropic phase. In the case of partial replacement, the core of brownmillerite is enveloped by a rim of the isotropic substance (Plate VIII – 1, 3, 6). Fully replaced grains are often of collomorphic structure. The replacement is a continuous process. In some grains, specks of iron oxides may be observed. The grains are anhedral and up to 0.2 mm across. n = 1.640 – 1.694. It seems that the refringence depends on the state of hydration. This phase is X-ray amorphous. Electron probe analyses of this phase are given in Table 9.

Table 9. Chemical analyses of calcium-aluminate-ferrite-hydrate.

Oxide	1	2
Al_2O_3	11.9	19.2
SiO_2*	3.2–5.8	0.6–3.0
TiO_2	3.5	4.2
Cr_2O_3	1.0	0.7
Fe_2O_3	37.7	36.0
CaO	9.7	10.4
MgO	n.d.	1.9
Total	67.0–69.6	73.0–75.4

* The distribution of silica is irregular.

1. Hatrurim, Sample S.G. 182. Microprobe analysis by F. Holoye (B.R.G.M.).
2. Hatrurim, Sample S.G., 181. Microprobe analysis by G. Socroun.

On the basis of the analyses of Table 9 and taking the difference to 100 as water, the composition of this phase is computed as follows:

1. $Ca(Fe_{1.37}, Al_{0.62}, Ti_{0.20}, Cr_{0.01})O_4$ $11.5H_2O$.
2. $(Ca_{0.80}Mg_{0.20})(Fe_{0.96}, Al_{0.80}, Ti_{0.22})O_4$ $5.7H_2O$.

The true content of water has to be higher, as some dehydration occurs in the electron probe. The conditions during both analyses, performed on different instruments, were also different. Si is not included in the calculation as it is an impurity.

Comparing these data with those of brownmillerites from the same samples (Table 7, columns 2 and 5) it will be seen that during the hydration process Ca and to a lesser extent Al are removed from the brownmillerite. This process is illustrated in the distribution pictures for Ca, Al, Fe, Ti, and Cr (Plates V, VI) and line scans across the grain. The micrographs show clearly that the amounts of Fe and Ti increase in the envelope in comparison with the brownmillerite core, while Ca and Al decrease.

The DTA curve (Fig. 5B) shows that the water is expelled below 300° with a large endothermic effect. The small subsidiary peak at 260° C is due to the presence of goethite. A small exothermic effect around 345° C represents the crystallization of Fe_2O_3. Separate grains were gradually heated and studied by optical and X-ray methods. After heating to 200° C cracks similar to cracks in a dried gel substance are observed (the same effect is caused by electron beams, see Plate VI – 1, 6, 7). At 400° C the formation of cracks stops. The colour of the grains changes to orange-red but they are still X-ray amorphous. After heating to 800° C the crystals turn red, become anisotropic, and the X-ray pattern is characteristic only of hematite.

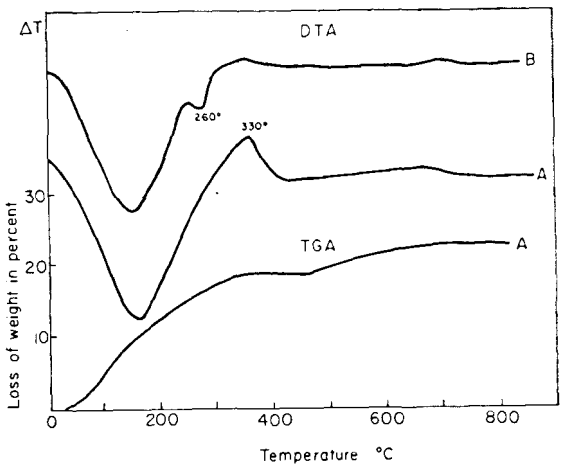

Figure 5. DTA and TGA curves of: A – $Cr_2O_3 \cdot nH_2O$ (samples SG 195); B–$Ca(Al, Fe)_2O_4 \cdot nH_2O$ (sample SG 182).

The hydration of synthetic brownmillerites was investigated by Steinour (1951), Bogue and Lerch (1934), Bogue (1955), Lea (1956), Jones (1960), and others. Bogue and Lerch obtained an amorphous hydrate, with n ~ 1.70, and suggested it was a dicalcium-ferrite-hydrate.

Hydration experiments on brownmillerite carried out by the writer, using air-isolated covered slides, showed that when a particle of brownmilerite was placed in contact with 3% acetic acid, no change was observed after 8 hours. After treatment of two hours with HNO_3 (1:7) a slight discoloration of the edges of the crystals was observed, and they became isotropic. This discoloration progressed slowly and the solution turned yellowish. Microchemical analyses showed the presence of Fe in the solution. With HCl (1:4) the discolouration was completed after about 4 hours, and with HCl (1:1) after half an hour only the crystal form was still observable. In one case, drop-like etching figures were found arranged parallel to the extinction of the crystal. In contact with water, no changes were observed even after 3 months. Under slightly alkaline conditions some Ca and Al were detected in the solution after a month. This process is very sluggish. In nature the replacement occurs in an alkaline environment in the presence of SO_3^{2-} and CO_2^{2-} ions. This is a very slow but continuous process depending on the supply of water. In a single thin section fresh brownmillerite crystals, brownmillerite cores with the "gel"-like phase, and fully replaced crystals can be observed. As the phase is X-ray amorphous, electron diffraction and especially selected-area diffraction are needed to test whether the phase has a low degree of crystallinity, and whether it can therefore be regarded as a new mineral.

$Cr_2O_3 \cdot nH_2O$

The material occurs as an earthy, loose and porous green matter in veins and pockets of carbonate rocks, in association with gypsum and zeolite. Skeletal hexagonal crystals, or parallel fibre growths appearing as prisms and stained by green matter, were observed in some calcitic veins cutting spurrite rocks. The skeletal crystals are hosts of an unidentified zeolite (?) (Plate VII – 6, 7). In transmitted light the matter is green, non-pleochroic and isotropic with n = 1.574. It is amorphous to X-rays. In one case diffuse lines at 3.63, 2.67 and 2.48 Å that can be attributed to eskolaite (Cr_2O_3) were observed. The substance is not attacked by cold 3% acetic acid, but is completely soluble in dilute hot HCl (1:1). Table 10 gives the results of a chemical analysis of a substance from a pocket, after dissolution of the calcite. In 3% acetic acid the insoluble residue consists of chromium oxide hydrate, amorphous silica, an unidentified zeolite, and some apatite.

The DTA curve (Fig. 5A) shows a broad endothermic peak with a maximum at 160° (removal of weakly bonded water) and an exothermic peak at 350° corresponding to the formation of eskolaite (Cr_2O_3). The first reflections of eskolaite appear at about 350°. The colour of the substance changes on heating from grass-green to dark green, and to nearly black at 400° – 450° C. In the range 450° – 500° it turns

Table 10. Chemical analysis of the residue insoluble in 3 % acetic acid

Oxide	Wt.%
Cr_2O_3	34.6
Al_2O_3	1.8
SiO_2	35.4
CaO	7.6
MgO	1.2
SrO	1.2
Fe_2O_3	0.2
K_2O	0.03
Na_2O	0.2
H_2O+	16.1
P_2O_5	n.d.
Total	98.3

Analysis by S. Ehrlich and I. Grudniewicz.

olive-green and at 700° C it is emerald-green. At 700° C, in addition to eskolaite, lines of cristobalite are detected (crystallization of amorphous silica). The TGA curve (Fig. 5A) shows a loss of 19.8% of weight below 370° and 3.5% between 500° – 700° C. Carruthers *et al.* (1967) showed that chrome oxide gel usually undergoes a strongly exothermic transformation when heated in air at about 400° C, with development of α-Cr_2O_3.

The analysed substance may be considered as a gel in the initial stage of crystallization.

V. CARBONATES

Siderite – $FeCO_3$

Siderite is found in a few specimens of lizardite limestone. It was identified by X-ray diffraction. It appears in thin section as brownish grains, bordered by a stain of iron oxides. On the DTA curve an endothermic peak is observed at 550° C. Siderite is a primary mineral.

Calcite – $CaCO_3$

Calcite is the most common and widely distributed mineral, occurring in nearly every sample. Two types of calcite may be distinguished: 1. Primary – mostly micritic with few organic remnants. 2. Secondary – formed by the decomposition of metamorphic calc-silicates, or as a late hydrothermal deposit in veins and cavities. The crystal habit of secondary calcite may be granular, prismatic, tabular, scalenohedral or rhombohedral (Plate IX – 2) and it is occasionally found as concentric bands, rosette-like aggregates, columnar and fibrous (Plate VIII – 3). Pseudomorphs after quartz, zeolites and calcium-silicates were also observed (Plate VIII – 4, 5, 6). The colour varies widely. Most of the calcite is white or colourless. Green, violet, brown and black calcite occur in veinlets. The colours are due to finely disseminated impurities such as chrome and iron compounds or organic matter. Table 11 lists analyses of minor elements from 3 coloured vein calcites. Ba was determined by emission spectrography,

Table 11. Minor elements in calcitic veins (p.p.m.).

Element	1	2	3
Fe	177	80	200
Zn	14	6	10
Mg	34,000	6,720	3,600
Cu	13	18	15
Sr	575	760	938
Mn	13	8	48
Ni	25	24	29
Ba	15	80	20
Cr	11,800	18,900	40
O.M.	–	–	900

Analyst, S. Ehrlich.
1. Violet calcite. Hatrurim, Sample S.G. 180
2. Green calcite. Hatrurim, Sample S.G. 292
3. Black calcite. Hatrurim, Sample B.T. 5991

organic matter by volumetric method, and other elements by atomic absorption.

The violet and green colours are due to finely disseminated Cr^{3+} compounds, and the black colour is due to the presence of organic matter. (The Cr^{3+} compound in sample (1) may be stichtite – $Mg_6 Cr_2 (OH)_{16} CO_3 .4H_2 O$).

Most of the secondary calcite is formed by recarbonation. The lime, formed by hydrolysis of the calc-silicate minerals, is converted to calcite by the action of CO_2 from the atmosphere or water. This reaction is very slow and under normal conditions of exposure is not completed even after a number of years. This calcite is very fine-grained and dissociates at lower temperatures than does primary calcite due to the poorly crystallized state of this calcite. The DTA curve shows an endothermic peak in the range 730° – 800° C. The oxygen and carbon isotopes in these carbonates are discussed in Bentor *et al.* (1972), and in Kolodny and Gross (1974).

Aragonite – $CaCO_3$

This mineral is common but occurs only in low concentrations, although in some calcareous and zeolitic rocks it constitutes 40 – 50% of the bulk carbonate. It is associated with calcite, gypsum, vaterite, tobermorites, afwillite, ettringite, zeolites and halite. It occurs as anhedral or prismatic crystals and forms radiating groups of acicular crystals in veins, cavities and crusts, converted partly to calcite. The larger crystals measure up to 0.5 mm across and are usually twinned. The twinning is of polysynthetic or of pseudohexagonal penetration type (Plate IX – 4, 5). The extinction is parallel, the elongation negative, biaxial negative, $2V \sim 18°$, $v < r$. The DTA curve shows an endothermic peak at about 450° C, corresponding to the inversion of aragonite to calcite.

The aragonite is of secondary origin. It is a low-temperature mineral formed by precipitation from aqueous solutions.

Vaterite – μ-$CaCO_3$

This mineral, long known as an artificial compound, has rarely been found in nature. It has been reported from Ballycraigy in hydrogel pseudomorphs after larnite by McConnell (1960), from the Pesyanoe meteorite by Dufresne *et al.* (1962) and from Hatrurim by Bentor *et al.* (1963) and by Gross *et al.* (1967). It was also found in mollusk shells (Skolkovski, 1951) and gastropod eggshells (Hall *et al.*, 1971). At Hatrurim, the vaterite has been found either as a rock-forming mineral in three samples, associated with calcite, aragonite, tobermorite, 7 Å-clay and hydrogarnets, or as a minor constituent in weathered metamorphic calc-silicate rocks, in slightly metamorphosed marls and conglomerates of the Hazeva Formation, and in weathering crusts.

The rock-forming vaterite occurs as a mosaic of anhedral, interlocking crystals up to 0.1 mm across, fibrous aggregates, and spherulites up to 0.15 – 0.30 mm in diameter (Plate VIII – 1, 2). In immersion preparations small globules or ellipsoids, 30 – 70 μ across, yielding a positive uniaxial figure, were observed. In thin section the mineral is colourless, usually uniaxial positive and rarely biaxial, with $2V \sim 0°$. nO = 1.550 ± 0.002, nE = 1.644 ± 0.002.nE–nO = 0.094. It is stained by Alizarin Red with an orange tint.

According to McConnell (1960), natural vaterite is unstable in the presence of water at room temperature and atmospheric pressure, and inverts to calcite in thin section. Northwood *et al.* (1969) reported the transformation of synthetic vaterite to calcite during grinding, the rate of transformation being greater at higher temperatures. DeKeyser *et al.* (1950) and Bischoff (1968) reported the transformation of vaterite to calcite or aragonite on heating above 400° C.

The vaterite from Hatrurim did not transform to calcite even after exposure of an uncovered thin section to atmospheric conditions for two

years. In Fig. 6 a DTA curve is presented of a rock sample consisting of vaterite and some aragonite with calcite. No exothermic peak in the range of 400° – 490° C (due to transition to calcite, as described by DeKeyser *et al.* (1950) and Turnbull (1973) for synthetic vaterite) is observed. Decarbonation starts gradually, with a broad endothermic effect having its maximum at 730° – 750° C and passing onto a more intensive effect with a double peak at 813° and 822° C. It was assumed that the first effect corresponds to the decarbonation of the vaterite, and the second effect to the decarbonation of calcite. To check this, 4 samples of vaterite-calcite rocks were heated gradually to different temperatures and were analysed by X-ray diffraction. The summary of the diffraction data is shown in Fig. 7. It seems clear that the vaterite from Hatrurim does not change spontaneously to calcite as does aragonite (Wray *et al.*, 1957), but undergoes decarbonation without conversion to another polymorph. No changes in the intensities of vaterite reflections were observed until 500° C; then they became weaker. At 600° C, first reflections of CaO began to appear, becoming more intense on further heating. At 650° no more vaterite reflections are observed and the intensities of the calcite ones remain unchanged. The diffraction data confirm that the broad endothermic peak at about 730° C on the DTA curve corresponds to the dissociation of vaterite.

The stability of vaterite on heating in aqueous solutions was studied in the range of 60° – 110° C. No transformation to another polymorph of $CaCO_3$ was observed after heating at 60° C for a week or after boiling for five hours.

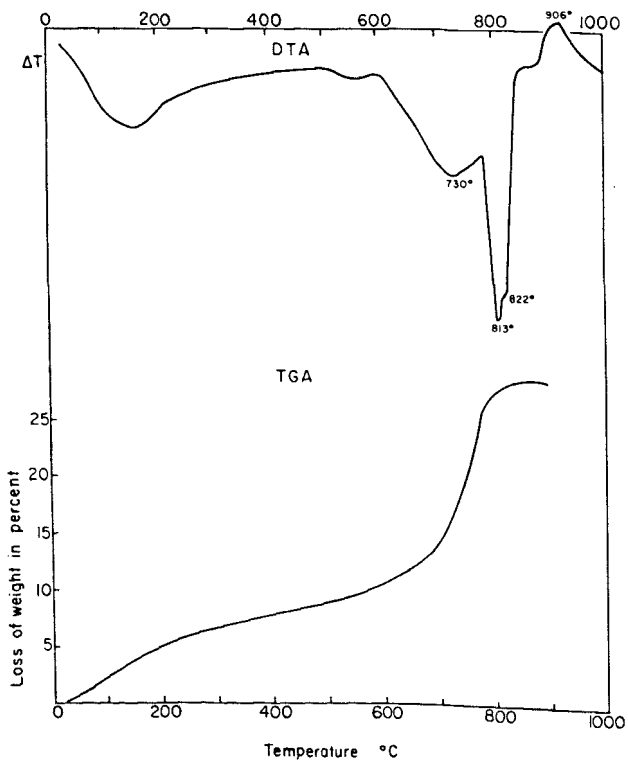

Figure 6. DTA and TGA curves of a vaterite – calcite rock (sample SG 344).

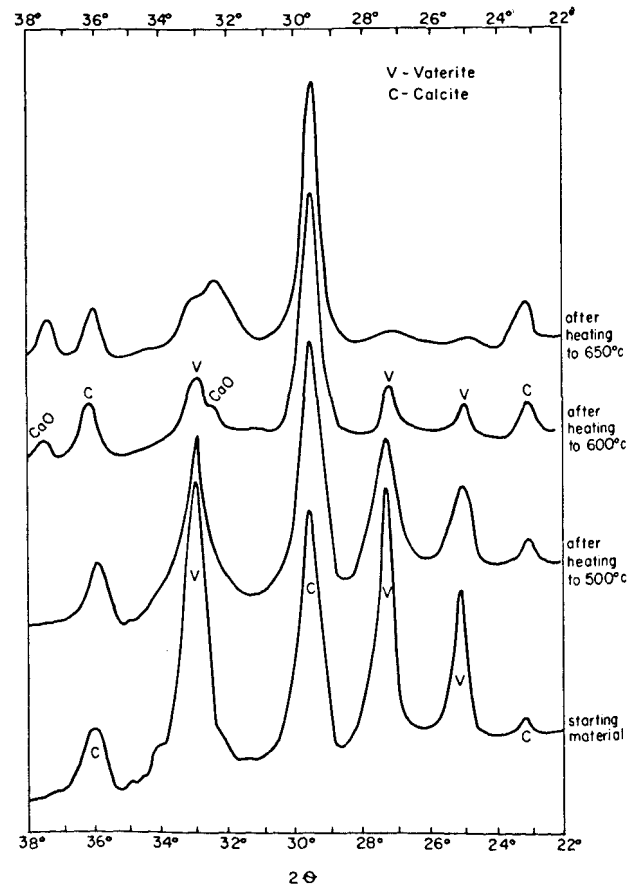

Figure 7. Smoothed tracing of X-ray diffractograms of a vaterite – calcite rock (sample SG 344).

When autoclaved at 110° C (at saturated steam pressure) the vaterite transformed slowly to aragonite. No changes occurred after curing for a day. After a week most of the vaterite had transformed to aragonite: the X-ray diffractogram showed only traces of vaterite, the reflections of aragonite became very intense, and no change in the intensity of calcite reflections was recorded.

Vaterite is considered to be the least stable polymorph of $CaCO_3$. It is known to form at 35° – 60° C (Faivre, 1946). McConnell (1960) suggested that imperfectly crystalline $Ca(OH)_2$ favours the development of vaterite. According to Taylor (1961), the presence of tobermorite minerals seem to favour crystallization of vaterite. The geological occurrences of vaterite seem to support both these suggestions. At Hatrurim it was formed by the hydration of calc-silicate rocks at low temperatures in the presence of atmospheric CO_2. Albright (1971) suggested that the vaterites from Ballycraigy and from Hatrurim are a metastable precipitate from aqueous solutions within the calcite stability field. The better crystallinity and stability of the vaterite from Hatrurim is probably due to impurities which facilitate crystal growth.

Dolomite – $CaMg[CO_3]_2$

Dolomite is a remnant of the parent rocks and occurs as rhombohedral crystals, 30 μ in diameter, stained by iron oxides. Today it is rare. Many pseudomorphs of calcite after dolomite are observed in some rock types, and especially in the lizardite limestone. Rare pseudomorphs of diopside after dolomite are also observed (Plate XIX – 7).

Hydromagnesite – $Mg_5[(OH)|(CO_3)_2]_2 4H_2O$

This mineral occurs as acicular crystals in the weathering crust of a melilite rock from Hatrurim, and in veinlets of a spurrite rock from Nahal Ayalon, associated with brucite, a serpentine mineral, hydrotalcite, and calcite. The elongation is positive, and birefringence nZ – nX = 0.023. The DTA curve (Fig. 3E) shows an endothermic peak at 420° C. It is formed by the weathering of Mg-bearing minerals.

Hydrotalcite – $Mg_6Al_2[(OH)_{16}|CO_3]4H_2O$

This mineral was identified on the basis of its X-ray powder diffraction pattern of a weathered melilite rock and in a sample of spurrite-monticellite rock. (Main spacings: 7.7, 3.9 and 1.97 Å.) The DTA curve (Fig. 3E) shows two endothermic effects, at 292° C and 486° C, corresponding to loss of molecular water and loss of CO_2 and hydroxyl water respectively. The mineral is characteristic of the weathering crust of rocks bearing Mg-minerals.

Calcium-aluminate-tricarbonate-hydrate – $3CaO.Al_2O_3.3CaCO_3.32H_2O$

This compound was mentioned by Jones (1938), and its existence was proven by Buttler (1958). Its X-ray pattern is very similar to that of ettringite and is characterized by an intense line at 9.4 Å. According to Carlson and Berman (1960) the indices of refraction of the synthetic compound, after losing 3 molecules of water on drying over $(MgClO_4)_2$, are: nE=1.456 and nO = 1.48. This mineral appears at Hatrurim in veins cutting calc-silicate-hydrate rocks, and overgrowing in optical continuity ettringite crystals (Plate X – 7). It occurs predominantly as thin films. The mineral is uniaxial, negative, with parallel extinction and negative elongation. The optical sign does not change on heating to 80° C as does that of ettringite. nE = 1.456 ± 0.002, nO = 1.476 ± 0.002, nO – nE = 0.020. It seems plausible that this carbo-aluminate grew directly upon the ettringite crystals after CO_2 entered the calcium aluminate solutions. Further work is needed to confirm identification of this mineral, as most lines of the X-ray pattern are overlapped by the more intense ettringite lines.

VI. SULFATES

Anhydrite – $CaSO_4$

The presence of anhydrite was assumed, on the basis of optical and X-ray data, in one sample only. It is associated with calcite, aragonite, halite, and volkonskoite. The mineral occurs as an aggregate of white prismatic crystals with perfect {001} and {010} cleavages.

Barite – $BaSO_4$

In the Hatrurim area numerous concretions of barite appear, and these were described by Bentor and Vroman (1960). The concretions are distributed in two units of the stratigraphic column, both equivalent to the Taqiye Formation. In the first one they occur in red, low-grade metamorphosed marly rocks. These concretions are rounded, bluish-grey in colour, of radial fibrous or columnar habit and are 1.5–4 cm in diameter. The barites of the second unit occur in porous carbonate-zeolite rocks rich in hydrogarnet, in association with hematite-maghemite nodules and concretions. They are rounded or ellipsoid in shape and up to 8 cm in diameter. Their colour is variable: grey, brown, yellow, reddish and almost black. They consist of granular, interlocking tabular crystals (Plate XI – 4). Some of them have a rim, about 2 mm thick, consisting of radiating columnar crystals. (Plate XI – 1). These concretions have grown into a groundmass containing calcite and clay, which may contain radial zeolites or small granules of garnets. Occasionally calcite has infiltrated along cleavages of barite. In a number of thin sections of marls, polycrystalline aggregates of barite were observed. Plate XI – 2 shows an idiomorphic zoned crystal of barite of about 0.25 x 0.5 mm. Table 12 presents analyses of the two kinds of barite concretions, made after the dissolution of cementing calcite.

The barite concretions are diagenetic. They were formed as colloid segregations in the sediment. While growing, they "captured" the surrounding sediment. During the metamorphic event minerals such as garnet and zeolites developed in the cement.

Table 12. Barite analyses

Oxide	1	2
BaO	64.8	65.0
CaO	0.1	0.1
SO_3	33.7	33.1
Fe_2O_3	neg.	0.8
Al_2O_3	neg.	neg.
SiO_2	1.3	1.4
Total	99.9	100.4

Analyst, M. Gaon.

1. Blue-grey, radial barite concretion. Hatrurim, Sample S.G. 366
2. Brownish-grey, tabular concretion. Hatrurim, Sample S.G. 381

Gypsum – $CaSO_4 .2H_2O$

Bentor and Vroman (1960) describe the appearance of gypsum at Hatrurim as: "microcrystalline, platy, undulatory aggregates; coarse-grained aggregates filling veins or forming rosettes, and also as individual transparent crystals up to 20 cm in size. In certain areas, gypsum is so widespread that the landscape assumes a typical karstic morphology."

Gypsum is a very common secondary mineral, occurring in low concentrations, especially in veins and crusts. In the lowermost part of the sections its distribution increases and in some specimens it composes up to 80% of the sample. Its occurrence may be massive, granular, fibrous, thick tabular, prismatic and acicular, colourless to white, or brown due to iron oxides. Curved acicular yellow aggregates of flower-like growth were observed on walls of exposures. In some gypsum crystals, minute hexagonal inclusions were observed of a mineral with very high birefringence in a uniform optical orientation. The mineral seems to be aragonite.

The gypsum was mostly derived by means of oxidation of FeS_2. This explains the common association of gypsum with iron oxides and hydroxides, in ocher-like gypsum rocks.

Ettringite – $Ca_6[Al(OH)_6]_2(SO_4)_3 . 26H_2O$

The known occurrences of ettringite are: Scawt Hill, N. Ireland (Bannister *et al.*, 1936); Crestmore, California, (Murdoch and Chalmers, 1958; Carpenter, 1963) – where it occurs overgrown by thaumasite; at Ettringen, Germany, the type locality (Lehman, 1874; Hentschel, 1961) associated with portlandite; at Boissejour, France (Grünhagen and Mergoil, 1963), at Franklin, New Jersey (Hurlburt and Baum, 1960) – in the high-temperature zinc deposit.

The mineral is relatively widespread in veins and cavities in the Hatrurim Formation (Bentor *et al.*, 1963; Gross *et al.*, 1967). At Hatrurim it forms thick, banded weathering crusts (up to 10 cm width) on larnite rocks, alternating with bands of prismatic afwillite and occasionally with hydrocalumite. Occasionally it appears as a rock-forming mineral. It forms hexagonal, short to long prisms up to 0.5 mm long, terminated usually by the base and rarely by low pyramids, or as fibrous, sometimes cotton-like aggregates. Plate X – 1, 2 shows SEM photomicrographs of ettringite crystals. The dehydrated and internally collapsed crystal shows striations along the prism axis. The colour varies from colourless to white and yellow of different shades. The yellow coloration is due to the presence of traces of iron and chromium. The incorporation of these ions increases also the birefringence. The crystals are transparent with a vitreous luster. The cleavage is perfect $\parallel \{10\bar{1}0\}$ and the prismatic crystals are striated parallel to the c axis. The fibrous ettringite forms radial aggregates, herringbone structures, or grows perpendicular to vein walls (Plate X – 4, 6). The mineral is uniaxial negative; the extinction is parallel and the elongation negative. Table 13 presents indices of refraction of several ettringite crystals, and their Cr and Fe content by atomic absorption.

An interesting phenomenon was observed when apparently single crystals were studied in immersion liquids: Each individual was composed of a gypsum crystal overgrown by ettringite. Single crystal oscillation and rotation photographs showed that the hexagonal c axis of the ettringite is parallel to the c axis of gypsum (Bentor *et al.*, 1963). Overgrowth of a carbo-aluminate on ettringite was also observed (see Page 23). Microchemical qualitative analysis indicates the presence of some Si and CO_2 in most fibrous and in some prismatic varieties.

A wet chemical analysis was made on 0.5 gr of yellow ettringite crystals, separated by handpicking (Table 14).

The composition of the ettringite is:

Table 13. Refractive indices and Cr and Fe content of ettringite

Sample	colour	nO	nE	nO–nE	Cr(p.p.m.)	Fe(p.p.m.)
SG 163	colourless	1.468	1.464	0.004	neg.	neg.
SG 175	yellowish	1.468	1.462	0.006	100	768
SG 173	yellow	1.470	1.458	0.012	1300	neg.
SG 233	yellow	1.470	1.456	0.014	965	124
SG 464	canary yellow	1.474	1.460	0.014	2080	914

Analyst, S. Ehrlich.

Table 14. Chemical analysis of ettringite.

Oxide	Wt. %	Oxide	ppm
CaO	27.4		
Al_2O_3	8.4	MgO	41
SO_3	16.2	SrO	246
Fe_2O_3	0.1	K_2O	neg.
SiO_2	0.4	Na_2O	300
Cr_2O_3	0.1		
CO_2*	0.8		
H_2O ±	45.1		
Total	98.5		

Analyst, M. Gaon.

* No calcite was detected in the X-ray pattern of this sample. Hatrurim Sample SG. 233.

$5.98CaO.Al_2O_3 . (2.49SO_3 .0.22CO_2 .0.07SiO_2)$ $30.56\ H_2O$. In Fig. 8, DTA and TGA curves of ettringite are presented. The DTA curve is characterized by an endothermic peak with a maximum at 170°. Different authors have reported peak temperatures for synthetic ettringite ranging from 110° to 150° C. The small subsidiary peak at 280° C is probably due to loss of the two hydroxyls bound to Al. According to Kalousek *et al.* (1949), two molecules of water remain at the temperature of glowing iron. The small endothermic peak at 770° C is due to decarbonation. TGA shows that the mineral loses about 20 molecules of H_2O below 120° C. Above this temperature the dehydration is much slower. At 200° C, $6H_2O$ are still left. The products of dehydration at 900° C are anhydrite and mayenite.

The ettringite was formed by hydration of calcium aluminates, especially of mayenite, at normal temperatures in the presence of gypsum or sulfate ions. Ettringite was experimentally synthesized by the author under similar conditions.

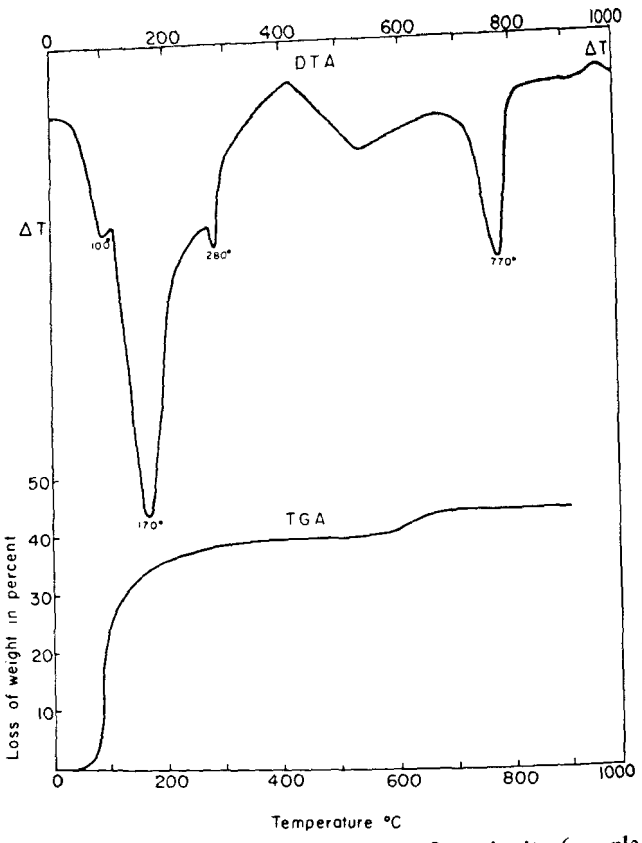

Figure 8. DTA and TGA curves of ettringite (sample SG 233).

VII. CHROMATES

Chromatite – $CaCrO_4$

This mineral was first identified in nature by Eckhardt and Heimbach (1963) in a specimen from Ma'aleh Adumim, on the Jerusalem-Jericho road, and it is also found in the Hatrurim area. It is a rare mineral occuring in crusts, veins, cavities and fissures in marls, calcareous and calc-silicate rocks. It is associated with calcite, aragonite, vaterite, portlandite, and gypsum. Idiomorphic crystals of chromatite are up to 100 μ in diameter. The bigger crystals were found on gypsum and portlandite. The mineral crystallizes in the form of tetragonal prisms with pyramids and dipyramids, as shown in Fig. 9, Plate XI – 6. The faces are striated. The mineral is bright yellow, transparent, and has a vitreous luster. Prismatic cleavage is rather

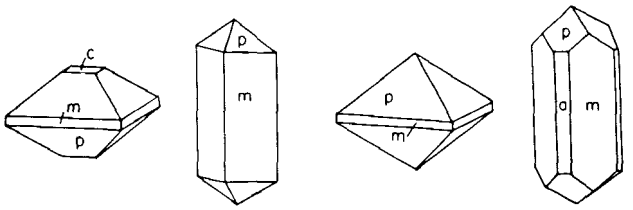

Figure 9. Idealized morphology of chromatite.

poor. Anhedral grains observed in thin section are yellow, non-pleochroic, with strong dispersion. The mineral is uniaxial positive or biaxial with 2V nearly zero; n > 1.80; nE – nO = 0.030. The X-ray powder photographs closely resemble those of the synthetic material. The mineral is easily soluble in water and gives a yellow solution. After heating in a closed tube, it turns emerald-green. Chemical analysis performed on single crystals separated by hand picking gave the following results: CaO – 32.0, MgO – 0.3, CrO_3 – 62.0, K_2O – 0.7, Na_2O – 3.6, Cl – n.d, total – 98.6%. K and Na were determined by flame photometry, Ca, Cr, Mg by atomic absorption. Na and K substitute for Ca, and the sodium may occur partly in the form of NaCl. Chromatite is found in weathering crusts and its preservation is possible because of the dryness of the region. According to Heimbach (1965) the source of Cr is the phosphorites. (According to Foa (1958), the phosphate rocks in the Negev contain about 0.015 – 0.05% Cr). The Cr^{3+} is presumably oxidized in an alkaline environment to Cr^{6+}, it ascends with solutions and then precipitates as chromatite.

VIII. PHOSPHATES AND VANADATES

Fluorapatite – $Ca_5[F|(PO_4)_3]$

Fluorapatite occurs as an ubiquitous mineral in the metamorphosed phosphorites, or as an accessory mineral in other metamorphic rocks. The crystals are equant, rounded, prismatic or acicular. The colour is grey-blue, cornflower-blue or greenish-blue. The crystals are usually very small, 10 – 50 μ in average. Only in one specimen (of a larnite rock) were grains up to 0.1 mm observed. The mineral was formed by natural calcination and often recrystallization of francolite. A SEM photomicrograph of a metamorphosed phosphorite is given on Plate XI – 7.

Francolite – $Ca_5[(F, OH)(PO_4, CO_3)_3]$

Francolite occurs as the main constituent of phosphorites and as a minor one in most rocks of the formation. Colourless to brownish in thin section. Occurs as rounded, isotropic ovulites, and anisotropic bone fragments.

Wilkeite – $Ca_5[(F, O)(PO_4, SiO_4, SO_4)_3]$

Wilkeite was identified on the basis of X-ray powder data. It occurs only in some specimens of larnite and larnite-gehlenite rocks. It is greenish or yellow in colour. n = 1.638. A curious occurrence of this mineral, as small yellow granules about 10 μ across, was observed in a sample probably derived by alteration of a metamorphic rock and consisting now predominantly of gypsum with some cristobalite.

Meta-autunite – $Ca[(UO_2)(PO_4)]_2 \cdot 2\text{-}6H_2O$

The mineral was found in a single sample as an efflorescence on a freshly exposed phosphatic chalk at Ma'aleh Adumim. It occurs as scaly aggregates of sulfur-yellow colour with perfect {001} cleavage. The mineral is biaxial, negative with a small 2V, r > v rather strong. The interference colour on (001) is an anomalous bluish-grey. nY = 1.644 ± 0.002. The index of refraction is higher than the indices reported by Leo (1960) for meta-autunite from Mt. Spokane which are: n = 1.620 – 1.635. The difference may be caused by different water content (The indices of refraction usually increase with decreasing water content.) The X-ray diffraction data are identical with those of

ASTM card 14–73, corresponding to meta-autunite II. The fluorescence under ultraviolet light is a weak yellowish-green.

Meta-autunite II is an orthorhombic phase with 0 – 6 H_2O, which is obtained by heating autunite to 80° C. This process is irreversible (Beintema, 1938). As the mineral was found in a very dry environment subjected to strong insolation, it is possible that it was converted to the II form.

Meta-tyuyamunite – $Ca[(UO_2)(VO_4)]_2\,3–5H_2O$

The mineral tyuyamunite was found at Tyuya-Muyun, Fergana, in Turkestan (Chirvinski, 1925). Meta-tyuyamunite is the less hydrous form. It is found in Israel in minor amounts in most deposits of phosphorites. It occurs at Hatrurim and in the Bethlehem area as an efflorescence on or in veinlets in phosphatic chalks, marls, and phosphorites, and is more common than meta-autunite. Occurs as aggregates of laths or "micaceous" crystals usually about 100 μ in diameter. The six-sided thin plates are elongated [100]. Cleavage {001} is perfect. The colour varies from canary-yellow to greenish-yellow. The optical properties of the mineral are: biaxial, negative, 2V ~ 45°, $r < v$ strong. Y = b, Z = a. It is faintly pleochroic in thicker tablets, with X = nearly colourless and Y, Z = yellow. Qualitative spectrographic analysis by S. Held shows, apart from the major elements, the presence of traces of sodium and potassium (Na > K). Meta-tyuyamunite is formed by dehydration of tyuyamunite (Stern *et al.*, 1956). The X-ray pattern is in good agreement with ASTM card 8–287.

Meta-tyuyamunite and meta-autunite are secondary minerals, probably recent, and are formed by ascending solutions which mobilized uranium, vanadium, and phosphate from the underlying phosphorite beds. The average uranium content of these phosphorites is about 100 ppm and the vanadium content about 60 ppm (Gross, unpublished data).

IX. SILICATES

a. Nesosilicates

Monticellite – $CaMg[SiO_4]$

Monticellite is a typical mineral of contact metamorphism. It is found at Crestmore (Moehlman *et al.*, 1934), in San Bernardino County, California (Schaller, 1935); Skye, Scotland (Tilley, 1951), and in many other localities. It occurs in several samples of spurrite and gehlenite-larnite rocks, mostly as an accessory mineral Only in two samples of a spurrite-calcite rock in contact with a lizardite limestone, does its content rise to about 10%. The mineral is associated with spurrite, melilite, larnite, brownmillerite, rankinite, and calcite. It occurs mostly as anhedral grains up to 20 μ across. Prismatic crystals are rare. The mineral is colourless in thin sections and is not stained by alizarin. The optical properties are: positive elongation, biaxial, negative, with 2V ~ 90°, nY = 1.640 ± 0.002, nZ – nX = 0.010. In polished sections monticellite turns brown by etching with 5% HF. The monticellite of Hatrurim was formed by thermal metamorphism of dolomitic marly limestones. Alteration of monticellite to lizardite is observed.

Merwinite – $Ca_3Mg[SiO_4]_2$

The mineral was identified by X-ray diffraction in a melilite rock, associated with melilite, larnite, spinel and andradite. Microscopic investigation of the heavy fraction reveals rounded grains with a mean index of refraction higher than 1.700. The mineral is biaxial, positive, with a large 2V. The birefringence is very low. Merwinite is characteristic of high-temperature metamorphism.

Dicalcium-silicates

Dicalcium-silicates have been recognized as constituents of Portland cement for almost a

century. Numerous investigations have been made of the polymorphism of dicalcium-silicate. The phase equilibrium studies reveal the existence of three stable forms, $\alpha-$, $\beta-$, and $\gamma-$ (Rankin and Wright, 1915). Bredig (1943) predicted the form α' and Trömel (1949) confirmed later the existence of this polymorph by X-ray diffraction. Toropov *et al.* (1957) suggested the presence of the β' phase. The presently accepted picture of thermal transformation of the dicalcium-silicates is that of Bredig (1950), and was revised by Nurse (1954), Roy (1958), Smith *et al.* (1961). The inversion sequences determined by Trömel (1949) and Nurse (1954) are presented in Fig. 10.

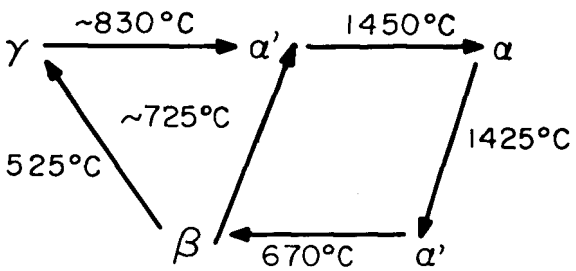

Figure 10. Inversion sequences of the dicalcium silicates.

At low temperatures the phases α, α' and β are stable only in the presence of stabilizers, such as P_2O_5, V_2O_5, BaO, Cr_2O_3, and Mn_2O_3. According to Nurse (1954), the major part of the P_2O_5 of the clinker is combined in solid solution within the dicalcium-silicate. This problem was briefly studied by Bredig (1943), Barret *et al.* (1942), Trömel *et al.* (1948), Nurse *et al.* (1959), and others. Nurse published a phase diagram showing a series of solid solutions between the α polymorph and a new high-temperature modification of the tricalcium phosphate, isomorphous with the α-disilicate. About 16% P_2O_5 can enter the dicalcium-silicate, $(PO_4)^{3-}$ substituting for $(SiO_4)^{2-}$ groups. The indices of refraction decrease with increasing P_2O_5 – content. The β form is known to occur in nature as the mineral larnite and the α' as bredigite. In the Hatrurim Formation the polymorphs – $\alpha-$, α' and β – are present. The predominant is the β form – larnite. In some specimens more than one modification occur together. Some crystals are composed of two phases as intergrowth of parallel lamellae of submicroscopic size.

The α modification occurs only in the lowermost part of the stratigraphic column at Hatrurim, corresponding to the Ghareb Formation. The β and α' polymorphs occur at Hatrurim and Ma'aleh Adumim in the lower part of the section, equivalent to the Ghareb Formation, and at Hatrurim they appear additionally in rocks equivalent to the Taqiye Formation.

Analyses of dicalcium-silicates from Hatrurim, obtained by electron probe analysis, are give in Table 15. They were carried out by P. Terrier, H. Hornain, and G. Socroun (1968) at the

Table 15. Electron microprobe analyses of dicalcium silicates.

Oxide	1	2	3
CaO	62.06	62.32	64.31
SiO_2	27.88	30.45	32.12
Al_2O_3	0.03	0.04	0.02
Fe_2O_3	0.02	0.02	0.02
MgO	0.05	0.05	neg.
SO_3	0.12	0.06	0.25
P_2O_5	8.27	4.63	2.67
Cr_2O_3	0.03	0.01	0.01
K_2O	0.84	1.16	0.19
Na_2O	0.82	0.68	0.77
MgO	0.03	0.02	0.02
Total	100.15	99.44	100.38

1. Nagelschmidtite, melilite-nagelschmidtite rock. Hatrurim.
2. Bredigite, gehlenite rock. Hatrurim.
3. Larnite, larnite-mayenite-brownmillerite rock. Hatrurim.

mineralogical laboratory of C.E.R.I.L.H. (France) on a CAMECA instrument.*

The minerals of this group are typical of the high-temperature sanidinite facies. Dicalcium-silicate is an initial product of solid-state reactions between lime and silica. The β form was obtained experimentally by heating normal Ghareb and Taqiye rocks in the temperature range of 450° – 650° C for a period of 30 days. The heating was performed in an open system.

Larnite–β-$Ca_2[SiO_4]$ – Monoclinic

The first natural occurrence of larnite was described by Tilley (1929). The larnite in the Hatrurim Formation is a rock-forming mineral. It occurs in three parageneses:

1. with brownmillerite and mayenite, composing about 15%– 80% of the rock;
2. with melilite – its content is about 20%;
3. with spurrite – in this paragenesis, which is rare, it is an accessory mineral.

The mineral occurs as rounded grains or tablets of 15 to 30 μ average size. Fairly large crystals up to 100 μ across are rare. Small, rounded microscopic inclusions in brownmillerite and rankinite grains were also observed. It is almost always polysynthetically twinned after (100) (Plate XII – 3). A SEM photomicrograph of twins is shown in Plate XII – 5. In thin section the mineral appears colourless or greyish. Extinction $X\Lambda c = 13° - 14°$. The mineral is biaxial, positive with $2V \sim 60°$. Dispersion $r < v$ weak. $nX = 1.700 - 1.705$, $nY = 1.715$, $nZ = 1.725 - 1.730$, $nZ - nX = 0.025$. In reflected light the mineral is grey. After etching of a polished specimen by alcoholic 0.25% HNO_3 it shows well-developed parallel or cross-hatched striations (Plate XIII – 3, 5). After exposure of the polished surface to vapour of 40% HF for 10 – 20 sec., the mineral turns blue and after a longer exposure the colour changes to red. The X-ray powder data are identical with those of ASTM 9–351. Scanning pictures presented in Plates II, IV, and XV show clearly the presence only of Ca and Si. The formula of larnite calculated from analysis 3 in Table 15 gives: $(Ca_{1.98}Na_{0.04})Si_{0.92}P_{0.07})O_4$. Larnite has hydraulic properties. In experiments on the hydration of larnite rocks at room temperature, performed by the present author, tobermorite minerals were the main products and tobermorites, afwillite, and gyrolite by autoclaving at 110° C.

Bredigite–α'-$Ca_2[SiO_4]$–(orthorhombic)

This is a very rare mineral, first recorded in nature at Scawt Hill, N. Ireland, by Tilley *et al.* (1948). It is also found at Muck, Scotland (Tilley *et al.*, 1948) and at Marble Canyon (Bridge, 1966). It was reported in cement clinker by Metzger (1953). According to Metzger (1953), the presence of K_2O and rapid cooling are good conditions for bredigite formation. It is typical of the contact metamorphism of limestones (Zharikov *et al.*, 1969). According to Smith *et al.* (1961), this mineral is formed slowly in the temperature range 725° – 860° C and converts on cooling to larnite. It occurs mainly in the "pseudo-conglomerate", associated with rankinite, melilite, perovskite and andradite, usually as irregular crystals up to 100 μ across. Some crystals show polysynthetic twins, sometimes only in one part of the crystal, the remaining part being untwinned (Plate XII – 4). In thin section the mineral is colourless. The two cleavages intersect at 60°. The mineral is biaxial, positive, 2V=20°– 30°, $r < v$, weak, nX=1.695, $nZ = 1.705$ (all ± 0.002). The main reflections in the diffraction pattern are: 2.73 Å, 2.66 Å and 261 Å. The formula of the bredigite calculated on the basis of data given in Table 15, is: $(Ca_{1.92}Na_{0.04}K_{0.04})(Si_{0.88}P_{0.11})O_4$.

According to the results of hydration experiments, performed by the author at temperatures ranging from 25° C to 110° C, the mineral

* The author takes this opportunity to thank them for the performance of the analyses.

hydrates slower than larnite.

Nagelschmidtite – α-$Ca_2[SiO_4]$–$Ca_{1.5}(PO_4)$–hexagonal

Name is taken from the synthetic compound, first reported in slags, by Nagelschmidt (1937) and Segnit (1950). This is the first record of the mineral in nature. It occurs in the lowermost part of the stratigraphic section of Hatrurim and forms up to 30% of the rock. It is found in close association with gehlenite, rankinite, perovskite, Ti-andradite, and magnetite. The crystals are anhedral. The average size is 50 μ, and the largest are up to 150 μ. In thin section the mineral shows a complex set of lamellae intersecting at angles close to 60° (Plate XII – 1, 2). It is usually uniaxial positive and rarely biaxial positive, with 2V nearly zero. Two phases were distinguished:

1. A colourless phase, which is clear and transparent. The refractive indices are: nX = 1.680, nZ = 1.698; nZ – nX = 0.018. (all ± 0.002). The main reflections in the X-ray pattern are: 2.66 (vs), 2.80 (s), 1.94 (m).

2. A cloudy phase (the most common one) – tends to be slightly brown or yellow and turbid. The indices of refraction are: nX = 1.638, nZ = 1.652; nZ – nX = 0.014. The cloudiness of the phase changes from sample to sample. In the most clouded ones it is impossible to obtain an interference figure. In some specimens the birefringence of the adjacent lamellae differ, the narrow ones having a higher index of refraction and an oblique extinction at about 20°. When a polished section was etched by dilute HNO_3, one set of striation was attacked more than the other. When heated to 1000° C and examined in immersion liquids, the cloudy phase retained the intersecting lamellar texture but turned clear and its birefringence increased. A SEM photomicrograph of such a crystal is shown in Plate XII – 6, 7. A single crystal from this phase was removed from thin section and X-rayed.

Table 16. **Nagelschmidtite; diffraction data for the cloudy phase**

d(meas) Å	I	phase
3.45	m	α
3.08	vw (diffused)	β
2.83	vs	α
2.76	m	β
2.29	w	α, β
1.94	m	α
1.84	m (diffused)	α, β

The X-ray data show that the cloudy phase consists of an intergrowth of two types of lamellae: the dominant one is the α–polymorph, the rarer is the β–modification, both arranged in parallel crystallographic orientation. The cloudiness must be related to the fact that during cooling the β modification cannot take as much P_2O_5 in solid solution as does the higher-temperature modification. An attempt was made to test the distribution of P by electron probe scanning. The distribution of this element seems to be homogeneous, but this may seem because the dimensions of the lamellae are too small to be resolved by the probe. The composition of the nagelschmidtite calculated from analysis 1 in Table 15 is as follows: $(Ca_{1.89}Na_{0.03}K_{0.03})(Si_{0.79}P_{0.20})O_4$. Inhydration experiments performed at room temperature and by autoclaving at 110° C, this form does not seem to undergo hydration.

The Garnet Group

The garnets are the most important accessory constituent and appear in nearly every sample examined. The group is subdivided into species representing the end members of the isomorphous series. Names are given according to the

dominant molecular type. Identifications are based on X-ray and optical data and partly on chemical analyses.

Grossular – $Ca_3Al_2[SiO_4]_3$

The occurrence of grossular in veins associated with glauconite is reported by Bentor and Vroman (1960). The mineral occurs mostly in calcite-zeolite rocks associated with diopside, and in anorthite-diopside and anorthite-diopside-wollastonite fels. This garnet occurs mostly as anhedral rounded grains (Plate XIV – 7) and less frequently as idiomorphic crystals (Plate XIV – 4, 9). Average crystal size ranges from 7 to 15 μ. Often they are clouded in the centre and surrounded by a thin shell of hydrogarnet (Plate XIV – 1). Sometimes one single rim envelops a group of grossular grains. Grape-like groups are also common. The colour of grossular is determined largely by the amount of iron present. The most common colour in thin sections is yellowish-green of various shades, a brownish-red variety is less common. Crystals surrounding inclusions of hematite and maghemite are larger, of dodecahedral habit, clear, and up to 100 μ across. The colour is more intense and they may be zoned. The grossular is isotropic with index of refraction ranging from 1.732 to 1.772. The cell edge a_0 varies from 11.90 to 11.95 Å. A chemical analysis of grossular is given in Table 18, analysis 1. Grossular is characteristic of thermally metamorphosed calcareous shales and marls.

Andradite – $Ca_3(Fe^{3+}, Ti)_2[SiO_4]_2$

The andradite appears in a few samples of zeolite-calcite rocks and in melilite rocks. It is the least common garnet in the rocks equivalent to the lower part of the Ghareb Formation near the flank of the syncline. In zeolite-calcite rocks it forms the nuclei of hydrogarnets. In melilite rocks it occurs usually as subhedral grains, as irregular rims about earlier minerals, or as interstitial irregular patches (Plate XVII – 2). The colour varies from brown to yellowish-brown and reddish-brown. The large crystals are up to 100 μ across. Isotropic, n = 1.800 ± 0.005. a_0 = 12.0 Å. A chemical analysis of andradite is given in Table 18, analysis 2. Apart from the normal andradite, the Ti-variety (schorlomite) is observed in two parageneses:

1. melilite, nagelschmidtite ± rankinite and perovskite;
2. gehlenite, pseudowollastonite ± rankinite and larnite.

This variety forms curious interfingering textures (Plate XIV — 5, 6), with irregular borders or rings surrounding square gehlenite grains. The cell edge varies from a_0 = 12.06 to 12.15 Å. Huckenholtz (1969) synthesized Ti-andradites between 1000° – 1400° C at 1 atm. pressure. The cell parameters of the synthetic andradites increase at a rate of 0.038 ± 0.002 Å per 10 Wt% TiO_2 in solid solution. This finding is in good agreement with data from chemical analyses of the Ti-andradites from Hatrurim, Table 18, analyses 4 and 5.

The Ti-andradite, as shown by its parageneses, is formed in intensively metamorphosed rocks of the sanidinite facies, at temperatures probably up to about 1100° C. The interfingering textures may be due to incipient melting of the Fe-Ti-rich liquid.

The normal andradite and the Ti-rich variety seem to be the last phase to crystallize.

Hydrogarnet – $Ca_3Al_2(OH)_{12}$ – $Ca_3Al_2[SiO_4]_3$

(Synonyms: hibschite, plazolite, hydrogrossular, hydrougrandite).

The first hydrogarnet (hibschite) was found by Cornu (1906) at Marianska Hora (Czechoslovakia) and was reexamined by Pabst (1942). The next was described as plazolite from Crestmore, California, by Foshag (1920a). Belyankin and Petrov (1939, 1941 a, b, c) described a hibschite from Nikorzminda (Caucasus). Hutton (1943) describes a hydrogrossular from Roding River (New Zealand), where it occurs as a constituent

of rodingites. Later hydrogrossular was described from Ayrshire, England (Bloxam, 1964), at Tokatoka, New Zealand (Mason, 1957), the Bushveld Complex, South Africa (Frankel, 1959), Ukraine, U.S.S.R. (Nalivkina ,1969), and Hsiaosungshan, China, (Tsao Yung Lung, 1964). In all these occurrences the hydrogarnets occur in contact metamorphic rocks, or as hydrothermal alteration of volcanic rocks. A comprehensive review on hydrogarnets has been given by Žabinski (1966).

Between grossular and the cubic $Ca_3Al_2(OH)_{12}$ exists a complete series of solid solution which were synthesized by Flint *et al.*, (1941). The term hydrogarnet is applied to define garnets in the crystal lattice in which hydroxyl groups substitute for $(SiO_4)^{4-}$ in the form of $[(OH)_4]^{4-}$ groups. The characteristic feature of the hydrogarnets is an increase in the size of their unit cell with an increasing content of hydroxyl groups. The lattice parameter increases from 11.85 for grossular to 12.56 Å for $Ca_3Al_2(OH)_{12}$. The substitution of Al by Fe^{3+} in the hydrogarnet also enlarges the unit cell which, in the case of complete substitution, is expressed by the magnitude of about 0.18 Å (Flint *et al.*, 1941). Zur Strassen (1958) concluded that it is impossible to replace all the Al by Fe, as a point is reached when the structure starts to be unstable. The hypothesis of McConnell (1942) on the possibility of substituting SiO_4 in garnets by $(OH)_4$ groups was confirmed by Cohen-Addad *et al.* (1963) by neutron diffraction and magnetic resonance. No members of the hydrogarnet series richer in the $Ca_3Al_2(OH)_{12}$ molecule than the hydrogarnet from Tokatoka, New Zealand, with a unit cell a_o = 12.24 Å (Mason, 1957), indicating a composition of approximately $Ca_3Al_2(SiO_4)(OH)_8$, had yet been encountered until now in nature. The compound $Ca_3Al_2(OH)_{12}$ is known as one of the phases of cement hydration.

Hydrogarnets with unit cells up to 12.2 Å occur in the Mottled Zone in the zeolite-calcite rocks and in low-grade metamorphosed marls. Hydrogarnets richer in water, including the end member $Ca_3Al_2(OH)_{12}$, occur in calc-silicate-hydrate rocks such as the tobermorite, jennite, and afwillite types, and in weathered spurrite and larnite rocks. They are usually associated with calcite, aragonite, vaterite, portlandite, ettringite, and calcium-aluminate-hydrates. In thin section the hydrogarnets are mostly colorless but some are yellowish and orange-reddish due to the presence of Fe and Ti. The hydrogarnets usually occur as anhedral individuals and sometimes in the form of octahedrons. Size ranges from 7 to 20 μ. The colourless crystals of hydrogarnet often contain a greenish nucleus of a garnet of the grossular-andradite series, or a less hydrous hydrogarnet with a smaller unit cell.

The thickness of the hydrogarnet shell does not exceed 3 μ. (Plate XIV – 1). The hydrogarnets appear also in the matrix and form undulatory thin veinlets (Plate XIV – 3). Some hydrogarnets are of submicroscopic size and could not be distinguished in thin sections. They were identified only by X-ray examination of residues insoluble in cold 5% acetic acid.

The refractive indices determined by the immersion method vary over a wide range: n = 1.618 – 1.735 according to the iron and water content.

In Table 17 the interplanar spacings of Hatrurim hydrogarnets are presented. As can be seen from this table the range of the unit cell varies within a very broad range from 11.92 Å to 12.56 Å, values much higher than reported before anywhere in nature. Analysis of a hydrogarnet from Hatrurim is presented in Table 18 (analysis 3). For comparison, analyses of two other hydrogarnets are given in columns 6 and 7

The DTA data on the cubic modification of $Ca_3Al_2(OH)_{12}$ are reported by Kalousek and Adams (1951), Majumdar and Roy (1956). In their studies two endothermic effects, one at 350° C and the other at 510° C, were observed.

Table 17. X-ray diffraction data for garnets and hydrogarnets

Mineral	Grossular		Grossular		Andradite		Schorlomite		Hydrogarnets														3CaO.Al_2O_3.$6H_2O$	
Sample	SG 495		SG 550		SG 314		SG 280		SG 547		SG 530		SG 253		SG 299		SG 514		SG 459		BT 5931		SG 460		SG 167		SG 452		SG 451	
a (Å)	11.85		11.89		12.00		12.06		11.92		12.01		12.12		12.17		12.20		12.25		12.30		12.33		12.38		12.42		12.56	
hkl	I	d(Å)	I	d(Å)	I	d(Å)	I	d(Å)	I	d(Å)	I	d(Å)	I	d(Å)	I	d(Å)	I	d(Å)	I	d(Å)	I	d(Å)	I	d(Å)	I	d(Å)	I	d(Å)	I	d(Å)
211			1	4.89	2	4.90			2	4.91	2	4.92	2	4.94	5	4.95	3	4.98	3	5.03	4	5.04	3	5.06	4	5.09	4	5.12	10	5.18
220			1	4.31	1	4.25	2	4.25					1	4.28	3	4.29	2	4.33	3	4.34	3	4.35	2	4.36	4	4.39	4	4.41	5	4.47
321									1	3.29			1	3.23	2	3.24	2.	3.26	2	3.27	3	3.29	2	3.30	2	3.31	5	3.32		
400	5	2.96	5	2.98	8	3.00	8	3.02	5	2.995	7	3.02	6	3.03	7	3.04	7	3.06	7	3.07	5	3.08	5	3.08	5	3.09	7	3.11		
420	10	2.65	10	2.66	10	2.68	10	2.70	10	2.67	10	2.69	10	2.71	10	2.72	10	2.73	10	2.74	10	2.75	10	2.76	10	2.77	10	2.78	10	2.81
332	2	2.52	2	2.54	4	2.56	2	2.58	2	2.55	4	2.56	1	2.59	2	2.60	1	2.60	1	2.61	1	2.63	1	2.63	1	2.64	1	2.67		
422	2	2.42	3	2.43	6	2.45	5	2.46	3	2.44	6	2.45	2	2.48	3	2.48	3	2.49	6	2.50	4	2.51	4	2.51	2	2.53	2	2.54	3	2.56
431,510	1	2.32	3	2.33	5	2.35	4	2.36	3	2.34	3	2.36	2	2.38	3	2.39	2	2.41	2	2.40	3	2.41	2	2.42	1.	2.42	2	2.43	3	2.47
521	1	2.16	3	2.17	6	2.19	4	2.20	4	2.18	3	2.19	5	2.21	5	2.22	4	2.24	5	2.24	5	2.25	5	2.25	6	2.25	4	2.26	10	2.30
440	1	2.09	1	2.10	2	2.10	2	2.12	1	2.12							1	2.16	1	2.17	1	2.18								
532,611	4	1.92	5	1.93	7	1.95	5	1.96	5	1.94	5	1.95	6	1.97	5	1.98	4	1.99	4	1.98	5	2.00	5	2.00	5	2.02	6	2.02	5	2.04
620	2	1.88	3	1.87	2	1.89	3	1.91	2	1.88	2	1.89	1	1.93			1	1.94	1	1.94	1	1.95	1	1.96			1	1.97		
541			1	1.82															1	1.89	1	1.88								
631			1	1.76					1	1.76									1	1.82	1	1.83	1	1.83			1	1.83		
444	2	1.71	4	1.71	6	1.73	3	1.74	2	1.72	4	1.73	1	1.76	1	1.76	1	1.77	1	1.78	1	1.78	1	1.73	2	1.79	1	1.79		
640	3	1.64	6	1.65	5	1.66	6	1.68	6	1.65	6	1.67	3	1.68	3	1.69	3	1.70	4	1.697	3	1.71	3	1.71	3	1.71	3	1.72		
552																			1	1.67	1	1.68					1	1.69		
642	4	1.58	8	1.585	8	1.604	8	1.62	5	1.614	6	1.61	4	1.62	4	1.63	7	1.64	5	1.635	5	1.64	5	1.643	5	1.651	4	1.663		
651,732																	1		1	1.563	1	1.56		1.566			1	1.552		
800	2	1.48	3	1.486	6	1.501	4	1.507	2	1.503	2	1.50	3	1.51	2	1.52	1.	1.53	2	1.531										
840					6	1.344							2	1.355					1	1.367	1	1.379	1	1.374						
n	1.725		1.765		1.780		>1.80		1.735				1.704								1.710				1.632					

Table 18. Analyses of garnets and hydrogarnets.

Oxide	1	2	3	4	5	6	7
SiO_2	37.61	34.37	32.95	22.53	27.71	34.01	34.48
Al_2O_3	17.84	8.80	17.78	2.38	2.55	8.45	19.87
Fe_2O_3	7.98	17.08	6.78	25.61	26.11	18.28	0.61
FeO		0.17				1.72	0.85
TiO_2	0.82	2.27	0.86	14.91	11.06	0.12	0.03
CaO	31.03	33.37	35.42	32.79	31.22	21.47	37.40
MgO	1.44	0.75	1.25	0.22	0.20	9.96	2.07
MnO		0.04				0.12	0.02
K_2O	0.16	0.07	0.35			0.10	0.01
Na_2O	0.14	0.08	0.27			0.30	0.02
Cr_2O_3	0.03	0.40	–			0.20	
H_2O+	0.66	2.58	4.55			5.29	4.65
H_2O-	2.12	–				0.18	0.23
Total	99.83	99.98	100.21	98.44	98.85	100.20	100.24
			Number of cations on the basis of 12 oxygens				
Ca	2.58	2.80	2.82	3.10	2.88		
Mg	0.17	0.09	0.14	0.03	0.03		
K	0.02	0.01	0.03				
Na	0.02	0.01	0.04				
Fe^{2+}		0.01					
Fe^{3+}	0.47	1.01	0.38	1.70	1.68		
Al	1.63	0.81	1.55	0.24	0.26		
Cr^{3+}		0.02					
Ti	0.05	0.13	0.05	0.99	0.71		
Si	2.98	2.69	2.45	1.99	2.38		
OH/4	0.09	0.34	0.56				
n	1.765	1.780	1.710	>1.800	>1.800		
a_o	11.89A	12.00A	12.30A	12.06A	12.06A		

1. Grossular, Hatrurim. Sample SG. 550. 2. Andradite, Hatrurim Sample SG. 314. 3. Hydrogrossular; Hatrurim. Sample BT 5931 4. Schlorlomite, Hatrurim. Sample SG. 268. 5. Schorlomite, Hatrurim. Sample SG. 277. 6. Hydrougrandite from Hsiaosung-Shan China. (Tsao-Yung-Lung, 1964). Contains also Cl-0.08%-P_2O_5 – 0.17% 7. Hydrogrossular from Champion Creek, New Zealand. (Hutton, 1943).
Analyses 1–3, gravimetric analyses by M. Gaon, Analyses 4–5, microprobe analyses by S. Gross.

Two-step loss of "hydroxyl water" is observed also on the DTA curves of the Hatrurim hydrogarnets. On Fig. 4B a curve of a hydrogarnet with a_o = 12.33 Å is shown. It shows a distinct endothermic effect at 355° and a smaller one at 485° C. Hydrogarnets with smaller amounts of water show a weak endothermic effect at about 380° – 395° C and a very weak one at about 510° C.

Hydrogarnets containing "nuclei" of another garnet, giving X-ray patterns of two distinct species, were subjected to heating up to 400° C. The dehydration products in all cases were mostly grossular and less frequently andradite.

The shells of hydrogarnets surrounding the anhydrous members point to their formation during retrograde metamorphism in an environment rich in water. The water-rich hydrogarnets occurring in the calc-silicate hydrate rocks were formed by hydration of the anhydrous metamorphic minerals at temperatures that did not exceed 200° – 300° C. A hydrogarnet with a cell edge of a_o = 12.31 Å was obtained by the author by autoclaving larnite-mayenite rocks at 110° C. The end member $Ca_3Al_2(OH)_{12}$ may be formed at lower temperatures, from the metastable hexagonal calcium aluminate hydrates.

Zircon – $Zr[SiO_4]$

Zircon occurs as the main accessory mineral in the sandstone of the Hazeva Formation and in a marl from Kefar Uria rich in detrital minerals. It occurs mostly as rounded grains and rarely as idiomorphic prismatic crystals. Maximum grain size is about 0.1 mm. In some quartz grains inclusions of idiomorphic zircon crystals, about 20 μ large, were observed.

Tricalcium silicate – $Ca_3[O|SiO_4]$

Proposed name: Hatrurite, after the name of the locality.

A Ca_3SiO_5 containing small amounts of foreign ions such as Al, Mg, is known to be the most important constituent of portland cement (known as "alite"). Jeffery (1952) shows that pure Ca_3SiO_5 is triclinic at room temperature, but small amounts of foreign ions in solid solution cause it to become monoclinic or trigonal. The pure tricalcium silicate is stable at room temperature.

The mineral was identified in a specimen of a larnite-brownmillerite-mayenite rock during examination by electron microprobe. It was later found in another sample of a similar rock of the same composition. In thin and polished section the mineral appears as pseudohexagonal crystals about 50 μ in diameter. After etching with water followed by alcoholic HNO_3 its colour is light grey, lighter than that of larnite. When etched by vapours of HF the colour turns a straw yellow. Plate XIII – 5 is a photomicrograph of another specimen of a larnite rock,

etched with 5% HNO_3 in alcohol. The six-sided zoned crystals are probably tricalcium silicate. The zone boundaries are parallel to the crystallographic boundaries of the grains and exhibit varying degrees of etching. In thin sections the mineral is colourless. Elongated prismatic or pseudohexagonal crystals of high refringence and very low birefringence (about 0.006) were observed. The elongation is negative. The mineral is biaxial negative with a small axial angle. Some crystals are cracked. As the major phase of this rock is larnite it is difficult to determine the mineral by its X-ray pattern. Identification can be made only on lines of medium intensity as the strongest lines are overlapped by those of larnite. It is possible to distinguish only the weak lines at 3.03 Å (m), 2.96 (vw), 1.767 (mv), 1.759 (vw), 1.484 (vw), 1.4521 (vw), which do not occur either in larnite or in mayenite and brownmillerite. In Plate XV – 2, 3, line scans across larnite and hatrurite with Si Kα and Ca Kα respectively are given. They show clearly an increasing Ca-concentration and a decrease in Si-concentration in Ca_3SiO_5 in relation to larnite. An analysis of hatrurite by electron microprobe performed on a single grain, using wollastonite as standard, is given in Table 19.

The composition of hatrurite is:

$Ca_{2.97}Al_{0.01}Ti_{0.01}SiO_5$

When the rock specimen was hydrated for half an hour at room temperature, $Ca(OH)_2$ was released. Neither larnite nor brownmillerite are attacked so quickly by water. Hatrurite is related to the high-temperature sanidinite facies.

Spurrite – $Ca_5[CO_3|(SiO_4)_2]$

Spurrite is a mineral typical of contact metamorphism of silica-deficient limestones formed by partial decarbonation at maximal temperatures and very low pressures. Spurrite is a relatively rare mineral. The best known occurrences are: Velardena (Wright, 1908); Crestmore, California (Foshag, 1920b); Scawt Hill, N. Ireland (Tilley 1929); Little Belt Mountains, Montana (Taylor, 1935); Lower Tunguska, Siberia (Sobolev, 1935), Reverdatto (1964, 1965); Camas Mor, Scotland (Tilley, 1947); Christmas Mountains, Texas (Clabaugh 1953); Tokatoka, New Zealand (Mason, 1957); and Kushiro, Japan (Kusachi *et al.*, 1971a). Its occurrence in cements is reported by Amafuji (1964). The first record of spurrite in the Hatrurim Formation was made by the writer in 1961 during investigation of some samples from Nahal Ayalon (Gross *et al.*, 1967). It was later found at Hatrurim (Bentor *et al.*, 1963a, b), and recently at Ma'aleh Adumim.

Table 19. Chemical analysis of tricalcium silicate (hatrurite).

Oxide	Wt.%	Cations per 5 oxygens	
SiO_2	26.1	Si	1.00
CaO	72.8	Ca	2.97
Al_2O_3	0.4	Al	0.01
TiO_2	0.3	Ti	0.01
Fe_2O_3	0.2	Fe^{3+}	0.003
MgO	traces		
Total	99.8		

Microprobe analysis by G. Socroun

Neglecting the later hydrated minerals, there are two groups of assemblages:

1. The most common: calcite-spurrite + brownmillerite, mayenite, and apatite, which is characteristic of the equivalents of the Ghareb Formation and to a lesser extent of the Taqiye Formation.

2. The less common: spurrite ± brownmillerite, mayenite, gehlenite, monticellite, and larnite. This assemblage is more characteristic of the metamorphosed Taqiye Formation.

Spurrite is one of the most abundant rock-forming minerals of the Mottled Zone, forming hard, dense, splintery, brown, red, grey-black, and violet rocks. The mineral appears mostly as a mosaic of minute anhedral crystals 3 to 15 μ across. Better crystallized samples consist of crystals up to 0.25 mm. In this type of rock, spurrite forms up to 80% of the rock. In the calcite-spurrite rocks most spurrite crystals, which reach up to 0.4 mm across, are poikiloblastic. They are idiomorphic to subhedral with pseudohexagonal or prismatic outlines. (Plate XVI – 1). The crystals appear granulated due to intense cracking and often contain droplike inclusions of calcite up to 20 μ across, and minute rounded inclusions of mayenite and prisms of brownmillerite. The mineral has a perfect {001} cleavage and a less pronounced {100} cleavage, the two intersecting at an angle of 79°. There are two sets of simple and polysynthetic twins at an angle of 57° (Plate XVI – 2, 3). The mineral is biaxial negative, 2V ~ 40°, $Y\Lambda c$ = -33° , dispersion r < v. The indices of refraction are: nX = 1.640, nY = 1.674, nZ = 1.678 (all ± 0.002), nZ – nX = 0.038.

The mineral dissolves with effervescence in HCl leaving a gelatin-like substance. In Fig. 11B, C a DTA-curve of a spurrite rock is presented. It shows a single endothermic effect with a maximum ranging from 845° to 990° C. The product of decarbonation is larnite and CaO. A method of semiquantitative determination of spurrite in the presence of calcite was elaborated by the author. The method is based on DTA in conjunction with the determination of CO_2 in the bulk sample (Gross, 1971). When hydrated in the presence of atmospheric CO_2 at room temperature for a period of two years, the spurrite was decomposed and only calcite was recorded by X-ray diffraction. The CO_2 content of the examined sample rises from 7.7% CO_2 to 26.2%. When hydrated at 60° C for a period of a month, aragonite was the main product formed. Analysis of the same sample in a powdered form stored at normal atmospheric humidity shows that CO_2 is absorbed. The content of CO_2 rises to 9.2% after a storage of 5 years and to 13.1% after 8 years.

This same process occurs in nature, but the process is very sluggish because of the density of the rock and the aridity of the environment.

The carbon and oxygen isotopic composition of fresh spurrite rocks and the recarbonated ones is discussed by Kolodny and Gross (1974).

The spurrite of the Hatrurim Formation was formed as a result of thermal metamorphism at elevated temperatures (probably not below 650° – 800° C) and at relatively low CO_2 pressure, in rocks strongly deficient in silica.

Thaumasite – $Ca_6H_4[(SiO_4)_2(CO_3)_2].26H_2O$

Thaumasite is a relatively rare hydrothermal mineral occurring in contact metamorphic rocks and in skarns. It is found only at Hatrurim (Bentor *et al.*, 1963) and is usually associated with calcite, aragonite, and ettringite.

The mineral occurs in veins and cavities of spurrite and afwillite rocks. Monomineralic veins are up to 2 cm wide. The thaumasite oc-

Table 20. Chemical analysis of thaumasite.

Oxide	Wt. %	Cations per 48 oxygens	
CaO	27.38	Ca	5.92
MgO	0.50	Mg	0.16
SiO_2	10.00	Si	2.02
Al_2O_3	0.08	Al	0.002
Fe_2O_3	0.14	Fe^{3+}	0.002
CO_2	6.73	C	1.86
SO_3	12.61	S	1.92
$H_2O\pm$	42.61	H	57.2
Total	100.05		

Hatrurim, Sample SG 262. Analyst M. Gaon.

curs in the form of thin elongated hexagonal prisms or as acicular or cotton-like aggregates. The prism faces are striated. The mineral is colourless or white and transparent. The luster is vitreous or silky. The mineral is uniaxial negative with negative elongation and parallel extinction. nE = 1.466 – 1.468, nO = 1.504, nO – nE = 0.036 – 0.038.

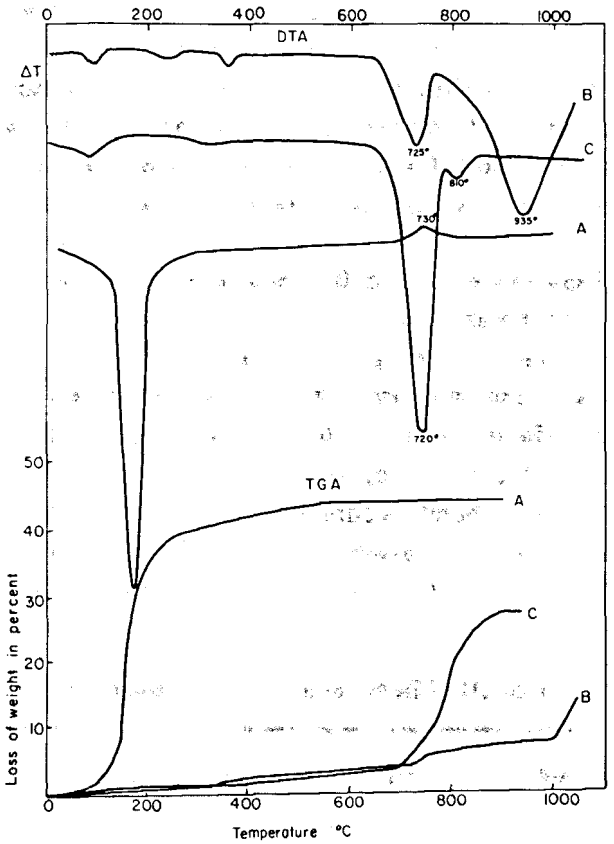

Figure 11. DTA and TGA curves of: A – thaumasite (sample SG 262); B – spurrite marble (sample BT 6000); C – spurritic limestone (sample SG 312).

The formula of thaumasite is: $(Ca_{5.92}Mg_{0.16})H_4[SiO_4)_{2.02}(SO_4)_{1.92}(CO_3)_{1.86}]26.6H_2O$

The X-ray powder pattern is identical with that of thaumasite from Country Down, North Ireland (Knill 1960). The DTA-curve of the thaumasite (Fig. 11A) shows a prominent endothermic effect with a maximum at 175° C, corresponding to the loss of water, and a small exothermic effect at 730° C. With runs of greater sensitivity two distinct exothermic peaks were obtained, the first one at 725° C and the second at 745° . The exothermic peaks are due to crystallization of larnite and anhydrite, as shown by X-ray diffraction of material heated to 850° C. On the TGA curve of the thaumasite a weight loss of 39.5% is observed below 250° C. In the temperature range of 250° – 500°, 5.1% of the weight is lost and between 500° – 750° a further 3% . The slow loss of weight above 300° C is due to decarbonation. According to Font-Altaba (1960) all the CO_2 is expelled together with the water before 300° C. Kirov *et al.* (1968) suggest that the CO_2 is expelled in two steps, most of it in the range of 200° – 500° C and a smaller amount in the range 900° – 1150° C. A difference of about 2% exists between the loss of weight recorded by TGA and the sum of $H_2O + CO_2$ as obtained by chemical analysis. It seems that this difference is due to the amount of CO_2 lost above 900° C – the temperature limit of the thermobalance used.

Thaumasite is a secondary mineral derived by the action of sulfate–bearing solutions on spurrite rocks.

Bultfonteinite – $Ca_2[F|SiO_3.OH].H_2O$

Bultfonteinite is a very rare mineral. It is found as a secondary mineral in the Bultfontein mine at Kimberley, South Africa (Parry *et al.*, 1932); at Crestmore, California (Murdock, 1955); and in skarns of Mihara, Okinawa, Japan (Miyake, 1965). In all these occurrences a close association of bultfonteinite with calc-silicates and calcium-silicate-hydrates is apparent. At Hatrurim the mineral was probably formed by hydrothermal alteration of larnite in the presence of F-ions, the latter possibly derived from the phosphorite beds. According to Parry *et al.* (1932) it is an alteration product of afwillite.

This mineral was identified by microscopic examination of larnite rocks. It is found here in veinlets and in cavities together with tober-

morite and afwillite, and fills occasionally fissures in the latter. It occurs as prisms up to 35 μ across or as small spherulites. The elongation is positive, Z $\wedge$c = 23° – 28°, birefringence low, n ~ 1.54, biaxial positive. In section $\perp$ to c, two systems of polysynthetic twins intersecting at a nearly right angle are observed (Plate XXIII – 1) The main reflections observed in the X-ray pattern and not overlapped by tobermorite and afwillite are: 8.1, 4.06, 2.92 and 1.93 Å.

Titanite – Ca Ti[O|SiO_4]

Titanite was found only in two specimens as a detrital accessory mineral. It occurs as rounded or wedge-shaped light brown grains of extreme refringence and birefringence.

b. Sorosilicates

Rankinite – $Ca_3[Si_2O_7]$

Rankinite is a very rare mineral. The first record is from Scawt Hill, N. Ireland, by Tilley (1942). It was also found at Camas Mor, Scotland (Tilley, 1947): at Kilchoan, Ardamurchan, Ireland (Agrell, 1965); Tokatoka, New Zealand (Black, 1969), Christmas Mountains, Texas; (Joesten, 1974), and lower Tunguska, (Kozoliuk *et al.*, 1974). It was also reported tentatively at northern Coahuila, Mexico (Temple and Heinrich, 1960). Rankinite has been observed by Nurse and Midgley (1955) in blast-furnace slags.

The rankinite of the Mottled Zone was found at Hatrurim and Ma'aleh Adumim at the base of the stratigraphic section and is associated with larnite, nagelschmidtite, gehlenite, pseudowollastonite, cuspidine, monticellite, andradite, perovskite, and magnetite. Rankinite occurs either as ameboid crystal or elongated irregular poikiloblastic patches, 3 x 0.5 mm across, arranged in parallel optical orientation (Plate XVI – 5). Prismatic crystals are rare. Some crystals are cracked and tobermorite is developed in the cracks (Plate XVI – 4). Occasionally a crystal of magnetite is found in the centre of a rankinite crystal with radiating cracks expanding towards the margins. The mineral is colourless and devoid of cleavage. The elongation is negative, it is biaxial positive, with large 2V and a weak dispersion r > v, X $\wedge$ c = 14°, nX = 1.642, nZ = 1.650, nZ – nX = 0.008 – 0.010 (all ± 0.002). It gelatinizes with HCl and shows no hydraulic properties. The X-ray pattern closely resembles that of ASTM card 11–317. The mineral fluoresces strongly under the electron probe. Analysis performed on a fairly large crystal by electron probe, using wollastonite as standard, gave: CaO – 58.6%, SiO_2 – 41.3%, Fe, Al and Mg negative, total 100.2%. Rankinite of the Mottled Zone is related to the highest grade of contact metamorphism – to the sanidinite facies.

Kilchoanite – $Ca_3[Si_2O_7]$

Kilchoanite is a polymorph of rankinite. It was obtained synthetically by Roy (1958 a, b) who called it "Phase z", and also by Speakman (1970). Roy obtained it from gels treated hydrothermally at 700° and from afwillite treated hydrothermally slightly above 200° C. Gard *et al.* (1960) obtained this phase at 200° C by hydrothermal treatment of $\gamma - Ca_2SiO_4$. It was found as a natural mineral by Agrell and Gay (1961) at Kilchoan, Ardnamurchan, Scotland and later at Tokatoka, New Zealand (Black, 1969). In both localities it occurs in metamorphic assemblages of the sanidinite facies. At Kilchoan it was formed in the period of retrograde metamorphism characterized by low $CO_2:H_2O$ ratio. At Kilchoan and Tokatoka it replaces rankinite.

Kilchoanite was found at Hatrurim in melilite-rankinite rocks containing some nagelschmidtite, cuspidine, and wollastonite. It is a rare mineral. It occurs as small (up to 50μ), scattered, irregular, colourless crystals with no visible cleavage, high refringence and weak anomalous interference colours. The crystals occur often close to the borders of

cavities filled by tobermorite. The mineral is biaxial, negative, with 2V moderate, $r > v$, $nZ - nX = 0.003$, $n = 1.644 \pm 0.002$. The spacings in the X-ray pattern, not overlapped by melilite or rankinite, are: 5.17 (m), 4.00 (w), 2.89 Å (s).

The kilchoanite of Hatrurim is a late-stage mineral. Its close association with tobermorite indicates a rather low temperature of origin.

The melilite group

The melilite group of minerals is an isomorphous series of solid solutions with the general formula $(Ca, Na, K)_2$ $(Mg, Fe^{3+}, Fe^{2+}, Al)$ $(Si, Al)_2O_7$. The principal members are gehlenite and akermanite. The most common in the Mottled Zone is gehlenite, less common are akermanite and the ferrian-gehlenite. The last was previously known only from slags. Melilites which crystallize from basic alkaline magmas rich in Ca, are found in thermally metamorphosed, impure limestones, and occur in blast-furnace slags and cements.

They have been found at Hatrurim, Ma'aleh Adumim, Tarqumiye, and Kefar Uriya.

The melilites occur in various metamorphic facies. The following assemblages are distinguished:

I. Sanidinite facies: (1) Melilite, nagelschmidtite, (larnite or bredigite are less common), rankinite, andradite ± spinel, magnetite, magnesioferrite, perovskite, wollastonite, merwinite, monticellite. (2) melilite, pseudowollastonite, schorlomite, ± larnite, rankinite. (3) spurrite, brownmillerite, mayenite with some melilite and larnite.

II. Pyroxene-hornfels facies: (4) Anorthite, diopside, grossular, melilite; (5) anorthite, wollastonite, diopside, melilite.

Assemblage (I), related to the sanidinite facies, is the most common. It occurs in rocks equivalent to the lower part of the Ghareb Formation. Assemblages (2) and (3) are rare: (3) occurs also in rocks corresponding to the Taqiye Formation. Assemblages (4) and (5) are characteristic at Hatrurim only of rocks of the Taqiye Formation. Assemblage (5) was found at Tarqumiye and Nahal Ayalon in rocks corresponding, according to geological setting, to the Ghareb Formation.

Gehlenite – $Ca_2Al[(Si, Al)_2O_7]$

Gehlenite constitutes up to 50 – 60 per cent of the rock and is present in the groundmass as squarish, tabular, or lath-like crystals elongated in the direction of the axis (Plate XVII – 1, 2, 3, 5). Anhedral individuals disseminated in the matrix are less common. Zoning is marked only in some cases, the core being gehlenite-rich and the rim akermanite-rich (examination by scanning with the microprobe). Marked {001} cleavage. Tabular crystals measure to 0.1 x 0.04 mm across. Minute squares of about 2 μ were also observed. In thin-section the colour varies from colourless for the Al-variety to yellowish-green for the ferrian variety. The change of colour may be observed in the same crystal, the core being greenish and the shell colourless. The mineral is uniaxial, negative and the elongation positive. The indices of refraction vary with composition and are: 1) the iron-poor variety: $nO = 1.670$, $nE = 1.662$, $nO - nE = 0.008$. 2) the iron-rich gehlenite is slightly pleochroic with O – pale yellow, E – greenish-yellow. The substitution of Al by Fe^{3+} raises the indices of refraction: $nO = 1.698$, $nE = 1.692$, $nO - nE = 0.006$, all ± 0.002.

Gehlenite with a certain content of the akermanite molecule has very low birefringence and anomalous blue to brown interference colours. The occurrence of small inclusions of gehlenite squares in rankinite and pseudowollastonite hosts indicate its early formation. Larnite and gehlenite are probably formed simultaneously. Wherever larnite is formed first, gehlenite is anhedral. The ferrian-gehlenite is less stable and iron is leached preferentially from the margins. This is indicated by electron probe

traverses and by microscopic examination. In samples having a weathering crust, the margins of the ferrian gehlenite crystals are stained by iron oxides. Distribution pictures for Ca, Si, Mg, Fe, Al, and Ti are presented in Plate III. Analyses of gehlenites obtained by electron probe are given in Table 21.

Table 21. Electron microprobe analyses of melilites

Oxide	1	2	3	4
SiO_2	25.6	24.8	24.9	28.8
CaO	37.9	38.6	39.2	38.7
MgO	1.6	1.2	1.7	2.0
Al_2O_3	22.8	26.2	27.4	21.4
Fe_2O_3	12.3	6.8	5.7	6.6
TiO_2	0.2	n.d.	n.d.	n.d.
Total	100.4	97.6	98.9	97.5
Numbers of cations on the basis of 7 oxygens				
Si	1.21	1.17	1.17	1.40
Ca	1.93	1.95	1.97	1.97
Mg	0.11	0.08	0.12	0.14
Al	1.26	1.45	1.50	1.20
Fe^{3+}	0.47	0.24	0.21	0.23
Ti	0.005	–	–	–

Analyses 2–4 by S. Gross.

1. Ferrian-gehlenite, gehlenite-nagelschmidtite rock, Hatrurim, Sample SG 281, Analyst G. Socroun.
2. Gehlenite, gehlenite-rankinite-andradite rock, Hatrurim, Sample SG 277.
3. Gehlenite, gehlenite-larnite rock, Hatrurim, Sample SG 268.
4. Gehlenite, pseudowollastonite-gehlenite rock, Hatrurim, Sample SG 214.

Gehlenite, according to its paragenesis, is a mineral of the highest grade of thermal metamorphism. It was formed from the marly rocks of the Ghareb and Taqiye formations. Synthetic iron gehlenite is stable, according to Bowen *et al.* (1933), at temperatures below 775° C. Gehlenite was obtained already at 450° C during prolonged heating experiments performed by the author, on the marls of Taqiye and Ghareb. This may have been the approximate temperature of metamorphism event at Kefar Uriya, as the gehlenite crystallites here do not exceed 1 μ.

Akermanite – $Ca_2Mg[Si_2O_7]$

Akermanite occurs, relatively rarely, in rocks rich in Mg. Akermanite is associated with gehlenite, larnite, merwinite, and spinel. It is found as colourless, anhedral or prismatic, disseminated individuals, measuring up to 80 μ across. Its positive sign indicates that it has a composition near that of pure akermanite. The anomalous interference colours and the refringence point toward the presence of a certain percent of the gehlenite molecule (about 25%). The elongation is negative, n = 1.644, birefringence about 0.004. Akermanite is usually formed later than gehlenite. In a few cases secondary crystallization of akermanite is also observed.

Cuspidine – $Ca_4[(F, OH)_2|Si_2O_7]$

Cuspidine is a rare mineral, characteristic of pneumatolytic metamorphism of limestones. The mineral occurs also in slags. It can be synthesized hydrothermally from crystallizing melts at temperatures above 500° C and by solid-state reactions at 1000° C (Van Valkenburg and Rynders, 1958).

Cuspidine is found at Crestmore (Tilley, 1928), Carlingford (Osborne, 1932a), Lower Tunguska (Sobolev, 1935), Skye, Scotland (Tilley, 1947), and other places. It occurs very rarely in the gehlenite-nagelschmidtite rocks at Hatrurim, associated with rankinite, perovskite, and magnetite. It forms small anhedral crystals with one fair cleavage, and moderate relief and birefringence. The mineral is biaxial positive, with $2V \sim 60°$. $X \wedge c = 5°$, dispersion $r > v$. Spacings in the X-ray pattern not interfered

with by other minerals: 3.26 Å, 2.94 and 2.90 Å

The mineral seems to be formed by solid-state reaction at elevated temperature, the source of fluorine being probably the francolite of the original marly rocks.

Pumpellyite – $Ca_2(Mg, Fe, Mn, Al)(Al, Fe, Ti)_2[(OH, H_2O)_2|SiO_4|Si_2O_7]$ (?)

The mineral occurs in a wide variety of rocks, but is characteristic particularly of the glaucophane-schist facies of metamorphism. At Hatrurim it is found, in minor amounts, in only one specimen of an altered lime-silicate rock, consisting of heterogeneous areas composed predominantly of calcite, ettringite, portlandite, hydrogarnets, and different calcium-silicate-hydrates such as afwillite, okenite, truscottite, and others.

Pumpellyite occurs in a "pocket" intimately associated with calcite and ettringite. It forms aggregates (about 0.6 mm across) of anhedral to prismatic and slightly corroded crystals. In thin-sections the mineral is pale greenish-yellow, slightly pleochroic, with high index of refraction and anomalous interference colours. The optical characteristics are: biaxial, positive, 2V ~ 30°, positive elongation, Z ∧ c = 8° – 10°, very strong dispersion r > v. nZ – nX = 0.010. Pleochroism: X, Y = pale greenish-yellow, Z = brownish-yellow. The X-ray powder pattern is almost identical with that in the ASTM Powder Diffraction File 10 – 447.

Pumpellyite, was probably formed by the action of hydrothermal solutions on the calc-silicate rock, and its formation preceded the later ettringitization process.

Vesuvianite – $Ca_{10}(Mg, Fe_2)Al_4[(OH)_4(SiO_4)_5(Si_2O_7)_2]$

Found at Hatrurim as a rare mineral in melilite-rocks and in anorthite-hedenbergite felses. It occurs mostly as idiomorphic prismatic crystals up to 90 μ across with poor {100} cleavage. In thin section the mineral is light green or brown. The elongation is negative, the extinction parallel. The mineral is uniaxial negative. nE = 1.708, nO = 1.712, nO – nE = 0.004 (all ± 0.002). The interference colours are anomalous in yellow and violet-blue tints. The mineral was formed by thermal metamorphism.

Prehnite – $Ca_2Al_2[(OH)_2|Si_3O_{10}]$

Prehnite is a common hydrothermal mineral found in cavities in igneous rocks and metamorphosed limestones. It is found at Hatrurim in cavities of an anorthite-gehlenite-diopside fels, associated with zeolites. It occurs as aggregates of prismatic or fibrous colourless crystals with positive elongation, and high relief as compared to the zeolites. The interference colours are slightly anomalous. The birefringence nZ – nX = 0.023. The main reflections in the powder diagram are: 3.28 and 3.49 Å. It is a secondary mineral formed by hydrothermal alteration of the metamorphic Ca-aluminosilicates.

c. Inosilicates

Diopside-hedenbergite – Ca (Fe, Mg) $[Si_2O_6]$

Diopside is a very common constituent of various igneous and contact metamorphic rocks. Hedenbergite is rare and found only in contact rocks and ore deposits. At Hatrurim the commonest pyroxene is diopside-hedenbergite. It occurs in three assemblages:

1) Calcite-zeolite rocks with hedenbergite and garnets of the grossular-andradite and hydrogarnet series;

2) anorthite-diopside-hedenbergite-grossular fels with some gehlenite;

3) anorthite-wollastonite-diopside-gehlenite fels.

Assemblages 1 and 2 are found only at Hatrurim, in rocks equivalent of the Taqiye Formation; assemblage 3 occurs only at Tarqumiye and seems, according to stratigraphic evidence, to be equivalent to the Ghareb Formation.

These pyroxenes occur as very small crystals, usually as rounded granules 3 to 10 μ in diameter. Prismatic crystals up to 0.2 mm are rare, and are found mostly in the vicinity of hematite inclusions, occasionally forming reaction rims. Only in one specimen prismatic or rhombic zoned crystals 0.3 x 0.1 mm large were observed (Plate XIX – 5). The borders of these crystals appear corroded and may include small vesicules filled by thomsonite. The extinction of the zonal crystals is not uniform. The core is darker than the borders. The colour of the mineral in thin-section is yellowish-green or faintly greenish-brown. The crystals are elongated in the direction with Z $\wedge$ c = 40° – 45°. The mineral is biaxial, positive, 2V ~ 60° with strong dispersion r > v. The sections parallel to {010} have strong anomalous interference colours. The indices of refraction are: nX = 1.725, nZ = 1.755; nZ – nX = 0.025 – 0.030 (all ± 0.025). Pleochroism is as follows: X = pale green, Y = yellowish green, Z = dark green. According to the optical and X-ray diffraction data, the mole per cent of diopside in the hedenbergite does not exceed 5 to 8. The diopside-hedenbergite was produced by thermal metamorphism of silica-poor dolomitic limestones and marls. The diopside-hedenbergite of the calcite-zeolite assemblage, which is very common at Hatrurim, was produced during retrograde metamorphism, in a system involving water. Its close association with hydrogarnets seems to indicate that the temperature probably did not exceed 350° C.

The diopside of assemblages (2) and (3) was formed by decarbonation reactions. Assemblage (2) was formed at temperatures corresponding to the pyroxene-hornfels facies (about 600°). The absence of grossular and the presence of wollastonite in assemblage 3 probably points to temperatures of about 860° C, when grossular decomposes to wollastonite + anorthite + gehlenite (Roy and Roy, 1962). This assemblage may be referred to the sanidinite facies and represents a silica-saturated assemblage, which is very rare in the Mottled Zone.

Fassaite – Ca (Mg, Fe^{3+}, Al) [(Si, Al)$_2$O$_6$]

The name fassaite is used to describe the aluminium-rich and sodium-poor pyroxenes (Deer *et al.*, 1965). The mineral was found in a specimen of anorthite-wollastonite-gehlenite-pyroxene fels from Tarqumiye. The mineral occurs in the form of short prismatic crystals terminated by (111) or (001). They are up to 100 μ in diameter. In thin-sections they display distinct cleavages at 87°. The colour is light green; the mineral is pleochroic, with X and Z – pale green, and Y – yellowish. One crystal was twinned on {100}. Z $\wedge$ c = 46°. The mineral is biaxial, positive, 2V ~ 60°, dispersion strong r > v. nZ – nX = 0.024. The interference colours are anomalous. For electron probe analysis a fairly large crystal, about 80 μ in diameter, was selected. Diopside served as standard. The result is given in Table 22 and compared with an

Table 22. Analyses of fassaite

Oxide	1	Cations per six oxygens		2
SiO_2	35.0	Si	1.40	41.36
CaO	26.8	Ca	1.11	25.27
Al_2O_3	17.5	Al	0.82	15.75
Fe_2O_3	13.9	Fe^{3+}	0.41	6.10
FeO				0.24
MgO	5.2	Mg	0.31	10.34
MnO	n.d.			0.03
TiO_2	3.0	Ti	0.09	0.76
Na_2O	n.d.			0.06
K_2O	n.d.			0.03
$H_2O\pm$	n.d.			0.10
Total	101.4			100.04

1. Fassaite from pyroxene-wollastonite-anorthite fels, Tarqumiye. Microprobe analysis by S. Gross.
2. Fassaite, Helena, Montana (Knopf and Lee, 1957).

analysis of a fassaite from Helena, Montana (Knopf and Lee, 1957).

The composition of the fassaite from Tarqumiye, calculating all iron as Fe^{3+}, is the following: $(Ca_{1.11}\,Mg_{0.31}\,,\,Ti_{0.09}\,,\,Al_{0.22}\,,\,Fe^{3+}{}_{0.41})\,(Si_{1.40}\,Al_{0.60})O_6$. This seems to be a fassaite richer in alumina than ever described previously.

Fassaite occurs in parageneses devoid of quartz, and Tilley (1938) has suggested that it is probably unstable in the presence of free silica.

The fassaite of Tarqumiye was formed by thermal metamorphism of marls.

Aegirine-augite – (Na, Ca) (Fe^{3+}, Fe^{2+}, Mg, Al) [Si_2O_6]

Aegirine-augite is very rare in the Mottled Zone, found only in some specimens of felses. It occurs as short prismatic crystals up to 0.2 mm in diameter. Green in thin section. The pleochroism is stronger than for other pyroxenes: X–grass green, Y–pale green, Z–yellowish green. The elongation is negative, $X\Lambda c = 13°$. It is biaxial negative, 2V large, dispersion $r > v$ strong, $nZ - nX = 0.037$. It is formed by thermal metamorphism of marls, the source of Na being probably halite.

Riebeckite – $Na_2\,Fe^{2+}_3\,Fe^{3+}_2\,[(OH,F)|(Si_4O_{11})]_2$

This is a detrital mineral found in the heavy fraction of the Ḥazeva sandstone. It occurs as rounded grains about 0.1 mm across. In the immersion preparation the mineral is blue in colour and strongly pleochroic: X – dark bluish-green, Y – smoky blue, Z – yellowish-green. The elongation is negative. The mineral is biaxial, negative, 2V moderate. The diffraction pattern seems to indicate a magnesioriebeckite.

Wollastonite – β-$CaSiO_3$

Wollastonite is a common constituent of thermally metamorphosed impure limestones. The mineral occurs in an anorthite-wollastonite diopside-fels with some gehlenite at Tarqumiye, in some melilite rocks of Ḥatrurim (Plate XIX – 1) associated with larnite and rankinite, and in a medium-grade metamorphosed rock from Kefar Uriya.

The mineral is rather rare in the Mottled Zone compared with other calc-silicates. It occurs at lath-like crystals, elongated in the c direction with distinct {100} and fair {001}cleavages, or as small needles. Larger crystals up to 0.1 mm are occasionally corroded by calcium-silicate-hydrates (Plate XIX – 2). It is biaxial negative, $2V \sim 40°$, $r > v$, elongation of laths either positive or negative. $X\Lambda c = 32° - 34°$, $Y\Lambda b = 4°$, $nZ - nX = 0.012$. Polysynthetic twins parallel to the direction of elongation are common. The analysis of a wollastonite from Tarqumiye, obtained by electron probe microanalysis with wollastonite as standard, gives:

CaO – 48.60%, SiO_2 – 51.49%, Al_2O_3 – 0.17%, MgO – neg., Fe_2O_3 – neg.

Total 100.26%.

The wollastonite was formed by thermal metamorphism of calcareous shales and marls. The scarcity of wollastonite may be explained by the silica deficiency of the parent rocks.

Pseudowollastonite – α-$CaSiO_3$

The high-temperature form of $CaSiO_3$ has been found in nature only in pyrometamorphosed rocks in south-west Persia (McLintock, 1932) where sediments have been baked by the burning of hydrocarbons. It is a common constituent of blast furnace slags (Nurse and Midgley, 1955). The synthetic compound was renamed cyclowollastonite (Strunz, 1970). An occurrence had been described under this name by Hochleitner (1972) from Pfaffenreuth,Bavaria. However, the new name has not been accepted by the IMA Commission of New Minerals. The mineral was found in Ḥatrurim in three samples associated with rankinite, gehlenite, schorlomite, and larnite. Pseudowollastonite forms up to 15% of these rocks. The mineral occurs mostly as

elongated, poikiloblastic, colourless crystals arranged in radial groups (Plate XIX – 4), or as anhedral small or subhedral larger crystals up to 0.5 mm across. The poikiloblastic crystals are about 1 x 0.04 mm, and filled like a sieve with minute square gehlenite crystals up to 10 μ. The elongation of these crystals is negative. The larger crystals are frequently twinned. The number of twin lamellae does not exceed 3 or 4 (Plate XIX – 3). In one sample, droplike pseudowollastonite grains about 20 μ across are enclosed in a rankinite host. The optical properties are: uniaxial, positive, rarely biaxial with (+) 2V ~ 0°, nZ = 1.650, nX = 1.610, nZ – nX = 0.040 (all ± 0.002). X Λ a = 2°.

Analysis of pseudowollastonite by probe with wollastonite as standard gave: CaO – 48.20%, SiO_2 – 51.92%, Mg – traces, Al_2O_3 – neg. Total = 100.12%. A SEM photomicrograph of a pseudowollastonite crystal is shown in Plate XVII – 4. The occurrence of pseudowollastonite indicates that the temperature must have exceeded the inversion temperature to wollastonite, i.e. 1125° ± 10° C (Buckner and Roy, 1955).

d. Calcium silicate hydrates

Okenite – $CaH_2[Si_2O_6].H_2O$

Okenite was originally found in Greenland by Von Kobell in 1838 (in Heller and Taylor, 1956) It was found later at: Faeroe Islands (Bøggild, 1922), Scawt Hill (Tilley and Alderman, 1934), Bombay, India (Gard and Taylor, 1956), Mull and Morven, Scotland (Walker, 1971), Skookumchuk, Washington (Tschernich, 1972). In all mentioned occurrences it is associated with basalts.

Okenite is an extremely rare mineral at Hatrurim, occurring in some cavities of calc-silicate rocks as tabular or prismatic crystals about 10 μ large, with one good prismatic cleavage, or as aggregates of curved fibers. The elongation is positive. The extinction is straight and parallel to c, and oblique in other directions. Multiple twinning on {010}. The mineral is biaxial, negative, with large 2V; n ~ 1.54. Observed X-ray spacings were: 21.0 (vvs), 8.8 (vs), 7.4 (m) 3.56 (s) and 2.93 (vs). Taylor (1964) suggested that synthesis of okenite is likely to be possible only at low temperatures, little above or perhaps even below 100° C. Okenite was obtained as a minor phase by the writer by autoclaving a gehlenite-larnite and a larnite rock at 110° C.

Xonotlite – $Ca_6[(OH)_2|(Si_6O_{17})]$

Xonotlite was first found in limestones near igneous contacts at Tetla de Xonotla, Mexico (Winchell, 1959), and is known at many other localities. Xonotlite is formed reproducibly when any sufficiently reactive starting material of 1:1 CaO/SiO_2 ratio is treated hydrothermally at 150° – 400° C (Taylor, 1964).

It is found in only two specimens of spurrite rocks at Hatrurim where it occurs as cavity-filling associated with jennite, tobermorite and truscottite. It occurs as fibrous aggregates with straight extinction and positive elongation. The index of refraction is higher than that of jennite and tobermorite. The spacings observed on the X-ray diffractograms are 4.27 Å (vw), 3.65 Å (s) 3.23 (m) and 1.95 (m). On the DTA curve an endothermic effect at about 800° C (attributed to xonotlite) was observed.

Xonotlite was obtained by the writer as a minor autoclave product of larnite rocks at 110°, and in the products of hydrothermal treatment at 500° C and 1 Kb pressure of a tobermorite rock.

Foshagite – $Ca_4[(OH)_2|(Si_3O_9)]$

The mineral was discovered at Crestmore by Eakle (1925). It is reported also from Mull and Morven (Walker, 1971b), Kushiro, Japan (Kusachi *et al.*, 1971) and probably from Velardena, Mexico (Heller and Taylor, 1956). Hydrothermal stability of foshagite is discussed by Speakman (1968).

Foshagite is a rare mineral at Hatrurim, where it is found in veinlets and cavities of a larnite rock. It occurs as elongated fibres of positive elongation, low birefringence, and has a refractive index higher than that of tobermorite. The main spacings observed on the X-ray diffractograms are: 6.8 (m), 3.36 (m), 2.93 Å (s). It is associated with minerals of the tobermorite group and afwillite. The synthetic compound is formed in the temperature range of 300° – 500° C. (Gard and Taylor, 1958, 1960; Flint *et al.*, 1938; Balitskiy and Gorbunov, 1967). The paragenesis of the mineral occurring at Hatrurim points to lower temperatures of formation, (about 100° – 150° C).

Hillebrandite – $Ca_2[SiO_4].H_2O$

The mineral was discovered at Velardena in Mexico by Wright (1908) and has been found also at Crestmore, California; Carlingford, Ireland (Nockolds and Vincent, 1947), in Lower Tunguska, Siberia (Reverdatto, 1964) and at Kushiro, Japan (Kusachi *et al.*, 1971b). It is found in the Hatrurim area in veins and cavities of melilite-larnite and spurrite rocks, and at Kefar Uriya and Ma'aleh Adumim in a calc-silicate-hydrate rock. It is rare.

Hillebrandite occurs as fibrous aggregates, radial spherulites (Plate XXIII – 5) or anhedral grains, lining occasionally cavities filled by tobermorite. In thin section it is colourless or yellowish. The optical properties are: positive elongation, parallel extinction, biaxial, negative, 2V moderate, nZ – nX = 0.006, n ~ 1.605 dispersion r < v strong. A characteristic feature of this mineral is its abnormal blue interference colour. The main reflections in the X-ray pattern are: 2.92 (vvs), 3.33 (s) and 4.76 Å (s).

Hillebrandite was synthesized by Heller and Taylor (1952) at 140° C. Roy and Harker (1962) indicate that hillebrandite can be a stable phase up to 300° – 350° C. The mineral was obtained by the author as a minor constituent by autoclaving larnite rocks at 110° C.

At Hatrurim it is a secondary mineral, formed by hydrothermal alteration of the calc-silicate minerals.

Tobermorite group

There are various calcium-silicate-hydrate compounds that are classified under the "tobermorite group". The name tobermorite was originally given to a mineral from Mull and Skye, Scotland (Heddle, 1880), a compound of approximate composition 5 $CaO.6SiO_2.5H_2O$. The name tobermorite s. str. is applied to the compound with an interplanar 002 spacing of 11.3 Å but is also used in a loose sense to cover a whole range of hydrated calcium-silicates differing in composition. The general formula is $xCaO.SiO_2.yH_2O$ where x varies between about 0.8 and 1.5 and y varies discontinuously between 0.5, and 2.0 or 2.5 (Heller and Taylor, 1956). These minerals have a layer structure, are similar to vermiculite (Taylor and Harrison, 1956), and are characterized by the value of the 002 interplanar spacing. This value increases with an increasing H_2O to SiO_2 ratio. It seems that the X-ray pattern is not dependent on the CaO to SiO_2 ratio but that this value influences the DTA curve (Kalousek, 1952; Van Bemst, 1955). The exothermic peak is shifted (from 830° C to 920° C) as the CaO/SiO_2 ratio of the hydrate increases, and in the same time it becomes less intense. Using the DTA technique, Kalousek (1952) differentiated two groups, one having a CaO/SiO_2 molar ratio of 0.8 – 1.33, the other a molar ratio 1.5 and above. Kalousek (1957) investigated the substitution of Si by Al in the tobermorite lattice and its influence on the X-ray and DTA patterns. Diamond (Diamond *et al.*, 1966) shows the upper limit of Al_2O_3 –solubility in crystalline tobermorite to be about 10% , and Majumdar and Rehsi (1970) estimated the MgO content to be about 2 – 3%. Gaze and Robertson (1956) ex-

pressed the opinion that $(CO_3)^{2-}$ may enter the tobermorite structure. The end product of the dehydration of tobermorites with a low Ca/SiO_2 ratio is wollastonite, and those with high CaO/SiO_2 ratio, larnite. Identification of the tobermorites was carried out by means of X-ray diffraction, and to a lesser extent by DTA, optical microscopy, and scanning electron microscopy.

The minerals of this group are widely distributed in low concentrations in the Hatrurim Formation (Bentor *et al.*, 1963; Gross *et al.*, 1967). They appear mostly in vugs, vesicles, and veins some mm across, associated with ettringite, gypsum, portlandite, aragonite, calcite, vaterite, bayerite, and calcium-aluminium oxide hydrates. Minerals of this group constitute up to 80 per cent of some specimens at the top of the formation at Hatrurim and Ma'aleh Adumim. The tobermorites were formed by hydration of calc-silicate rocks, especially the larnite ones. They reacted with meteoric water and hydrothermal solutions introduced along fractures.

Plombierite – $Ca_5H_2[Si_3O_9]_2 .6H_2O$ – 14 Å tobermorite

The name is used as a synonym for 14 Å tobermorite (McConnell, 1954, 1955). It has been synthesized from lime-silica slurries at 60° C (Kalousek and Roy, 1957). The mineral appears in most samples in close intergrowth with other hydrates of this group and occurs mostly as a white powder. It is very poorly crystallized compared with the other hydrates of this group. The X-ray powder photograph resembles closely the sample from Crestmore (Heller and Taylor, 1956). It appears as shapeless lumps or as irregular plates in SEM photomicrography (Plate XXI – 4). The thickness of a foil, calculated from the peak broadening on the diffractogram, is about 53 – 113 Å, corresponding to 4 – 8 elementary layers. Dehydration to 11.3Å tobermorite occurs after heating overnight at 60° C. In a hydrothermal run of a week at a temperature of 600° C and a pressure of 100 bar it becomes a mixture of wollastonite and xonotlite.

Analyses of the 14 Å hydrate by means of a electron microprobe with wollastonite as standard gave: CaO – 32.94%, SiO_2 – 41.43%, Al_2O_3 – traces. Taking the deficit as H_2O, the composition would be: 0.84 CaO . SiO_2 . 2.06-H_2O. In reality, the content of water is higher, as the mineral is partly dehydrated during the performance of the analysis. The DTA curve of this hydrate (Fig. 12E, F) shows an endothermal effect at 130° – 140° C due to loss of interlayer water, and an exothermal peak at 820° – 830° C due to crystallization of wollastonite.

Tacharanite (?) – 12.6 Å tobermorite

The name tacharanite has been used (Sweet, 1961) to designate a mineral from Skye, Scotland, with a 12.7 Å spacing and apparently belonging to the tobermorite group. Another occurrence is at Mull and Morven, Scotland (Walker, 1971), in amygdules of basalt. The 12.6 Å tobermorite was found also at Crestmore, California, intergrown with the 10 Å – tobermorite (Heller and Taylor, 1956). According to Taylor (1964), the relationship of tacharanite to the 12.6 Å tobermorite mineral from Crestmore is uncertain, as these phases were not fully investigated.

Table 23. Diffraction data for the 12.6 Å hydrate, Hatrurim

d (meas.) Å	I	hkl
12.6	vs	002
5.5	vw	201
3.07	vs	220
2.79	vs	400
1.83	s	040
1.66	mw	620
1.52	mw	440

The mineral from Hatrurim appears as bundles of radiating fibres in cavities of calc-silicate rocks in association with other hydrates of this group, ettringite, and gypsum. The fibres are white and of a silky lustre. The elongation of the fibres is negative, the extinction straight and the mean index of refraction about 1.50.

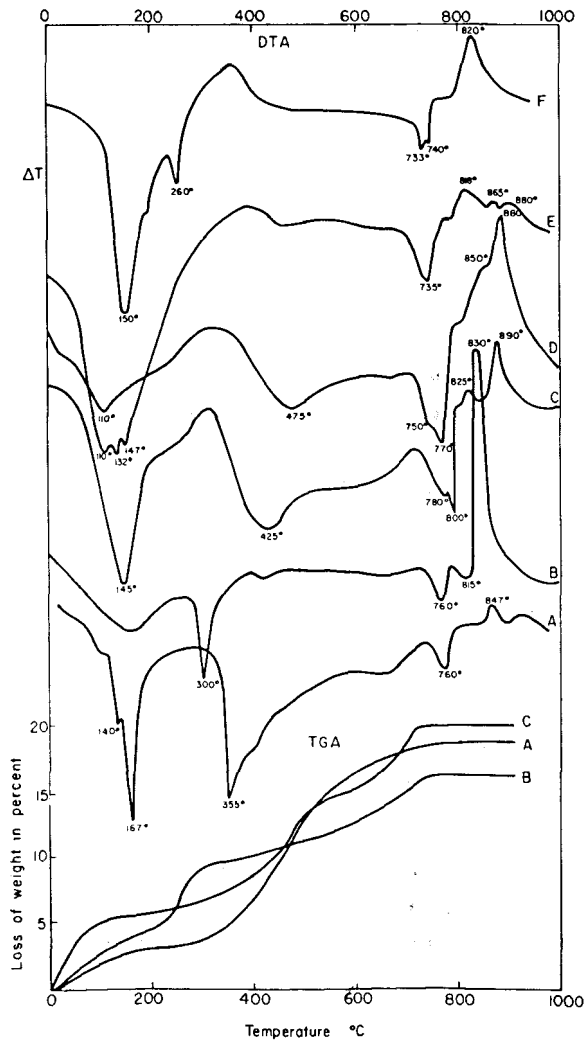

Figure 12. DTA and TGA curves of calcium silicate hydrates. A – afwillite rock (sample SG 532); B – 11.47 Å tobermorite rock (sample SG 210); C – jennite rock (sample SG 459); D – rock consisting of 11 Å tobermorite with dicalcium silicate hydrate α. (sample SG 451); E – 14 Å, 12.6 Å, 10 Å and 11.3 Å tobermorites (sample SG 214); F – 14 Å and 11.3 Å tobermorites (sample SG 281).

On the DTA curve an endothermic effect at 130° – 150° C, corresponding to the loss of interlayer water, and a small and mild exothermic effect at 865° C are observed (Fig. 12E). The dehydration curve given by Sweet (1961) shows two distinct breaks at 350° C and 650° C.

Table 24 presents the results of a chemical analysis by electron microprobe of the 12.6 Å hydrate, occurring as a cavity filling associated only with calcite in a rock consisting of larnite, rankinite, pseudowollastonite, and gehlenite. (For comparison, the data for the tacharanite from Skye are given).

Table 24. Chemical analyses of two 12.6 Å hydrates

Oxide	1	2
SiO_2	32.8	41.8
CaO	48.3	33.6
Al_2O_3	1.2	5.6
Fe_2O_3	n.d.	0.3
MgO	traces	3.2
Na_2O	n.d.	0.6
K_2O	n.d.	0.1
H_2O	n.d.	15.2
Total	82.3	100.4

1. 12.6 Å tobermorite from Hatrurim. Electron microprobe analysis by S. Gross.
2. Tacharanite from Skye (Sweet, 1961).

The molar ratio of CaO/SiO_2 of the Hatrurim mineral is 1.54 CaO/ (0.98 SiO_2 + 0.02 Al_2O_3), much higher than for the Skye mineral. The amount of water calculated as deficit is 1.75 H_2O and must be higher, taking into consideration the conditions of vacuum and heating of the microprobe. It seems that the mineral from Hatrurim does not correspond to the mineral from Skye and corresponds more to the synthetic "CSH (II)" of Taylor, a calcium silicate

hydrate (Taylor, 1961) with CaO/SiO_2 ratio 1.54 – 2.0.

The 12.6 Å hydrate was obtained by the present author as the main phase by the hydration of some larnite rocks at room temperature. This synthetic compound forms thin fibers a few microns in length and a tenth of a micron wide (Plate XXI – 1).

Tobermorite – $Ca_5H_2[Si_3O_9]_2.4H_2O$ – 11.3Å – 11.7 Å tobermorite

This is the principal calcium-silicate-hydrate occurring in the Hatrurim Formation. X-ray examination reveals its pronounced crystallinity. This mineral has been synthesized hydrothermally at 100° – 200° C (Flint *et al.*, 1938; Heller and Taylor, 1951, 1952). It consists of a tough white material made up of interlaced fibres with a silky lustre, and mostly forms radiating aggregates or bundles of fibres, arranged perpendicular to the walls of veins. Locally lenses up to 3 mm in size consist of rosettes or crisscrossing fibres (Plate XXII – 1). In thin sections the mineral is colourless and consists of aggregates of fibres, mostly in approximately parallel orientation, showing parallel extinction and ± elongation. The fibre bundles are up to 100 μ in length. The mineral is biaxial negative with moderate 2V and dispersion r < v. The mean index of refraction is n = 1.554 ± 0.002, nZ – nX = 0.004 – 0.006. The microstructure of freshly fractured surfaces of tobermorite-containing rocks has been studied by SEM. Photomicrographs are shown in Plate XX. They are in agreement with observations of other workers. The X-ray powder photographs are similar to those of the material from Ballycraigy (Heller and Taylor, 1951). The 11 Å modification probably corresponds to a better crystallized and a lower hydrated state of the 14 Å hydrate, since the hko spacings are identical for both hydrates.

Two varieties can be distinguished according to their thermal behaviour:

1) Normal tobermorite, with a basal spacing of 11.3 Å. When heated to about 300° C a part of the water is lost and a 9.3 Å tobermorite is formed. After heating to 400° C it becomes X-ray amorphous, and at 800° C it gives the pattern of wollastonite. The DTA curve (Fig. 12F) shows an endothermic peak at 260° C corresponding to dehydration, and two exothermic peaks: a very weak one at 360° C and a stronger one at 820° C. The effect at 820° C is due to crystallization of wollastonite. The morphology of this variety as it appears on SEM microphotographs is mostly of platy laths or aggregates of laths, crossing each other at angles of 60° – 90°. Occasionally crumpled foils are observed. The laths are about 5 – 10 μ long and 1 – 2 μ broad. The foil thickness as calculated from the peak broadening on X-ray diffractograms is about 110 – 166 Å (10 – 15 elementary layers).

2) Abnormal tobermorite. The basal spacing 002 does not shrink up to 700° C. Above this temperature the peak weakens and becomes diffuse, disappearing at 800° C, when wollastonite is formed. Its thermal behaviour resembles that of the Loch Eynort tobermorite (Gard and Taylor, 1957). The reason for this behaviour is unknown. According to Gard and Taylor: "The cohesive forces between the layers are unusually strong and, in fact, stronger than those operating in the a-direction within the layers themselves". McConnell (1954) suggested the stability of the basal spacing might be caused by alkali ions in interlayer positions. Taylor (1964) suggested that it could possibly be attributed to Si–O–Si links between the adjacent layers, perhaps in the manner proposed by Mamedov and Belov (1958). Kalousek (1957) prepared synthetic tobermorites with about 4% of Al_2O_3 in the structure. He found that the DTA curve of these synthetic tobermorites was affected by substitution of Si by Al. They exhibit a much stronger exothermic peak shifted to slightly higher temperatures. The basal spacing of the Al-substituted tobermorites

Table 25. Chemical analysis of 11.47 Å, tobermorite calculated from bulk analysis of rock

Oxide	Wt%	Deducted for calcite 1	Deducted for quartz 2	Deducted for orthoclase 3	Deducted for apophyllite 4	Deducted for gypsum 5	Deducted for apatite 6	Deducted for *hematite* 7	Deducted for *titanite* 8	remainder for *tobermorite*
SiO_2	42.07		1.50	2.91	3.0				0.20	34.40
CaO	31.22	2.90			1.5	0.25	0.51		0.21	25.85
MgO	0.50									0.50
Fe_2O_3	1.70							1.70		
Al_2O_3	4.30			0.83						3.56
TiO_2	0.28								0.28	
K_2O	1.33			0.76	0.3					0.27
Na_2O	0.72									0.72
F	0.14				0.1		0.04			
P_2O_5	0.39						0.39			
CO_2	2.28	2.28								
SO_3	0.36					0.36				
H_2O+	10.97				0.9	0.16				9.90
H_2O-	3.51									
Total	99.77	5.18	1.50	4.50	5.8	0.77	0.94	1.70	0.69	75.20

Analyst M. Gaon

1. Assuming that it contains all the CO_2. On microscopic investigation a smaller amount of calcite is observed. It is possible that part of the CO_2 is incorporated in the tobermorite. 2. Estimated by counting in two thin sections. 3. Estimated by counting in two thin sections. 4. Assuming that it contains all the remaining F after deduction of the apatite. This gives a good correlation with the amount of apophyllite as estimated in thin sections. 5. Assuming that it contains all the SO_3. 6. Assuming that it contains all the P_2O_5. 7. Assuming that it contains all the Fe_2O_3. 8. Assuming that it contains all the TiO_2 (single crystals identified in thin section).

shifts from 11.1 Å to 11.7 Å with the increase in the Al content.

Mitsuda (1970) synthesized a tobermorite rich in Al by treating a zeolite (clinoptilolite)–lime mixture under saturated steam at 90° – 180° C. This tobermorite, with spacing 11.4 – 11.7 Å, was found to be anomalous in thermal behaviour like the Loch Eynort specimen. The DTA curve of this synthetic tobermorite shows a broad endothermic peak at about 110° – 300° and a strong exothermic one at 840° – 850° C.

In Table 25 the analysis of an abnormal tobermorite with a spacing of 11.47 Å is given. It constitutes about 75% of a former sandstone, altered to tobermorite rock. The composition of the 11.47 Å tobermorite is accordingly: $(Ca_{4.52}Mg_{0.13}Na_{0.23}K_{0.06})H_2[(Si_{2.80}Al_{0.33})O_9]_2$ $4.38H_2O$.

The DTA and TGA of this sample are given in Fig. 12, curve B. The DTA curve exhibits a broad endothermic valley up to 250° C owing to the loss of free and absorbed water; on the TGA it corresponds to a loss of about 5% of water. The endothermic effect at 300° C is due to loss of interlayer water of a well-crystallized tobermorite. On the TGA curve a corresponding break appears in the range 250° – 300°. The small endothermic peak at 760° is attributed to calcite. The exothermic peak at 830° is due to the conversion of tobermorite to wollastonite. Its intensity probably demonstrates that Al proxies for Si. A SEM photomicrograph of the abnormal tobermorite is shown in Plate XX – 1, 2. It forms groups of parallel or fan-shaped platy crystals elongated in one direction, up to 15 μ long and 165 to 200 Å thick. Some platy sheets are slightly rolled.

The 11 Å tobermorite rock was probably formed by the hydrothermal action of lime waters, formed as result of hydration of the adjacent calc-silicate rocks. The penetrating liquid reacted with quartz grains and chert fragments. It is known (Krauskopf, 1956) that the solubility of silica minerals increases significantly as the pH rises above 8.5. In thin-section, layers of

tobermorite fibres are observed replacing quartz grains. Some unreacted quartz cores and unaltered feldspars are still present, pointing to incomplete reaction. The reaction between quartz and lime is slow below 120° C. The presence of calcite only in thin veinlets cutting the tobermorite rock serves as evidence that the reaction took place in the absence of CO_2.

10 Å-tobermorite

This mineral occurs mostly in intergrowth with other members of the tobermorite group. Analysis by microprobe of a fibrous aggregate, filling a void in a larnite-rankinite-pseudowollastonite-gehlenite rock, gave the following results: CaO – 56.2%, SiO_2 – 32.1%, Al_2O_3 – 0.2% . The molecular ratio of CaO/SiO_2 = 1.7. Copeland and Schulz (1967, in Taylor, 1962) obtained a compound with a similar composition by hydration of a larnite rock at room temperature. It seems that Taylor's hypothesis, that the 10 Å tobermorite may in reality be a well-crystallized form of "CSH II" and represents a less hydrated form of the 12.6 Å mineral, analogous to the supposed relation between the 14 Å and 11.3 Å tobermorites, is correct.

On an SEM photomicrograph (Plate XXI – 2, 3) of an afwillite rock in which the presence of the 10 Å hydrate was indicated by the X-ray pattern, undulating foils and sheets were observed that were split along their length and appeared to have a corrugated structure. They might be related to the 10 Å hydrate. The 10 Å hydrate was obtained by the present author by autoclaving a larnite rock at 110° C.

Riversideite – $Ca_5H_2[Si_3O_9]_2.2H_2O$ – 9.3 Å tobermorite

Riversideite occurs less frequently than the other tobermorites and is found only in close intergrowth with other hydrates of the tobermorite group. It is probably formed by heating of the normal 11.3 Å tobermorite. Foil thickness, as evident from X-rays, is about 270° Å corresponding to 28 elementary layers.

Jennite – $Na_2Ca_8Si_3O_{30}H_{22}$ (?)

Bentor *et al.* (1963) reported an unknown mineral, occurring intergrown with some ettringite and tobermorite. X-ray investigation and the thermal behaviour of this mineral led L. Heller to the suggestion that it may be a mineral of the tobermorite group with a composition x $CaO.SiO_2.yH_2O$ where $1 < x < 2$. It was impossible to isolate pure material for chemical analysis as X-ray photographs of fibres taken from different parts of the specimen show it to be intergrown with tobermorite. The powder data agree with those of jennite, a new mineral from Crestmore, published by Carpenter *et al.* (1966). Jennite occurs in Hatrurim as vein and cavity fillings in spurrite, larnite, and gehlenite-nagelschmidtite rocks, and as a main constituent of some calcium-silicate-hydrate rocks. The mineral is associated with tobermorite minerals, ettringite, truscottite, portlandite, gypsum, calcite, and vaterite.

The larger cavity fillings and veins have a layered structure. The outer zone consists usually of jennite intergrown with tobermorite, the inner layers are formed by tobermorite and the centre by ettringite. Jennite occurs as fibrous aggregates, often fan-shaped, or as blades (Plates XXII – 2 and XXIII – 2). The optical properties are: negative elongation, parallel extinction with the blades lying on the edge. Y makes an angle of 32° – 36° with the prism axis. The mineral is biaxial negative with moderate 2V. The birefringence is higher than that of the tobermorites. nZ – nX = 0.014. The mean refractive index is n = 1.562 ± 0.002. The morphology of the jennite is shown by SEM micrographs (Plate XXI – 4, 5). It is known from X-ray examination to be the principal calcium-silicate-hydrate present in the sample. It forms parallel groups of laths about 150 μ long with a good cleavage. The thickness of the laths, as evident from X-rays, is about 320 –

400 Å. Jennite is converted in the vacuum of the SEM to meta-jennite. This form is obtained from jennite by heating to about 80° C (the basal spacing of 10.5 Å of the jennite being shifted to 8.8 Å). The basal spacing persists on heating up to 300° and above this temperature the mineral becomes X-ray amorphous. The first reflections of wollastonite appear at 600° C. On heating of fibres up to 850° , well oriented wollastonite and partially oriented larnite are obtained with their b-axes in the fibre direction (Bentor *et al.*, 1963). Grinding of jennite with water does not affect its X-ray pattern, and autoclaving at 110° does not convert it to meta-jennite.

The chemical analysis of a rock consisting predominantly of jennite reveals sodium to be present only as traces. It seems therefore that sodium is not incorporated in the jennite, a possibility acknowledged by Speakman and Taylor themselves (personal communication). In Fig. 12C the DTA of the jennite rock is shown. The curve exhibits a broad endothermic effect with a maximum at 425° C due to dehydration. The exothermic effect at 890° C is due to the crystallization of a mixture of wollastonite and larnite. Jennite is formed by hydration of calc-silicate rocks. The formula proposed by Carpenter *et al.* (1966), has to be confirmed. No sodium ions seem to replace calcium.

Gyrolite – $Ca_2[Si_4O_{10}].4H_2O$

This compound was discovered as a natural mineral in Skye, Scotland, by Anderson (1851, in Taylor 1964), and was found later in many other localities. It is a very rare mineral at Ḥatrurim, where it occurs in veins as radiating fibrous aggregates. The elongation is negative, the mean index of refraction is about 1.54. nZ – nX = 0.008. The X-ray powder pattern is almost identical with that quoted by Mackay and Taylor (1954). The mineral appears associated with truscottite, afwillite, tobermorite, and ettringite.

Meyer and Jaunarais (1961) and Harker (1960, 1964) synthesized gyrolite at temperatures as low as 145° – 150° C. In the present investigation gyrolite was obtained with afwillite and some 14 Å – tobermorite by autoclaving of a larnite rock in excess of water at 110° C.

Gyrolite is formed by hydrothermal alteration of calc-silicate rocks.

Truscottite – $Ca_2[Si_4O_{10}].H_2O$

The mineral was discovered in 1914 in Sumatra by Hövig (in Mackay and Taylor, 1954) It was described recently from the Toi mine (Japan) by Minato and Kato (1967). According to Taylor (1964), reviewing syntheses of truscottite, it appears to form as a stable product at a temperature range from somewhat below 200° to over 300° C.

Truscottite is very rare at Ḥatrurim, where it is found in some calc-silicate rocks and their weathering crusts as spherulitic aggregates, up to 0.4 mm across (Plate XX – 4), or as fibres of low birefringence, negative elongation and straight extinction. n = 1.55 ± 0.002. It was identified by its X-ray pattern which is identical with that given by Mackay and Taylor (1954).

Truscottite is a late hydrothermal mineral derived by alteration from calc-silicate rocks.

Afwillite – $Ca_3[SiO_3.OH]_2.2H_2O$

Afwillite is a very rare mineral. It occurs at Kimberley, S. Africa (Parry and Wright, 1925); Scawt Hill, N. Ireland (Tilley, 1930); Crestmore, California (Switzer and Bailey, 1953); Boissejour, France (Grünhagen and Mergoil, 1963), near Mayen, Laacher See (Jasmund and Hentschel, 1964), Azerbaidzhan (Annenkova, 1964). It was described at Naḥal Ayalon by Gross *et al.* (1967).

In these occurrences, excluding Naḥal Ayalon, afwillite is a late hydrated phase connected with rocks formed by contact metamorphism. In the Mottled Zone, afwillite (Gross *et al.*, 1967)

occurs in close paragenesis with ettringite, portlandite, tobermorite, hillebrandite, hydrocalumite, gypsum, foshagite, aragonite, and calcite. It is relatively abundant as vein and cavity fillings in calc-silicate rocks. It occurs as a rock-forming mineral in several samples from Hatrurim, from the upper part of the stratigraphic section equivalent to the Taqiye Formation. The rock-forming afwillite appears as a groundmass of radial aggregates of fibres or as spherulites (Plate XXII – 6). Afwillite occurring in veins lines the walls while the interior is filled by tobermorite and ettringite. The crystals show a prismatic or tabular habit and are inclined to the walls of the veins. They are up to 2 mm in length, the faces of some of them being pitted and corroded by calcite (Plate XXII – 4). Afwillite filling cavities occurs as sheaflike aggregates. The mineral is white or colourless, has a perfect {001} and a poor {100} cleavage (indices according to the optical orientation of Parry and Wright, 1925). The prismatic crystals are elongated in the b-direction and the tabular ones parallel to {101}. The optical properties are: biaxial, positive, 2V ~ 50°, dispersion $r < v$, $X \wedge c = 31°$, elongation (±), $nX = 1.618$, $nY = 1.620$, $nZ = 1.634$. $nZ - nX = 0.016$ (all ± 0.002). The mineral dissolves in HCl and is stained orange-red by alizarin.

In Fig. 12A the DTA and TGA curves of an afwillite rock are shown. The water is expelled in a broad and asymmetric peak beginning at 320° C, with a maximum at 355° – 390° C. A small exothermic effect at 845° – 850° is due to crystallization of larnite with some rankinite. It is a secondary mineral formed hydrothermally at 110° – 160° C according to Heller and Taylor (1952b). In hydration experiments performed by the present author, afwillite was one of the main phases obtained by autoclaving larnite rocks at 110° C.

Dicalcium-silicate-hydrate – α-$Ca_2[HSiO_4]OH$

This compound was synthesized by Thorvaldson and Shelton (1929), Wells *et al.* (1943) and others. It is readily formed hydrothermally at temperatures between 100° and 200° C. The crystal structure was studied by Heller (1952). In its cryptocrystalline form it was identified only by DTA curves (Kalousek *et al.*, 1954). Until now it was not known as a natural mineral and this is its first report as such. The mineral occurs as a cavity filling in melilite-larnite rocks. It occupies the centre of the cavity and is surrounded by tobermorite and jennite. The dicalcium-silicate is also a minor constituent of rocks consisting predominantly of calcium-silicate hydrates. In microscopic investigation of samples in which it appears, well-crystallized aggregates of prismatic crystals of high relief, positive elongation and parallel extinction were observed. Twinning is simple or cruciform (Plate XXIII – 2, 3). The mineral is biaxial positive, $nX - nZ = 0.007$. In the SEM photomicrograph orthorhombic tablets (Plate XX – 3) characteristic of this compound are observed. The strongest spacings recorded were: 4.22 (vs), 3.90 (s) and 3.27 Å (vs). A DTA-curve of a rock in which the dicalcium-silicate-hydrate is one of the main phases is given in Fig. 12, curve D. It exhibits an endothermic effect in the range of 470° – 480° C and an exothermic one at 880° – 900° C, showing thereby that it has a high CaO/SiO_2 ratio. Heating the specimen to 800° C gave larnite. Microprobe analysis of this sample confirms the ratio of CaO/SiO_2 to be 2. The dicalcium-silicate-hydrate was obtained as one of the minor phases by autoclaving a sample of larnite-mayenite-brownmillerite rock at 110° C with a small amount of water.

e. Phyllosilicates

Apophyllite – $KFCa_4[Si_4O_{10}]_2.8H_2O$

Apophyllite in nature occurs mainly in: amygdules in basalts, cavities in granites, fissures in metamorphic rocks, and in calc-silicate rocks, where it is sometimes an alteration

product of wollastonite. (Bailey, 1941; Vorma, 1961; Kostov, 1962; Tatekava, 1969; Chukhrov *et al.*, 1973).

The apophyllite of Hatrurim is associated with tobermorite, calcite, quartz, and occasionally with stilbite. It occurs in veinlets, fissures, and cavities of a tobermorite rock in the Hazeva Formation, and is especially abundant in the altered sandstones and conglomerates of the Hazeva Formation (Kolodny *et al.*, 1973). In thin-section, single crystals of apophyllite occur in the centre or at the borders of quartz grains replaced by fibrous tobermorite. Quartz grains replaced in the centre by apophyllite and surrounded by bundles of stilbite were also observed. Apophyllite occurs as colourless, tabular or prismatic crystals terminated by dipyramids up to 0.6 mm in diameter, with perfect basal cleavage on {001} (Plate XXIV – 1). Twinning on {111} was also observed. The mineral is uniaxial negative, n = 1.538 ± 0.002. It is distinguished by its anomalous ultra-blue to brown interference colours. Some crystals are zoned (Plate XXIV – 6). An analysis by electron microprobe (by Y. Kolodny) gave the following results: K_2O – 5.1%, SiO_2 – 56.4%, CaO – 26.2% . The DTA-curve of apophyllite (Fig. 13) exhibits two endothermic effects, a strong one at 310° and a second, weak one at about 400° . At about 395° a weak exothermic effect is observed. The DTA data agree with those given by Kostov (1962) for a specimen from Bulgaria.

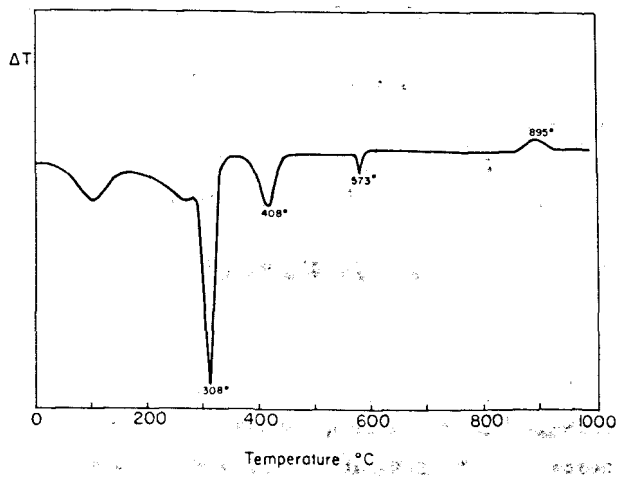

Figure 13. DTA curve of apophyllite (sample SG 625).

Apophyllite is a secondary mineral and is formed through the action of hydrothermal solutions, rich in lime and containing some fluorine, on quartz grains at temperatures below 300° (the temperature of its decomposition) and possibly at much lower temperatures. Orthoclase present in the sandstone served as a source of the potassium.

Pyrophylite – $Al_2[Si_4O_{10}](OH)_2$

Pyrophylite was found in two samples of melilite rocks. It occurs in voids and veinlets as groups of lamellae, or as radiating spherulitic aggregates. The optical properties are: elongation positive, biaxial-negative with a moderate 2V, nZ – nX = 0.045. The microscopic identification was verified by X-ray diffraction. On the DTA-curve an endothermic effect at about 760° C was observed due to dehyroxylation. The mineral is associated with tobermorites and lizardite. It was formed by hydrothermal alteration of the melilite rocks.

Biotite – $K(Mg, Fe)_3(AlSi_3O_{10}](OH, F)_2)$

Biotite is found as detrital flakes in the silt fraction of a low grade metamorphosed marl from Kefar Uriya, and in the Hazeva sandstone at Hatrurim. In some quartz grains minute inclusions of hexagonal scaly habit, about 80 μ across, were observed. The mineral is pleochroic from colourless or yellowish to reddish brown. It is biaxial negative with 2V nearly zero and dispersion r < v.

Xanthophyllite – $Ca(Mg,Al)_3[Al_2Si_2O_{10}](OH)_2$

Xanthophyllite occurs usually in talc-and chlorite-schists and in metasomatically altered limestones (Knopf and Lee, 1957). The mineral was identified optically in a sample of melilite

rock from Hatrurim, associated with melilite, spinel, vesuvianite, rankinite, and garnet. The colour of the mineral is bottle green. Cleavage is micaceous on 001 . It is pleochroic with: X-pale olive green, Z,Y-olive green. nY = 1.662 ± 0.002, nZ − nX = 0.012, biaxial negative, 2V ~ 10° . The X-ray pattern resembles that of the xanthophyllite from Crestmore (Forman, 1951). Christophe-Michel-Levy (1964) reported that xanthophyllite was obtained during the hydrothermal synthesis of melilite at 500° C at a vapour pressure of 500 bar. The xanthophyllite of Hatrurim seems to have been formed by hydrothermal alteration of the melilite rocks at temperatures probably lower than those suggested by Christophe-Michel-Levy.

Chlorite – $(Mg, Fe, Al)_6\ [(Si, Al)_4 O_{10}](OH)_8$

Chlorite is very rare at Hatrurim. Two varieties of chlorite were observed:

1) In most instances it occurs as fine-grained scaly aggregates of dark green colour in spurrite rocks, together with iron sulfide and organic matter. The scales are up to 17 μ across. They are biaxial negative with a small 2V. Pleochroic in green shades. n = 1.660 ± 0.002. Birefringence weak. According to the optical properties this chlorite is probably thuringite.

2) More rarely chlorite occurs in cavities of weathered carbonate-zeolite rocks as aggregates, characterized by a 7 Å spacing. On heating to 500° C this spacing weakens and the 14 Å one appears. This chlorite is destroyed by hot HCl. It seems to be a chamosite.

Illite-$K_{0.5-0.75}$ $(Al, Fe, Mg)_2[(Si, Al)_4 O_{10}](OH)_2$

This mineral occurs in small amounts in bituminous marls and gypsiferous rocks of the Ghareb Formation. Identification is based on DTA and X-ray examination.

The illite is a primary, unchanged sedimentary mineral.

The smectite group

Montmorillonite is by far the dominant clay of the shales, marls and gypsiferous rocks of the Ghareb Formation. It is less common in the metamorphosed marls equivalent to the Taqiye Formation. The clay occurs as fine-grained aggregates of pale yellow, grey or bricklike colour. The indices of refraction, depending on composition and hydration state, vary in the range of 1.480 to 1.580, and the birefringence from 0.020 to 0.35. The crystal size as measured by peak broadening on the diffractogram d_{001} is about 40 Å.

Identification of species is based on X-ray, DTA, microchemical test, chemical analyses and determination of phases obtained after heating the clay to 1000° C.

Montmorillonite

The most widely distributed montmorillonite in the Mottled Zone is the trioctahedral one, the dioctahedral being less common.

In Table 26, column 3 the result of a chemical analysis of a ditrioctahedral montmorillonite is given. After subtraction of apatite the following structural formula is obtained:

$(Ca_{0.13} Mg_{0.21} Na_{0.12} K_{0.10})(Al_{2.09} Fe^{3+}_{0.57}$
$Ti_{0.10} Mg_{1.24})(Si_{7.75} Al_{0.25})O_{20}(OH)_4$

Curve D on Fig. 14 is a curve of a "normal" montmorillonite according to the definition of McKenzie (1957). It shows a large, double low-temperature peak due to loss of absorbed moisture, a small endothermic peak at 710° C, and an S-shaped endothermic-exothermic peak system at 825° C and 850° C respectively. The peaks at 710° and 825° C are due to dehydroxylation and the exothermic one is attributed to the formation of spinel, cristobalite and hematite.

Curve C is a curve of an "abnormal" dioctahedral montmorillonite. The sample exhibits an endothermic peak at 540° C. The S-shaped peak

Table 26. Analyses of clay minerals

	1	2	3	4	5	6	7	8	9
SiO_2	45.08	46.24	47.39	25.23	30.70	24.1	27.60	67.66	23.52
Al_2O_3	10.18	12.87	11.90	9.95	12.25	9.0	8.05	11.12	8.66
Fe_2O_3	1.86	2.26	4.69	14.78	12.07	11.6		2.22	15.28
FeO	neg.	neg.	neg.	neg.	n.d.	n.d.	neg.	n.d.	0.20
Cr_2O_3	7.68	6.67	n.d.	n.d.	n.d.	n.d.		n.d.	n.d.
TiO_2	0.33	0.37	0.81	0.65	n.d.	n.d.	1.03	0.48	n.d.
MgO	5.37	5.20	6.04	16.93	20.80	27.4	38.82	5.16	24.78
CaO	2.45	2.33	5.05	5.89	3.46	2.6		1.17	5.95
MnO	n.d.	n.d.	0.07	0.21	0.81	n.d.	2.13	n.d.	0.39
K_2O	0.03	0.01	0.44	0.01	n.d.	n.d.		0.10	0.13
Na_2O	0.12	0.08	0.40	0.07	n.d.	n.d.		0.10	0.44
P_2O_5	0.64	0.45	2.25	2.06	2.21	1.7		0.67	2.00
SO_3	0.39	0.08	0.14	2.91	n.d.	n.d.		neg.	n.d.
H_2O+	7.21	10.12	9.77	12.62	10.35	9.0		11.28	14.27
H_2O-	16.97	14.67	10.77	8.51	6.35	13.3	22.37	n.d.	2.96
Org. mat.	n.d.	n.d.	n.d.	n.d.	0.10	n.d.		n.d.	n.d.
Total	98.31	101.35	99.72	99.82	99.10	98.7	100.00	99.96	98.58
				Number of ions					
Si	7.67	7.48	7.75	3.18	3.42	2.92	2.92		2.80
Al	8.00	8.00	8.00	4.00	4.00	4.00	3.92		4.01
	0.33	0.52	0.25	0.82	0.58	1.08	1.00		1.21
Al	1.70	1.93	2.09	0.64	1.02	0.20			
Fe^{3+}	0.24	0.28	0.57	1.40	1.00	1.06			1.37
Cr^{3+}	1.03 4.00	0.85 4.00	4.00	5.32	5.54	6.14		Fe^{+2}	0.02 5.82
Ti	0.04	0.05	0.10	0.06			0.08		
Mg	0.99	0.89	1.24	3.20	3.46	4.88	6.16		4.43
Mn				0.02	0.06				
Ca	0.24	0.31	0.13	0.16					
Mg	0.38 0.64	0.37 0.70	0.21 0.56	0.17					
Na	0.02	0.02	0.12	0.01					
K			0.10						0.10 0.12
									0.02
OH	4.00	4.00	4.00	4.00	7.68	7.30	8.00		8.00
O	20.0	20.0	20.00	5.00	10.00	10.00	10.00		10.00
H_2O	2.07	3.48	3.38	1.16					

1. Volkonskoite, Nahal Ayalon. Sample SG. 131. 2. Volkonskoite, Hatrurim. Sample SG 157. 3. Montmorillonite with some apatite, Hatrurim. Sample SG. 413. 4, 5. Lizardite with some montmorillonite and apatite as impurities. Hatrurim. Samples SG 408 and SG. 503 6. Lizardite with apatite as impurity. Hatrurim. Sample SG. 361. 7. Lizardite from Hatrurim, recalculated from bulk analysis of a lizarditic limestone after deduction of calcite and apatite. Sample SG. 364. 8. Mixture of silica "gel" (?) and Al-serpentine. Hatrurim. Sample SG. 333. 9. Lizardite with apatite as impurity. Hatrurim. Sample SG. 159.
Analyses 1–4, 7, 9 by M. Gaon. Analyses 5, 6 and 8 by S. Ehrlich.

characteristic of "normal" montmorillonites is absent.

Montmorillonite of non-metamorphosed phosphorites is dehydroxylated at 720° C. The montmorillonite of the thermally-metamorphosed phosphorite does not exhibit the low-temperature endothermic peak, and the dehydroxylation peak appears at 565° C. It seems that this montmorillonite was dehydroxylated at the time of the thermal event and was later rehydroxylated. The difference of the dehydroxylation temperatures of both types is about 150° C. This agrees with the experiments of Heller *et al.* (1962).

Saponite

This clay mineral is relatively abundant. The spacing $d_{0.01}$ = 14.8 Å collapses after heating, to 9.7 Å. The DTA-curve of a specimen of saponite mixed with an Al (?)-serpentine is shown in Fig. 14, curve E. The endothermic effects characteristic of the saponite are: the low

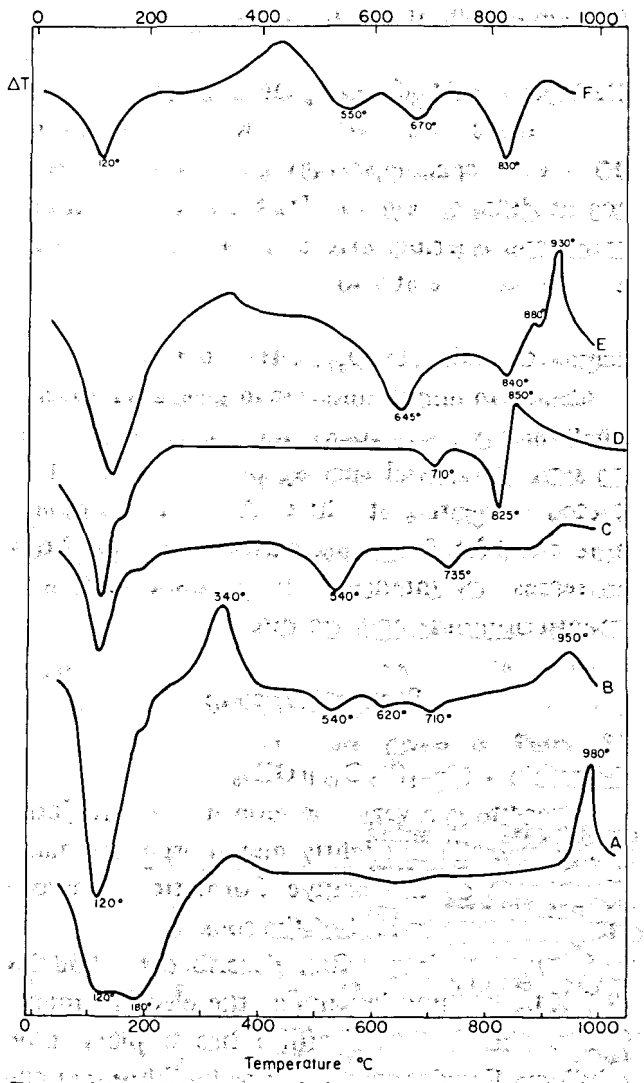

Figure 14. DTA curves of clay minerals: A – allophane (sample SG 337); B – volkonskoite (sample SG 131); C – nontronite (sample SG 524); D – trioctahedral montmorillonite (sample SG 169); E – saponite with Al – serpentine (sample SG 413); F – illite with montmorillonite (sample SG 202).

temperature peak at 100° – 200° C due to loss of absorbed moisture, and a single peak at 840° C due to dehydroxylation. This peak is followed by an exothermic one at 880° C. The phases formed upon dehydroxylation are: enstatite, cristobalite, spinel and sillimanite. The SEM micrograph (Plate XXIV – 4) of this sample shows its platy character, and a notable tendency to elongation.

Nontronite

Nontronite occurs in some marls and in the weathering crusts of melilite rocks, associated with brucite, tobermorites and a serpentine mineral. It is brown and slightly pleochroic from pale brown to brown. It does not swell with glycol. The dehydroxylation peak on the DTA curve appears in the range of 450° – 540°C and the weak exothermic effect at 845° C. The nontronite of the weathering crust was formed by the alteration of the ferrian-gehlenite.

Volkonskoite

Volkonskoite is a dioctahedral clay of the montmorillonite group in which Cr substitutes for Al in the octahedral layer. The mineral is widely distributed throughout the lower part of the Hatrurim Formation. The rocks of this sequence are cut by numerous irregular and winding veins which range in width from a few millimetres to a few centimetres. They may reach a few metres in length (Gross and Bentor, 1966; Gross *et al.*, 1967). Transitions between these veins and the host rocks may be sharp or gradational. Apart from the volkonskoite the veins are filled by calcite and small amounts of gypsum, anhydrite, halite, apatite or aragonite. The volkonskoite is bluish-green and earthy. At Nahal Ayalon round concretions up to 5 mm in diameter of grass-green volkonskoite occur in an argillaceous limestone. In immersion liquids the colour varies from grass-green to pale bluish-green. The optical properties of this clay are: non-pleochroic; the elongation of the flakes is positive. The mineral is biaxial negative with a small 2V. The mean index of refraction varies in a broad range: n = 1.496 – 1.556, nZ – nX = 0.020. The mineral swells with glycol and the basal spacing – 14.5 Å – shrinks to 9.6 Å after heating to 500°.

Two analyses of volkonskoite are given in Table 26, columns 1 and 2. The structural formulae, calculated after subtracting the impurities as gypsum and apatite, are:

1) $(Ca_{0.24}Mg_{0.38})(Al_{1.70}Fe^{3+}_{0.24}Cr^{3+}_{1.03}Mg_{0.99}Ti_{0.04})(Si_{7.67}Al_{0.33})O_{20}(OH)_4$

2) $(Ca_{0.31}Mg_{0.37})(Al_{1.93}Fe^{3+}_{0.85}Cr^{3+}_{0.85}Mg_{0.89}Ti_{0.05})(Si_{7.48}Al_{0.52})O_{20}(OH)_4$

Chemical analysis reveals a Cr_2O_3 content higher than in any other occurrence of volkonskoite described so far (Serduchenko, 1933; Kiselev, 1938; McConnell, 1953; Andritzky, 1965). A DTA-curve for volkonskoite from Israel has been published by Holdridge and Walker (1968). The sample examined was a mineral mixture containing some 4.5% Cr_2O_3, appreciable lower than typical samples from the area. The DTA-curve of a typical volkonskoite from Hatrurim is given in Fig. 14, curve B. The interlayer water is expelled with a broad low-temperature effect with a maximum at 120° C. The small exothermic peak at 340° C is due to crystallization of eskolaite (Cr_2O_3). Three small endothermic peaks at 545°, 620° and 715° are due to expulsion of hydroxyls. At 950° C another exothermic effect appears and is attributed to the crystallization of new phases. The phases obtained by X-raying of a specimen heated at 1000° C are: cristobalite, eskolaite, enstatite, and spinel. The volkonskoites of Ural and Caucasus are genetically connected with ultrabasic rocks containing Cr-minerals. Andritzky and McConnell leave the problem of the genesis of the volkonskoites open. The volkonskoite of the Hatrurim Formation was formed by hydrothermal alteration. Along the numerous cracks formed by cooling of the metamorphosed rocks, Al, Si, Fe, Cr and Mg are leached by ascending solutions from the host rocks and crystallize later as Cr-clay. The chromium came from the black shales and from phosphorites, in which it is a typical trace element.

Kaolinite – $Al_4[Si_4O_{10}](OH)_8$

Kaolinite occurs only in one sample of a chalk from Hatrurim. It was identified in the clay fraction together with montmorillonite. After heating to 600° it is X-ray-amorphous.

Halloysite – $Al_4[Si_4O_{10}](OH)_8.4H_2O$

Identified in a marl from Kefar Uriya by the 10 Å basal spacing,shrinking to 7.4 Å after heating at 200° C. On the DTA curve it exhibits a small endothermic effect at 540° C and a weak exothermic one at 930° C.

Sepiolite – $Mg_4[Si_6O_{15}](OH)_2].6H_2O$

Occurs in minor amounts in several samples of chalk and gypsum rocks. Identified by its X-ray pattern. The basal spacing of 12.5 Å is not affected by heating at 300° C. Above this temperature the 12.5 Å spacing weakens and the 7.6 Å increases in intensity. It is associated with montmorillonite and lizardite.

Serpentine group

Lizardite – $Mg_6[Si_4O_{10}](OH)_8$

Lizardite is a very common mineral at Hatrurim, especially in slightly metamorphosed marly limestones of the Taqiye Formation, where it constitutes up to 35% of the rock.

The mineral was first described by Midgley (1951). Examination under the electron microscope shows that lizardite has a platy morphology. Powder examinations by Whittaker and Zussman (1956) on Midgley's samples suggested that it has a single-layered unit cell and is pseudo-orthohexagonal. This was confirmed by the single-crystal analysis of Rucklidge and Zussman (1965). Lizardites generally show some chemical substitution of trivalent Al and Fe ions for Mg or Si, or both. According to Gillery (1959),platy crystals with high Al content may have a one-layered or six-layered orthohexagonal cell, those with the highest Al content having six-layered structure. Recent electron microprobe studies by Page (1968) show that lizardite is consistently more iron-rich than other serpentine minerals. The natural six-layered serpentines were described by Brindley

and Von Knorring (1954), Zussman and Brindley (1957), and Bailey *et al.* (1960). An iron-lizardite was described by Chie Pin-Wen *et al.* (1964).

Lizardite occurs either homogeneously disseminated throughout the rock or in aggregates up to 30 μ across. The colour of the mineral in thin section is usually a very faint pale yellow, brownish, or greenish. Some specimens are turbid because of the presence of a fine hematite dust. In a specimen from a calcareous sandstone a white lizardite was observed. The mineral is extremely fine-grained. The crystal size calculated from the X-rays: d_{001} = 100 – 170 Å. Preparates for optical investigation are homogenized or intimately mixed with some iron oxides. The mineral is biaxial negative with small 2V, n = 1.550 – 1.558 (± 0.002). nZ – nX = 0.008 – 0.010. X-ray diffraction data of different lizardites are given in Table 27. The basal spacing varies from 7.40 Å to 7.19 Å, decreasing with increasing Al content (Zussman and Brindley, 1957). X-ray diffraction shows that most of the specimens are not a pure phase but contain some montmorillonite, apatite, hematite or bayerite.

In Table 26, columns 4, 5, 6, 7 chemical analyses of serpentines are given, calculated on the basis of 18 (O, OH) and assuming that the tetrahedral layer is completely filled. Sample 7 is a pure Mg-lizardite, samples 4, 5, 6 have some montmorillonite as impurity. Iron, which was present in all other samples, was incorporated in the formula if no X-ray, DTA, or microscopic evidence was found for the presence of hematite or other iron oxides. Highly sensitive DTA runs in the range up to 400° C were made for the detection of Al $(OH)_3$ phases and, if found, TGA runs were made and the amount of Al $(OH)_3$ was calculated according to the loss

Table 27. Diffraction data for serpentine minerals

Sample	1		2		3		4		5		6		
hkl	d(meas.)Å	I	d(meas.)Å	I	d(meas.)Å	I	hkl	d(meas.)Å	I	d(meas.)Å	I	hkl	d(meas.)Å	I
001	7.36	vvs	7.25	vvs	7.19	vs	006	7.13	vvs	7.08	vvs	002	7.2	m
020	4.62	m	4.49	m	4.59	m	020,110	4.57	m	4.49	m	020	4.55	vs
002	3.67	s	3.64	s	3.60	s	022,112	4.48	vw					
220	2.65	m	2.63	w			024,114	4.21	vw					
201	2.51	vs	2.495	vs	2.51	vs	026,116	3.85	vw	3.86	vw			
003	2.41	s	2.38	w	2.39	m	027			3.66	w			
202	2.15	m	2.14	m	2.14	w	0012	3.56	s	3.55	s	004	3.57	m
004	1.84	w	1.84	vw	1.84	w	028,118	3.48	vw	3.47	wv			
310	1.74	w	1.74	w	1.74	vw	029	3.29	vw					
311	1.69	vw			1.66	vw	0210	3.13	vw					
060	1.536	s	1.532	s	1.538	s	202,132	2.63	m	2.63	m			
061,204	1.504	m	1.497	w			204	2.58	m	2.57	w	201	2.59	m
005	1.461	vvw			1.47	w	206	2.48	w	2.48	m	202	2.50	m
							0018,208	2.38	s	2.37	m		2.30	vw
							209			2.31	vw		2.38	vw
							2010	2.25	w	2.25	vw			
							2012	2.13	vw	2.13	vw			
							2014	2.00	w					
							0220	1.94	vw					
							2016	1.88	vw					
							310,150	1.735	w					
							0224	1.67	w					
							0420,2022	1.57	w					
							060	1.531	m	1.530	m	060,062	1.53	m

1. Lizardite from a matrix of a metamorphosed sandstone, Sample SG. 192. 2. Lizardite, lizarditic limestone, Sample SG 429. 3. Lizardite, lizarditic limestone, Sample SG. 503. 4. Al-serpentine, calcite-garnet rock, Sample SG. 333. 5. Al-serpentine, slightly metamorphosed "marl", Sample SG 316. 6. Poorly crystallized serpentine, from weathered melilite rock, Sample SG 281.

of water in the range 200° – 350° C. In no case more than 2.5 per cent of $Al(OH)_3$ was found. It was not possible to deduct the montmorillonite impurity when present.

It was found that in all cases Al substitutes for Si in the tetrahedral layer. The octahedral layers are filled entirely only in the case of pure Mg-lizardite; in all other cases Fe^{3+} and Al proxy for Mg, and the octahedral total is low. The same feature, a deficit in octahedral total, is reported for lizardites from other localities.

The calculated structural formulae for the lizardites are:

SG. 408 – $(Si_{3.18}\,Al_{0.82})(Mg_{3.20}\,Al_{0.64}\,Fe_{1.40})(OH)_8\,O_{10}$

SG. 503 – $(Si_{3.42}\,Al_{0.58})(Mg_{3.46}\,Al_{1.02}\,Fe_{1.00})(OH)_8\,O_{10}$

SG. 361 – $(Si_{2.92}\,Al_{1.08})(Mg_{4.88}\,Al_{0.20}\,Fe_{1.06})(OH)_8\,O_{10}$

SG. 364 – $(Si_{2.92}\,Al_{1.00})(Mg_{6.16}\,(OH)_8\,O_{10}$

SG. 159 – $(Si_{2.80}\,Al_{1.20})(Mg_{4.43}\,Fe^{+3}{}_{1.37}\,Fe^{+2}{}_{0.02})(OH)_8\,O_{10}$

The DTA and TGA curves of the lizardites are given in Fig. 16.

Lizardites dehydroxylate at lower temperatures than do antigorites. Low-temperature endothermic peaks represent the loss of absorbed water, and the broad and deep endothermal effect with maximum at 625° – 635° is due to dehydroxylation. The TGA curve shows

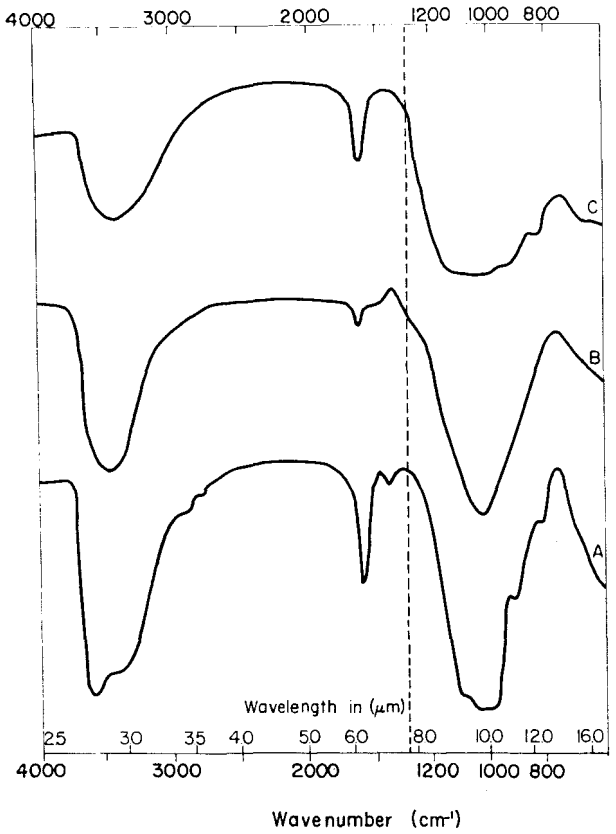

Figure 15. Infrared absorption spectra of clay minerals: A – volkonskoite (sample SG 131); B – montmorillonite (sample SG 413); C – "Isotropic matrix" – consisting of silica gel (?) and Al-serpentine (sample SG 333).

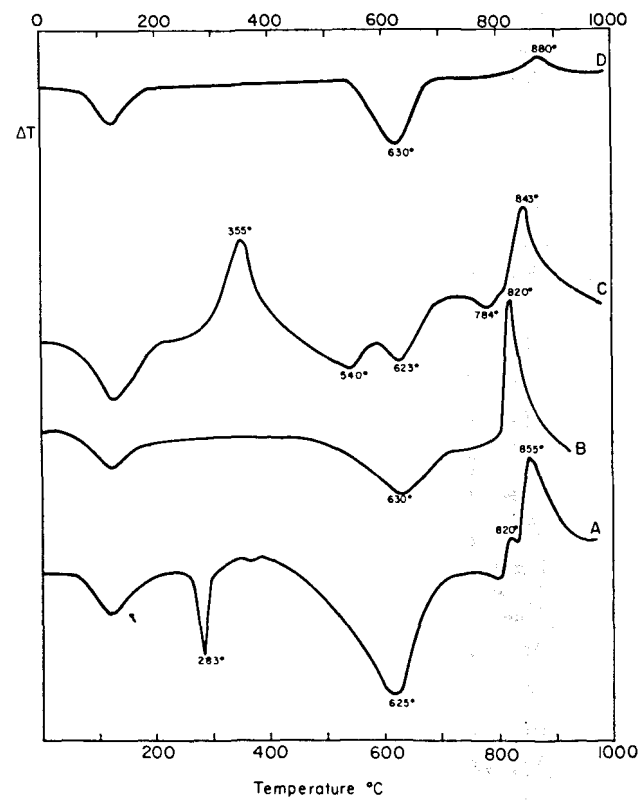

Figure 16. DTA curves of serpentine minerals: A – Al-serpentine with lizardite (sample SG 364a); B – lizardite (sample SG 429); C – poorly crystallized serpentine mineral with montmorillonite (sample SG 281); D – Al-serpentine (sample SG 420).

the water to be lost in the range of 400° – 750° C. At 820° – 830° C the curves exhibit strong exothermic peaks, related to the formation of forsterite in the case of pure Mg-serpentine, and of a mixture of forsterite ± spinel, and hematite in lizardites with substitutions of Al and Fe, as estimated by X-ray examination of those specimens after heating to 1000° C. The endothermic effect at 180° C is due to bayerite as an impurity. The basal spacing 7.3 Å is not affected by treatment with boiling HCl 1:1, but in the DTA curve no more peaks are visible. The basal spacing remains unaffected by heating up to 600° C. After prolonged heating at this temperature a broad reflection appears in some specimens at about 13.6° – 14.6 Å and in others at 12.6Å. On heating to 700° C an additional spacing at 11.3 Å is observed, beside the spacings of olivine. According to Nelson and Roy (1954, 1958), these reflections may belong to transition phases on the course of transformation to olivine. The 14 Å spacing is characteristic of a two-layered cell: 2 x 7.3 = 14.6 Å.

The I.R. spectra of typical lizardites from Hatrurim, recorded by S. Yariv of the Hebrew University, are presented in Fig. 17. They can be divided into two groups: Curve A is typical for magnesium lizardites (Table 26, analyses 6, 7) with basal spacings in the range 7.36 – 7.28 Å and is similar to curves of lizardites given by Brindley and Zussman (1959), Veniale *et al.* (1963), and Luce (1971). The strong band at 3680 cm^{-1} appears at low wave numbers compared to other published lizardite spectra. Curve B is typical of Al-substituted lizardites (Table 26, analyses 4, 5) with basal spacings in the range 7.19 – 7.25 Å. The band at 3680 cm^{-1} is absent. The broad and strong absorption band observed on both curves in the range 3700 – 3200 cm^{-1} may be interpreted as due to a combination of free hydroxyl ions and hydrogen-bonded water molecules.

The dehydroxylation of group A, as observed on DTA curves, occurs at about 630° and

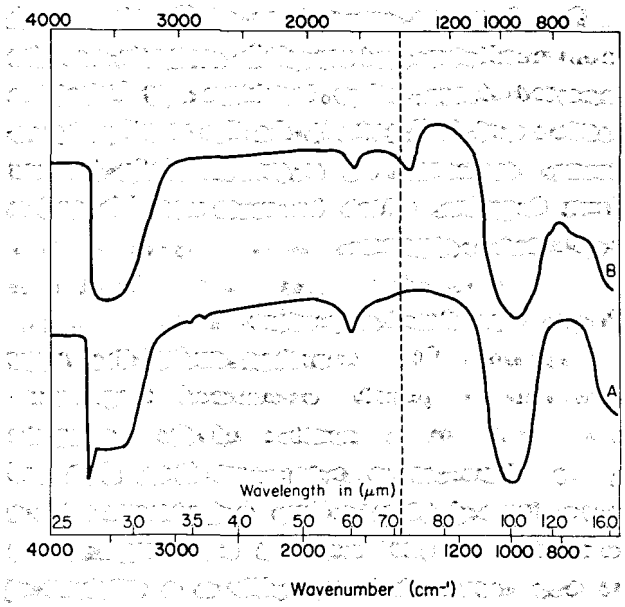

Figure 17. Infrared adsorption spectra of lizardites: A – sample SG 408; B – sample SG 503.

of group B at about 625° C.

The lizardites from Hatrurim were formed by dedolomitization of the dolomitic biomicrites of the upper Ghareb or Taqiye Formation (Danian). The sediments underwent heating during the thermal event to a temperature that probably did not exceed 400° C. During this phase water vapours enriched in CO_2 were liberated from the underlying sediments which were heated to a much higher degree. These waters penetrated the overlying sediments, dissolving material from them. From these solutions, which were saturated in Mg, Si and Al, lizardites crystallized during the cooling phase. The reaction might be as follows:

$$6CaMg(CO_3)_2 + 4(SiO_2 + Al_2O_3) + 4H_2O \longrightarrow (Si, Al)_4 (Mg, Al)_6 (OH)_8 O_{10} + 6CaCO_3 + 6CO_2$$

In thin sections of some of these rocks, relict rhombohedra, built of micritic calcite and bordered by iron pigment, are observed. The trace element content of Co and Ni in the lizardites also points to their sedimentary origin as it does not exceed a few parts per million. In Landenian marls, lizardite is usually associated with saponite.

The frequent association of lizardites with montmorillonite and especially saponite was also reported from other localities by Ushakova (1959) and Ball (1964). As the weathering intensity increases, Mg is preferentially leached from lizardite, which becomes unstable and is converted to saponite.

Poorly crystallized serpentine

Lapham (1961) described under the name deweylite a poorly crystallized magnesium-silicate-hydrate, a member of the serpentine group, deficient in octahedral ions, that had been formed from colloid suspensions at low temperature. The work of Faust and Fahey (1962) shows that deweylite is a mixture of stevensite and clinochrysotile, or lizardite. Speakman and Majumdar (1971) synthesized "deweylite" by hydrothermal treatment of magnesia-silica gels of various compositions and at temperatures up to 180° C. Their synthetic preparations were mixtures of poorly crystallized talc and poorly crystallized serpentine.

A very badly crystallized serpentine mineral occurs in weathering crusts of melilite rocks in close association with a dioctahedral montmorillonite, brucite and tobermorite. It is reddish brown and has an index of refraction of about 1.500 ± 0.002. Its X-ray pattern consists only of weak and broad peaks (Table 27, column 6). The crystal size, as calculated from peak broadening, is about 60 Å. The thermal behaviour and the resistance to acid attack agree with the observations of Lapham. The DTA-curve of a mixture of this serpentine with montmorillonite is given in Fig. 15,curve C. The curve exhibits 4 endothermic peaks. The low-temperature peak at 125° C represents the loss of absorbed water. The endotherms at 540° and 784° C are due to the dehydroxylation of the montmorillonite (probably a nontronite). The effect at 623° C is attributed to a serpentine mineral. The exothermic peak at 843° C indicates the crystallization of new phases. X-ray examination shows the presence of enstatite, forsterite and hematite. The small exothermic peak at 355° C points probably to crystallization of a ferric gel.

The mineral was formed by weathering of a melilite rock. Its association with brucite and tobermorite point to a temperature of formation that did not exceed 100° C.

Al – serpentine

The most commonly occurring clay in the retrograde metamorphic rocks of the Taqiye Formation is a 7 Å clay which is usually trioctahedral, rarely dioctahedral. It is insoluble in cold HCl 1:1. The basal spacing of 7.07 – 7.13 Å does not collapse on heating to 600° C and is still visible at 700° C, although slightly weaker. The clay does not swell with ethyleneglycol treatment. The X-ray diffraction pattern (Table 26, columns 4, 5) is almost identical to that of natural and synthetic aluminous serpentines. Naturally occurring Al-serpentines are described by Bailey and Tyler (1960) and Zhukov (1971). Synthetic ones are discussed by Gillery (1959), Brindley and Von Knorring (1954), and Zussman and Brindley (1957). The general composition of the synthetic Al-serpentines is: $(Si_{4-x}Al_x)(Mg_{6-x}Al_x)O_{10}(OH)_8$, where x may vary in the range 0 – 2.50. According to Gillery (1959) the serpentines with a low Al content have a single-layer unit cell, and the Al-rich ones a six-layered cell.

The clay is of light cream colour and appears by optical examination to be a single phase n = 1.506 – 1.514. X-ray examination reveals only the presence of Al-serpentine. Crystal size as calculated from peak broadening is, d_{001} = 105 – 175 Å. In a SEM photomicrograph (Plate XXIV – 3) of a fresh rock surface consisting predominantly of calcite, 7 Å clay and garnets, spherical particles up to 2 μ in diameter are observed. These may be silica gel or allophane (?) particles. The hexagonal plates, about 0.5 μ across, shown in Plate XXIV – 5 are most likely

Al-serpentine particles. The chemical analysis of the clay fraction, which according to X-ray seems to be composed only of the 7.09 Å serpentine (Table 26, analysis 8), shows it to consist predominantly of silica. The ratio of Mg + Si to Al is such that it is impossible to derive a structural formula for this clay.

The percentage of Al in the tetrahedral sites can be estimated from the basal spacing, using the charts of Nelson and Roy (1958). Following this technique 0.74 – 1.66 Al replaces a part of the Si in the Al-serpentines from Hatrurim (this Al number is calculated for four sites in the tetrahedral layer). The amount of aluminium in the Al-serpentines can also be confirmed from its decomposition temperature observed on the DTA curve, and from a graph presented by Jahanbaglao and Zoltai (1968). This latter curve reveals the linear relationship between the Al_2O_3 –content (in wt %) and the decomposition temperature, and is in agreement with observations by Roy and Roy (1954) of the increase of thermal stability of serpentine with increasing Al-content.

The weight percent of Al_2O_3 in the Al-serpentines as calculated from the above-mentioned graph may range from about 15 to 28%. The DTA curve reveals the sample to be a mixture of an amorphous material and Al-serpentine. The DTA-curve of a specimen treated with cold HCl 1:1 is given in Fig. 15, curve D. The shape of the low-temperature endothermic peak is typical of amorphous material. At 620° – 630° C an endothermic effect characteristic of serpentine dehydroxylation is observed. A moderate to weak exothermic effect appears only at 855° – 880° C. X-ray examination of samples after heating to 600° and 650° C reveals, beside the basal spacing of 7.1 Å, the presence of the first lines of olivine and enstatite at 650° C. On further heating until 800° C these lines become stronger. Olivine and enstatite start to appear before the serpentine is completely destroyed. At 900° C the main phases are cristobalite, sillimanite, and olivine. The I.R. curve is given in Fig. 15, curve C.

In the light of the experiments of Nelson and Roy (1958) on the synthesis of chlorites, the Al-serpentines seem to be a metastable phase obtained at temperatures not exceeding 300° C, while at higher temperatures the product might be a chlorite. The subject of the serpentines of Hatrurim and especially those containing Al is being further investigated.

Allophane – $nAl_2O_3.mSiO_2.pH_2O$

This is an X-ray-amorphous mineral which is a mixture of hydrogels of Al_2O_3 and SiO_2. According to Ross and Kerr (1934) the water is presumably in an absorbed form. The index of refraction varies from 1.490 to 1.512. The DTA curve (Fig. 14, curve A) exhibits a large and broad endothermic peak in the range of 100° – 250° C. At 980° C a strong exothermic peak related to the crystallization of the amorphous matter is observed. Al is leached by 15% HCl, leaving SiO_2-gel. The mineral occurs in association with other clays in marly rocks.

f. Tectosilicates

Analcite – $Na[AlSi_2O_6].H_2O$

This mineral is found in small amounts in some carbonate and gypsum rocks, associated with α–cristobalite, thomsonite, phillipsite, and clay (identification was based on X-rays). It occurs as interstitial grains of radiating aggregates. It is nearly isotropic, with a very low index of refraction. Analcite is a late-stage mineral. It is considered to have been formed by the action of sodium-containing solutions on clays.

Orthoclase – $K[AlSi_3O_8]$

Detrital. The predominant feldspar in the bituminous chalk, in the sandstone and conglomerate of the Hazeva Formation, and in a sample of tobermorite rock. In the sandstone it is partly replaced by calcite, the replacement

starting from the margins and advancing along cleavage cracks. For some reason it is more resistant to replacement by tobermorite than are quartz and albite. The grains are up to 0.15 mm across.

Microcline – $K[AlSi_3O_8]$

Microcline is a detrital mineral found in sandstone, and as a relict in a tobermorite rock. Only single crystals up to 0.1 mm across, with the characteristic cross-hatched twinning, were observed.

Albite – $Na[AlSi_3O_8]$

Albite is a detrital mineral. Single grains were observed in a tobermorite rock corroded and replaced by tobermorite along the cleavage and the borders.

Anorthite – $Ca[Al_2Si_2O_8]$

Anorthite is a common mineral in the anorthite-diopside-gehlenite fels, occurring with grossular and sometimes with vesuvianite or wollastonite. It occurs mostly in rocks equivalent to the Taqiye Formation at Hatrurim, and rarely in equivalents of the Ghareb Formation at Nahal Ayalon and at Tarqumiye. In thin-section the mineral is colourless, prismatic, with polysynthetic twinning on (010). Crystal size ranges from 10 to 50μ. The mineral is biaxial, negative, $2V = 77°$, $v > r$, $X' \wedge (001) = -(36° - 38°)$; $X' \wedge (010) = -40°$, $nZ - nX = 0.012$. The anorthite of Hatrurim is formed by the thermal metamorphism of marls and belongs to the pyroxene-hornfels facies.

Hyalophane – $(K,Ba)[Al(Al,Si)Si_2O_8]$

This mineral was identified in vugs of one specimen of a sandstone, associated with barite and clay. The X-ray pattern is almost identical with that of the mineral from South-west Africa described by Vermaas (1953). The mineral is colourless, biaxial negative, $2V \sim 75°$, $r > v$. $nZ - nX = 0.005$. The origin of the hyalophane is not clear. It may be a result of the metamorphism.

Zeolites

This group of minerals is widely distributed in the Hatrurim area, though sporadic at Tarqumiye and absent elsewhere. It occurs mostly in rock types equivalent to the Taqiye Formation. The most common are: thomsonite, phillipsite, and gismondite. They compose from single percents up to 50 percent of the rock. They occur in masses, veins, and vugs, associated with calcite, aragonite, garnets, diopside, and 7Å clay. The zeolites of Hatrurim are relatively poor in silica. They were formed in permeable rocks by retrograde metamorphism at temperatures not exceeding 300° C. Occasionally calcite replaces zeolites, and pseudomorphs of calcite after zeolites are observed (Plate VII – 4).

Scolecite – $Ca[Al_2Si_3O_{10}].3H_2O$

Scolecite is found in vugs of two samples of felses, associated with phillipsite and thomsonite. It occurs in the form of prismatic crystals with one good prismatic cleavage. The elongation is negative, $X \wedge c = 18°$. The mineral is biaxial, negative, $2V \sim 40°$, $r < v$ strong; $nZ - nX = 0.008$. The index of refraction is higher than that of phillipsite.

Mesolite – $Na_2Ca_2[Al_2Si_3O_{10}]_3.8H_2O$

Mesolite occurs as bundles of thin radiating fibres, up to 0.4 mm in length, in thomsonite and calcite crystals. The elongation is positive and the extinction inclined. The refringence is lower than that of thomsonite, and the birefringence very low. In the diffraction pattern a single, relatively strong spacing was observed at 5.74 Å, not overlapped by thomsonite spacings.

Thomsonite–$NaCa_2[Al_2(Al,Si)Si_2O_{10}]_2.6H_2O$

This is the most common zeolite. It occurs

Table 28. Diffraction data for zeolites

1		2		3		4		5		6	
d (Å)	I	d (Å)	I	d (Å)	I	d(Å)	I	d (Å)	I	d (Å)	I
9.3	vw	7.24	s			7.4	m	8.1	w	9.6	vvs
		7.15	s	7.1	s						
6.6	s	6.8	w			6.9	vs	7.15	vvs	6.96	m
5.9	s	6.5	w	6.5	w	6.3	w	6.36	vw	6.40	w
								5.34	m		
5.37	w	5.9	w			5.2	w	5.02	m	5.57	vs
4.63	s	5.8	w	5.71	w	4.9	m	4.96	m	5.03	vs
4.37	m	5.35	vw			4.57	w			4.65	w
4.13	s	4.98	m			4.23	m	4.26	w	4.33	vvs
3.95	vw	4.87	vw	4.87	m	4.04	s	4.09	s	3.98	w
3.79	vw	4.68	w	4.64	w			3.96	m	3.88	s
3.50	m	4.48	w	4.44	w			3.64	vw	3.58	s
3.27	w	4.26	vvs	4.25 } 4.18 }	vs	3.49	w	3.46	m	3.46	s
3.20	m							3.44	m	3.37	w
3.17	m	4.08	m	4.02	m			3.30	w	3.25	w
2.94	vs	3.76	w							3.18	w
		3.63									
2.85	vvs							3.25	m	2.92	vvs
2.79	w	3.42	w	3.54	w	3.18	vs	3.18	vvs	2.88	s
2.68	s	3.35	m	3.30	m			3.14	m	2.83	w
2.56	w	3.29	m							2.77	w
2.42	vw	3.20	s	3.16	s			3.10	w	2.69	m
2.29	vw	3.15	m	3.12	m	2.92	m	2.94	m	2.60	m
2.25	w	3.02	w					2.90	w	2.57	w
2.19	w	2.95	m	2.98	m			2.88	wv	2.50	m
2.12	vw	2.92	w	2.90	w			2.80	vw	2.35	vw
2.09	w	2.86	w			2.71	m	2.74	m	2.29	m
2.06	vw	2.78	m	2.79	m			2.69	m	2.28	w
1.88	w			2.72	m			2.65	w	2.23	w
1.83	w	2.66	w			2.52	m	2.53	m	2.16	w
1.81	w	2.58	w			2.38	m	2.38	m	2.12	w
1.71	vw	2.53	w	2.53	w	2.16	w	2.16	w	2.09	m
		2.45	w	2.44	w	1.97	m	2.01	m		
		2.36	w			1.76	m				
		2.34	vw	2.35	w	1.66	w				
		2.20	w								
		2.13	w								
		2.07	w								
		1.95	w								
		1.89	w								
		1.87	mw								

1. Thomsonite, Sample SG. 370. 2. Gismondite, Sample SG. 419. 3. Gismondite, Sample MK. 108. 4. Phillipsite, Sample SG. 448. 5. Ba-Phillipsite, Sample SG. 206. 6. Chabazite, Sample SG. 540.

as white or colourless crystals in vugs of felses, in fissures and cavities, and as the matrix of the calcite-zeolite rocks, where the content reaches up to 65% . The vugs or veins may be composed of thomsonite only, or it may occur with another zeolite – generally phillipsite. It is always well crystallized and occurs as prismatic or fibrous radiating groups and as anhedral grains when it comprises the matrix (Plate XXV–1). The crystals are vertically striated. The average crystal is about 0.1–0.25 mm long and 0.02 mm thick. Crystals measuring 0.5 mm and more are rather rare. Perfect {010} and poor {100} cleavages are observed.

The optical properties are: elongation ±, extinction straight, biaxial, positive, 2V ~ 50° , r > v strong.

nX = 1.526 – 1.530
nY = 1.528 – 1.532 } all ± 0.002
nZ = 1.538

nZ –nX = 0.006 – 0.008

Table 29. Chemical analysis of thomsonite

Oxide	Wt %	Cations per twenty oxygens	
SiO_2	38,83	Si	5.21
Al_2O_3	29.81	Al	4.70
Fe_2O_3	0.16		
FeO	neg.		
TiO_2	traces		
CaO	13.54	Ca	1.95
MgO	0.58	Mg	0.12
K_2O	0.15	K	0.03
Na_2O	3.33	Na	0.86
H_2O+	1.23		
H_2O-	12.25	H_2O	6.04
Cl	neg.		
Total	99.88		

Hatrurim. Sample S.G. 370. Analyst, M. Gaon.

The X-ray diffraction pattern is given in Table 28. Table 29 gives the result of a wet chemical analysis of thomsonite from vugs in a fels.

The formula of thomsonite from Hatrurim calculated on the basis O = 20, is: $(Ca_{1.95}Mg_{0.12}Na_{0.86}K_{0.03})(Si_{5.21}Al_{4.70})O_{20}.6.04H_2O$

The DTA curve for thomsonite is given in Fig. 18, curve D. The dehydration occurs in steps: The mineral loses water with a broad and mild low-temperature effect that is completed at 300° C, and with three strong and sharp endothermic peaks at 358° , 428° and 523° C respect-

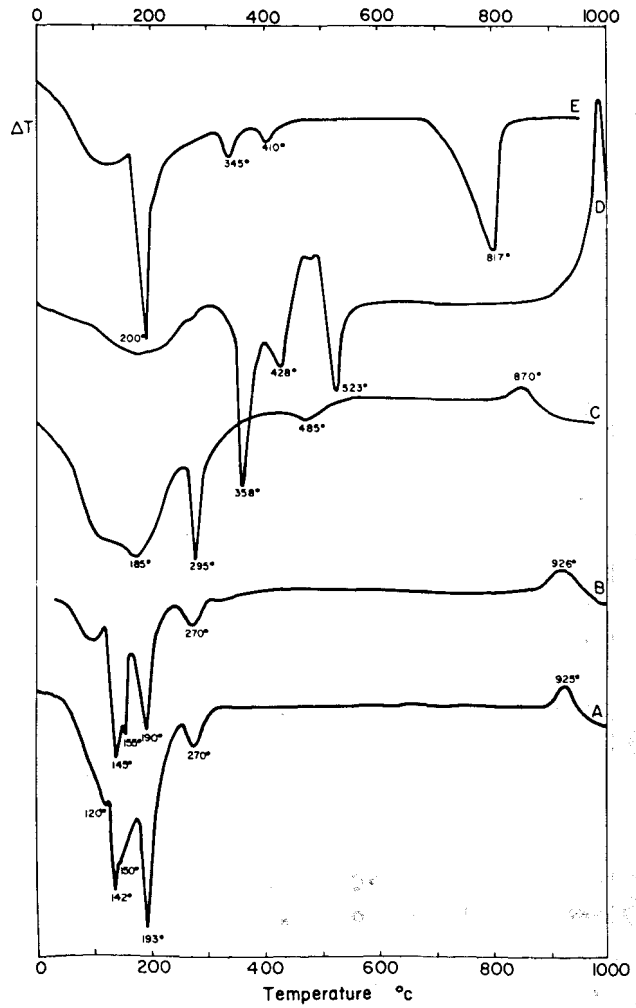

Figure 18. DTA curves of zeolites: A – gismondite (Sample MK 108); B – gismondite (sample SG 419); C – chabazite (sample SG 438); D – thomsonite (sample SG 370); E – phillipsite (sample SG 448).

ively. At 1000° C the curve exhibits a strong exothermic effect.

The DTA curve of the Hatrurim thomsonite is in good agreement with data given by Koizumi (1953). Anorthite is produced by dehydration of thomsonite.

Heulandite – $Ca[Al_2Si_7O_{18}].6H_2O$

Heulandite is found in marls and in vugs in felses, associated with calcite, thomsonite and levyne. It occurs in thin-section as anhedral colourless crystals about 30 μ across. One good cleavage is observed. The elongation is negative and the extinction oblique. The mineral is biaxial, positive, $2V \sim 35°$, $r > v$. $nZ - nX = 0.006$. The main reflections in the diffractograms are: 8.8 (s), 3.96 (m), 3.89 (m), 3.40 (m), 2.96 Å (ms). According to Walker (1951), heulandite is formed at 240° C.

Epistilbite – $Ca[Al_2Si_6O_{16}].5H_2O$

Epistilbite is found in the matrix of the Hazeva conglomerate. The mineral is associated with apophyllite and occasionally surrounds the latter. It occurs in thin-section as bundles of colourless fibres up to 0.6 mm length. The elongation is positive and the extinction oblique. The mineral is biaxial, negative, 2V moderate, $v > r$ strong. $nZ - nX = 0.012$. Its index of refraction is slightly lower than that of apophyllite. On the X-ray diffractogram only reflections not masked by apophyllite can be detected. They are: 8.8 (w), 6.7 (vw), 4.92 (m), 3.72 (w), 3.44 (m), 3.21 (m), 2.40 Å (w).

On the DTA curve of apophyllite (Fig. 13) an endothermic effect at about 265° C is attributed to epistilbite.

Gismondite – $Ca[Al_2Si_2O_8].4H_2O$

Gismondite is the second most important zeolite after thomsonite. In some specimens it appears as a rock-forming mineral and constitutes up to 50% of the rock. In other samples it occurs as monomineralic veins or it is associated with phillipsite, thomsonite, and aragonite. In one specimen thin gismondite rims enveloping garnets were observed. The mineral occurs mostly as anhedral grains or as pseudotetragonal bipyramids produced by twinning (Plate XXV-2, 3). Basal sections of such individuals show four segments with oblique extinction. Crystals are up to 0.5 mm across. The optical properties are: $Y \wedge c = 5° - 11°$; biaxial, negative, $2V \sim 85°$, $r < v$ strong. $nX = 1.528$, $nY = 1.540$, $nZ = 1.546$, $nZ - nX = 0.008$ (all ± 0.002). Small granules of diopside are included in the large gismondite grains and give them a cloudy appearance. In Table 30 a chemical analysis of gismondite, recalculated from the bulk analysis of sample S.G. 419, is given after deduction of calcite and small amounts of apatite, diopside, and hematite.

Table 30. Chemical analysis of gismondite

Oxide	Wt. %	Adjusted to 100 %	Cations per eight oxygens		
SiO_2	18.87	38.18	Si 2.25	3.92	
Al_2O_3	11.94	24.16	Al 1.67		
CaO	7.55	15.27	Ca 0.96	1.03	
Na_2O	0.26	0.53	Na 0.06		
K_2O	0.08	0.16	K 0.01		
H_2O-	4.79	9.69			
H_2O+	5.94	12.01	H_2O 4.15		
Total	49.43	100.00			

Analyst, M. Gaon.

The structural formula of gismondite, calculated on the basis of O = 8, is as follows: $(Ca_{0.96}Na_{0.06}K_{0.01})(Si_{2.25}Al_{1.67})O_8.4.15H_2O$. The X-ray data of two different samples of gismondite are given in Table 28 and the DTS-data in Fig. 18, curves A and B. Hoss and Roy (1960) reported two hydrate phases, in the temperature range between 90° – 190° C. Reeuwijk (1971) pointed to five different metastable crystallographic phases, before the irreversible feldspar phase is reached. The DTA curve (A) of sample MK 108 is identical with the

DTA curve of the specimen investigated by Reeuwijk with the composition $(Ca_{0.80}Na_{0.12}K_{0.20})(Si_{2.11}Al_{1.86})O_8.4.3H_2O$. The DTA curve B of speciment SG 419 also exhibits distinct endothermic peaks. A very weak one at about 105° C, stronger ones at 145° , 155° and 195° C, and a weak one at 270° C. The strongest endothermic peak is at 145° and not at 195° C, as in specimen MK 108. At about 900° C the curve exhibits a small exothermic effect. The TGA of this sample shows two breaks, at 120° C and 225° C. The difference in retention of water molecules is probably due to differences in composition. Reeuwijk's mineral is richer in K and Na ions and correspondingly poorer in Si than specimen S.G. 419. The anhydrous phase formed after dehydration is anorthite.

Phillipsite – $KCa[Al_3Si_5O_{16}].6H_2O$

Phillipsite occurs as colourless cruciform penetration twins (Plate XXV – 4, 5) up to 0.15 mm across. Cleavage is distinct on {001}. Some crystals are zoned. The elongation is positive, n = 1.500 – 1.506, nZ – nX = 0.003 – 0.008.

Optically, two varieties may be distinguished:

a) Biaxial, negative with moderate 2V, r < v, Z ∧ c = 23° – 28°. This variety is the most common. An optically negative phillipsite is mentioned by Dunham (1933).

b) Biaxial, positive, 2V ~ 60° , r < v weak, Z ∧ c = 10° – 15° . The X-ray pattern given in Table 27 is almost identical with the data given by Hoss and Roy (1960) for a specimen of phillipsite containing Ba. Other specimens have X-ray patterns similar to ASTM 2-0084. The mineral is associated with thomsonite, chabazite, gismondite, and barite. Phillipsite seems to be a later mineral in rocks in which gismondite composes the matrix. The DTA curve of a rock consisting predominantly of phillipsite with some thomsonite and calcite is given in Fig. 18, curve E. It exhibits a broad endothermic low-temperature peak at about 110° C and a sharp one at 200° C, attributed to philipsite. The small endothermic peaks at 345° and 410° C are attributed to thomsonite admixture and the peak at 817° C to calcite.

Harmotome – $Ba[Al_2Si_6O_{16}].6H_2O$

Harmotome was identified microscopically in vugs of two samples of fels in the horizon where barite concretions are frequent. The crystals occur in the form of penetration twins up to 70 μ across. Biaxial, positive, 2V large, the elongation is ±, X ∧ a = 60° , Y ∧ c = –30° ; nY = 1.506; nZ – nX = 0.006.

Gmelinite – $(Na_2,Ca)[Al_2Si_4O_{12}].6H_2O$

Gmelinite was identified in two samples of gypseous carbonate rocks. It occurs as spots 2–3 mm across, consisting of white prismatic crystals of positive elongation, and with perfect cleavage along the prism. The mineral is biaxial, positive, with a very small optic angle; nZ – nX = 0.003. The powder diffraction pattern is identical with that of gmelinite from the Isle of Mayen (Mikheyev, 1957).

Chabazite – $(Ca, Na_2)[Al_2Si_4O_{12}].6H_2O$

Chabazite occurs as the only zeolite present or is associated with phillipsite and thomsonite in "brick"-like rocks. The mineral occurs as rhombohedrons or anhedral grains (Plate XXV – 6). Uniaxial negative, or biaxial negative, with small 2V. nX = 1.484, nZ = 1.488, nZ –nX = 0.004 (all ± 0.002). In addition to Na the mineral also contains K and Sr. The molar ratio of $Na_2O:K_2O:SrO$ = 6:3:1. The X-ray diffraction pattern corresponds to ASTM 15-618. The DTA curve is given in Fig. 18, curve C. The mineral loses water continuously with a broad endothermic effect up to 270° C and a maximum at about 185° C. The sharp endothermic peak at 295° C is attributed to the presence of gibbsite.

Levyne – $Ca[Al_2Si_4O_{12}].6H_2O$

This mineral was found only in two samples, associated with gismondite and chalcedony. It occurs as single tabular colourless crystals up to 40 μ across, with negative elongation. The mineral is biaxial, negative, n ~ 1.500; nZ – nX = 0.004. Levyne seems to be later than gismondite. In the diffractogram the following reflections, not overlapped by gismondite, were observed: 8.2 (s), 6.4 (m), 5.3 (m), 4.04 (s), 2.82 (vw), 2.60 Å (ms).

Unidentified zeolite (?)

In a number of calcitic veins cutting spurrite rocks, greenish, skeletal crystals with cleavage along the prism zone and with prismatic or hexagonal outlines were observed (Plate VII – 6, 7). The elongation is positive and the extinction straight. The mineral is biaxial, negative, with small axial angle. r < v. In thin sections it is green, and occasionally weakly pleochroic. By microchemical qualitative analysis the following elements were found: Si, Al, Ca, Mg, Sr, Cr, and traces of K and Na. In the X-ray pattern single weak reflections at 7.1, 3.16, 4.01 and 2.67 Å were detected. The reflections resemble the patterns of synthetic zeolites of the phillipsite group (Taylor and Roy, 1964). This zeolite may be orthorhombic or monoclinic. The high index of refraction as compared with other zeolites is explained by absorbed Cr ions, causing the coloration. This compound needs further investigation.

REFERENCES

AGRELL, S.O. and GAY P., 1961, Kilchoanite, a polymorph of rankinite. *Nature*, Vol. 189, p. 743 M.A. Vol. 15, p. 541.

AGRELL, S.O., 1965, Polythermal metamorphism of limestone at Kilchoan, Ardnamurchan (Scotland), *Min. Mag.*, Vol. 34, pp. 1–15.

ALBRIGHT, J.N., 1971, Vaterite stability, *Amer. Min.*, Vol. 56, pp. 620–624.

AKHLESTINA, E.F., 1972, Melnikovite in the Upper Pliocene formations of the Caspian depression, *Chem. Abs.* 77, No. 26, 167144. (*Vop. Geol. Yuzh. Urala Povolzh'ya*, 1970 No. 7, pp. 129–37).

AMAFUJI, M., 1964, Occurrence of spurrite in the cement manufacturing process, *Journ. Min. Soc. Japan*, Vol. 6, pp. 285–312.

ANDRITZKY, G., 1963, Ein Vorkommen von Volkonskoit in einer verquarzten tektonischer Brekzie bei Küru, *Geol. Blätter, NO-Bayern*, Vol. 13, pp. 186–191.

ANNENKOVA, G.A., 1964, Xonotlite from the Kel'bodzhare District of the Azeirbaidzhan S.S.R., *Trudy Min. Muz. Akad. Nauk SSSR*, Vol. 15, pp. 184–188.

AVNIMELECH, M., 1936, Etudes géologiques dans la region de la Shéphélah en Palestine, *Ann. Univ. Grenoble, Trav. Lab. Geol.* Grenoble, p. 144.

AVNIMELECH, M., 1965, Remarks on the occurrence of unusual high-temperature minerals in the so-called "Mottled Zone" comples of Israel, *Israel J. Earth-Sci.*, Vol. 13, pp. 102–110.

BAILEY, E.H., 1941, Skeletonized apophyllite from Crestmore and Riverside, California, *Amer. Min.*, Vol. 26, pp. 565–567.

BAILLEY, E.B. and TYLER, S.A., 1960, Clay minerals associated with the Lake Superior iron ores, *Econ. Geol.*, Vol. 55, pp. 150–175.

BALITSKIY, V.S. and GORBUNOV, L.V. 1967, Some formation conditions of hydrous calcium silicates in alkaline silica-bearing solutions at elevated temperatures and pressures, *Geokhimiya*, Vol. 10, pp. 1071–1075.

BALL, D.F., 1964, Saponite and lizardite veins on the Island of Rhum, *Clay Minerals, Bull.*, V.5, pp. 434–442.

BANNISTER, F.A., HEY, M.H. and BERNAL, J.D., 1936, Ettringite from Scawt Hill, County Antrim, *Min. Mag.*, Vol. 24, pp. 324–329.

BARRETT, R.L. and McCAUGHEY, W.J., 1942, The system $CaO–SiO_2–P_2O_5$, *Amer. Min.*, Vol. 27, pp. 680–695.

BASTA, E.J., 1959, Some mineralogical relationships in the system $Fe_2O_3–Fe_3O_4$ and the composition of titanomagnetite, *Econ. Geol.*, Vol. 54, pp. 698–719.

BEINTEMA, J., 1938, On the composition and crystallography of autunite and meta-autunites, *Rec. Trav. Chim. Pays-Bas*, Vol. 57, pp. 155–175.

BELYANKIN, D.S. and PETROV, V.P., 1939, Hibschite in Georgia, *Dok., Akad. Nauk. S.S.S.R.*, Vol. 24, pp. 349–352.

BELYANKIN, D.S. and PETROV, V.P., 1941a, On hibschite and plazolite, *Dokl. Akad. Nauk. SSSR*, V. V. 32, pp. 66–68.

BELYANKIN, D.S. and PETROV, V.P., 1941b, The grossularoid group (hibschite, plazolite), *Amer. Miner.*, Vol. 26, pp. 450–453.

BELYANKIN, D.S. and PETROV, V.P. 1941c, An attempt to revise the chemical formula of the mineral hibschite, *Dokl. Akad. Nauk. SSSR*, Vol. 30, pp. 420–423.

BENDER, F., 1968, *Geologie von Jordanien;* Beitrage zur Geologie der Erde, Gebrueder Borntraeger, 230 p.

BENTOR, Y.K., ed. 1960, Israel, in: *Lexique Stratigraphique International, Asie*, Vol. III, (10.2), Paris.

BENTOR, Y.K. and VROMAN, A., 1960, *The geological map of Israel 1:100,000, Sheet 16–Mount Sedom (with explanatory text)*, Geol. Surv. Isr., Jerusalem.

BENTOR, Y.K., GROSS, S. and HELLER, L., 1963a, High temperature minerals in non-metamorphosed sediments in Israel, *Nature*, Vol. 199, pp. 478–479.

BENTOR, Y.K., GROSS, S., and HELLER, L., 1963b, Some unusual minerals from "Mottled Zone" complex, Israel, *Amer. Min.*, Vol. 48, pp. 924–930.

BENTOR, Y.K., GROSS, S. and KOLODNY, Y., 1972, New evidence on the origin of the High Temperature Mineral Assemblage of the "Mottled Zone" (Israel), *24th International Geological Congress*, Section 2, pp. 265–275.

BERNER, R.A., (1964). Iron sulfides formed from aqueous solutions at low temperatures and atmospheric pressure, *Journ. Geol.*, Vol. 72, pp. 293–306.

BISCHOFF, J.L., 1968, Catalysis, inhibition and the calcite-aragonite problem: II, the vaterite-aragonite transformation, *Amer. J. Sci.*, Vol. 266, pp. 80–90.

BLACK, P.M., 1969, Rankinite and kilchoanite from Tokatoka, New Zealand, *Min. Mag.*, Vol. 37, pp. 517–519.

BLOXAM, T.W., 1964, Hydrogrossular from the Girvan-Ballantrae Complex, Ayrshire, *Min. Mag.*, Vol. 33, pp. 814–815.

BØGGILD, O.B., 1922, Re-examination of some zeolites. *Kgl. Danske Vidensk. Selsk. Math-Phys. Medd.*, Vol. 4, No. 8, (M.A. 2–59).

BOGUE, R.H. and LERCH, W., 1934, Hydration of portland cement compounds, *Ind. Eng. Chem.*, Vol. 26, pp. 837–847.

BOGUE, R.H., 1955, *The chemistry of portland cement*, (Reinhold Publishing Corp., New York).

BOWEN, N.L., SCHAIRER, J.F. and POSNJAK, E., 1933, The system $CaO–FeO–SiO_2$, *Amer. Journ. Sci.*, Vol. 26, pp. 193–297.

BOWEN, N.L., 1940, Progressive metamorphism of siliceous limestone and dolomite, *J. Geol.*, Vol. 48, pp. 225–274.

BRADY, L.F. and GREIG, Y.W., 1939, Note on the temperature attained in a burning coal seam, *Am. J. Sci.*, Vol. 237, p.116–119.

BREDIG, M.A., 1943, Phase relations in the system Ca_2SiO_4–orthophosphate, *Amer. Min.*, V. 28, pp. 594–601.

BREDIG, M.A., 1950, Polymorphism of calcium orthosilicate, *J. Amer. Ceram. Sec.*, V. 33, pp. 188–192.

BRIDGE, F.E., 1966, Bredigite, larnite and γ dicalcium silicates from Marble Canyon, *Am. Min.*, Vol. 51, pp. 1766–1774.

BRINDLEY, G.W., and von KNORRING, O., 1954, A new variety of antigorite (ortho-antigorite) from Unst, Shetland Islands, *Amer. Min.*, Vol. 39, pp. 794–804.

BRINDLEY, G.W. and ZUSSMAN, J., 1959, Infra-red absorption data for serpentine minerals, *Amer. Min.*, V. 44, pp. 185–188.

BUCKNER, D.A. and ROY, R., 1955, Phase equilibria in the system $CaO–Al_2O_3–SiO_2–H_2O$. II. The system $CaSiO_3$ and the influence of Sr^{++} in solid solution, *Bull. Geol. Soc. Amer.*, Vol. 66, p. 1536 (abstract).

BURNHAM, C.W., 1959, Contact metamorphism of magnesian limestones at Crestmore, California, *Bull. Geol. Soc. Amer.*, Vol. 70, pp. 879–920.

BUTTLER, F.G., 1958, Ph.D. thesis, Aberdeen, in: Taylor, H.F.W., 1964, *The chemistry of cement hydration.*

BUTTLER, F.G., DENTGLASSER, L.S., and TAYLOR

H.F.W., 1959, Studies on $4CaO.Al_2O_3.13H_2O$ and the related natural mineral hydrocalumite, *Journ. Amer. Ceram. Soc.*, Vol. 42, pp. 121–126.

CARLSON, E.T., and BERMAN, H.A., 1960, Some observations on the calcium aluminate carbonate hydrates, *J. Res. Nat. Bur., Stand.* 64A, pp. 333–341.

CAROBBI, G., 1940, Ricerche Vesuviane, B. Volcan., Vol. 7, pp. 3–42.

CARPENTER, A.B., CHALMERS, R.A., GARD, J.A., SPEAKMAN, K., and TAYLOR, H.F.W. 1966, Jennite, a new mineral. *Amer. Min.*, Vol. 51, pp. 56–74.

CARRUTHERS, J.D., SING, K.S.W., and FENERTY, J., 1967, Glow phenomenon of chromium oxide, *Nature*, 213, pp. 66–68.

CHIE PIN–WEN and CHIEN T'SE, 1964, Ferro-lizardite, a new mineral species of the serpentine group, *Acta Geol. Sinica*, Vol. 44, pp. 86–98, (M.A. 1966, Vol. 17, p. 504).

CHIRVINSKY, P.N., 1925, Tyuyamunite from the Tyuya-muyun radium mine in Fergana, *Min. Mag.*, Vol. 20, pp. 287–295.

CHRISTOPHE–MICHEL–LEVY, M., 1964, Synthèses hydrothermales dans le système gehlénite–akermanite, $CaAl_2SiO_7$–$Ca_2MgSi_2O_7$ en milieu carbonaté, *Bull. Soc. Franç. Min. Cryst.*, LXXXVII, pp. 28–30.

CHUKHROV, F.V. and BONSHTEDT–KUPLETSKAYA, M., (editors): *Mineraly:* 1960, Vol. I; 1963, Vol. II/I; 1965, Vol. 11/2; 1967, Vol. II/3; 1972, Vol. III/1; "Nauka", Moscow.

CHUKHROV, F.V., YERMILOVA, L.P., and SHANIN, L.L., 1973, On the age of apophyllite in the late hydrothermal associations. *Proc. AN. USSR, IZV*, Vol. 2, pp. 3–14.

CLABAUGH, S., 1953, Contact metamorphism in the Christmas Mountains, Brewster County, Texas, *Bull. Geol. Soc. Amer.*, Vol. 64, p. 1408.

COHEN–ADDAD, C., DUCROS, P., DURIF–VARAMBON, A., BERTAUT, E.F., and DELAPALME, A., 1963, Etude de la position des atoms d'hydrogène dans l'hydrogrenat $Al_2O_3.3CaO.6H_2O$, *Solid state communications, 1.* Pergamon Press.

COLVILLE, A.A., and GELLER, S., 1971, The crystal structure of brownmillerite, Acta Cryst., Vol. 27B, pp. 2311–2315.

COPELAND, L.E., BRUNAUER, S., KANTRO, D.L., SCHULTZ, E.G., and WEISE, C.W., 1959, Quantitative determination of the four major phases of portland cement by combined X-ray and chemical analyses, *Anal. Chem.*, Vol. 31, pp. 1521–1530.

DE KEYSER, W.L. and DEGUELDRE, L., 1950, Contribution a l'etude de la formation de la calcite, aragonite et vaterite, *Bull. Soc. Chim. Belg.*, Vol. 50, pp. 40–71.

DEER, W.A., HOWIE, R.A., and ZUSSMAN, J., 1962, *Rock-forming minerals*, Vols. I, II, III, IV, V, Longmans, London.

DELL, C.I., 1972, An occurrence of greigite in Lake Superior sediments, *Amer. Min.*, Vol. 57, pp. 1303–1304.

DIAMOND, S., WHITE, J.L., and DOLCH, W.L., 1966, Effects of isomorphous substitution in hydrothermally synthesized tobermorites, *Amer. Min.*, Vol. 51, pp. 388–401.

DRAPER, R.B., 1935, The synthesis of magnesioferrite and some observations on "mineralization", *Amer. J. Sci.*, Vol. 23, pp. 106–115.

DUFRESNE, E.R., and ANDERS, F., 1962, On the retention of primordial noble gases in the Pesyanoe meteorite, *Geochim. Cosmochim. Acta.*, Vol. 26, pp. 251–262.

DUNHAM, K.C., 1933, Crystal cavities in lavas from the Hawaiian islands, *Amer. Min.*, Vol. 18, pp. 369–385.

EAKLE, A.S., 1917, Minerals associated with the crystalline limestone at Crestmore, Riverside County, California, *Univ. Calif. Bull. Dept. Geol.*, Vol. 10, pp. 327–360.

EAKLE, A.S., 1925, Foshagite, a new silicate from Crestmore, California, *Amer. Min.*, Vol. 10, pp. 97–99.

ECKHARD, E.J., and HEIMBACH, W., 1963, Ein natürliches vorkommen von $CaCrO_4$, chromatite, *Naturwiss.*, Vol. 50, p. 612.

FAIVRE, R., 1946, Recherche des conditions physico-chimiques de précipitation des trois formes crystallines du carbonate de calcium préparé par double decomposition du chlorure de calcium et du carbonate de sodium, *Compt. Rend. Acad. Sci., Paris*, Vol. 222, pp. 140–141.

FAUST, G.T., and FAHEY, J.J., 1962, The serpentine

group minerals, *U.S. Geol. Sur. Prof. Paper* 384–A, 92 p.

FLEISCHER, M., 1956, New data–bayerite, *Amer. Min.* Vol. 41, p. 959.

FLEISCHER, M., 1968, Melnikovite vs. greigite, *Amer. Min.* Vol. 54, p. 328.

FLINT, E.P., McMURDIE, H.F., and WELLS, L.S., 1938, Formation of hydrated calcium silicates at elevated temperatures and pressures, *J. Res. Nat. Bur. Stand.*, Vol. 21, pp. 617–638.

FLINT, E.P., McMURDIE, H.F., and WELLS, L.S., 1941, Hydrothermal and X-ray studies on the garnet hydrogarnet series and the relationship of the series to hydration products of portland cement, *J. Res. Nat. Bur. Stand.*, Vol. 26, pp. 13–33.

FOA, F., 1958, Minor constituents and trace elements in Negev phosphate rocks, *Nature*, Vol. 181, p. 1676.

FONT–ALTABA, M., 1960, A thermal study of thaumasite, Min. Mag., Vol. 32, pp. 567–572.

FORMAN, S.A., 1951, Xanthophyllite, *Amer. Min.*, Vol. 36, pp. 450–457.

FOSHAG, W.F., 1920a, Plazolite, a new mineral, *Amer. Min.*, Vol. 5, pp. 183–185.

FOSHAG, W.F., 1920b, Thaumasite and spurrite from Crestmore, California, *Amer. Min.*, Vol. 5, pp. 80–81.

FRANKEL, J.J., 1959, Uvarovite garnet and South African jade (hydrogrossular) from the Bushveld complex, Transvaal, *Amer. Min.*, Vol. 44, pp. 565–591.

FUNK, H., 1957, The products obtained by the action of water on $-Ca_2SiO_4$ up to 120°, *Z. anorg. Chem.*, Vol. 291, pp. 276–293.

GARAVELLI, C.L., and NUOVO, G., 1971, La greigite della argille di Montemesola, *Periodico Mineral.* Vol. 40, pp. 305–327.

GARD, J.A., and TAYLOR, H.F.W., 1956, Okenite and nekoite (a new mineral), *Min. Mag.*, Vol. 31, pp. 5–20.

GARD, J.A., and TAYLOR, H.F.W., 1957, A further investigation of tobermorite from Loch Eynort, Scotland, *Min. Mag.*, Vol. 31, pp. 361–370.

GARD, J.A. and TAYLOR, H.F.W., 1958, Foshagite: Composition unit cell and dehydration, *Amer. Min.*, Vol. 43, pp. 1–15.

GARD, J.A., NICOL, A.W., and TAYLOR, H.F.W., 1960, New data for the calcium silicate "phase Z", *Nature*, Vol. 188, pp. 1187–1188.

GARD, J.A., and TAYLOR, H.F.W., 1960, The crystal structure of foshagite, *Acta Cryst.* Vol. 13, pp. 785–793.

GAZE, R., and ROBERTSON, R.H.S., 1956, Some observations on calcium silicate hydrate:I – Tobermorite, *Mag. Concrete Res.*, Vol. 8, pp. 7–12.

GEDEON, T.G., 1956, Bayerite in Hungarian bauxite, *Acta Geol. Acad. Sci. Hung.*, Vol. 4, pp. 95–105.

GILLERY, G.H., 1959, X-ray study of synthetic Mg-Al serpentines and chlorites, *Amer. Min.*, Vol. 44, pp. 143–152.

GROSS, S. 1970, Mineralogy of the "Mottled Zone" Complex in Israel. List of minerals, *Israel J. Earth-Sci.* Vol. 19, pp. 211–216.

GROSS, S., 1971, Determination of spurrite, associated with calcite, by means of differential thermal analysis, *Israel J. Chem.*, Vol. 9, pp. 601–606.

GROSS, S., and HELLER, L., 1963, A natural occurrence of bayerite, *Min. Mag.*, 33, pp. 723–724.

GROSS, S., and BENTOR, Y.K., 1966, Pseudo-hydrothermal clays–volkhonskoite, in: Bentor, Y.K., *The clays of Israel*, The International Clay Conference, Jerusalem.

GROSS, S., MAZOR, E., SASS, E., and ZAK, I., 1967, The "Mottled Zone" complex of Nahal Ayalon (Central Israel), *Israel J. Earth-Sci.*, Vol. 16, pp. 84–96.

GROSS, S., and HELLER, L., 1970, Brownmillerite in the "Mottled Zone" complex, Israel, and its resistance to weathering, *IMA–IAGOD Meeting 70, collected abstracts*, p. 160, Sci. Council of Japan.

GRÜNHAGEN, H. et MERGOIL, J., 1963, Decouverte d'hydrocalumite et afwillite associeés a l'ettringite dans les porcélanites des Boissejour près Ceyrat (Puy de Dome), *Bull. Soc. Fr. Min.*, Vol. 86, pp. 149–153.

GRUZDEV, V.S., BRYGALOV, I.A., CHERMITSOVA, N.M., and SHUMKOVA, N.G., 1972, Greigite from Yakutiya and its optical properties, *Dokl. Akad. Nauk. SSSR*, Vol. 202, pp. 132–136.

GVIRTZMAN, G., and BUCHBINDER, B., 1966, *The Tertiary Project in Semi-Annual Progress Report on the Geol. Res. Projects.* Inst. for petroleum research and geophysics, Israel. Report 1018, pp. 11–17.

GVIRTZMAN, G., and BUCHBINDER, B., 1969, Outcrops of Neogen formations in the central and

southern coastal plain, Hashephela and Be'er-Sheva regions, Israel. *Geol. Surv. Isr. Bull.* No. 50.

HALL, A., and TAYLOR, J.D.D. 1971, The occurrence of vaterite in gastropod eggshells, *Min. Mag.*, Vol. 38 pp. 521–523.

HARKER, R.I., 1960, Dehydration series in the system $CaSiO_3$–SiO_2–H_2O, *Bull. Geol. Soc. Amer.*, Vol. 71, p. 1881.

HARKER, R.I., 1964, Dehydration series in the system $CaSiO_3$–SiO_2–H_2O, *Amer. Cer. Soc.*, Vol. 47, pp. 521–529.

HEDDLE, M.F., 1880, in: HELLER, L., and TAYLOR, H.F.M., 1956, *Crystallographic data of the calcium silicates.*

HEIMBACH, W., 1965, Zum Vorkommen von Chromatit, $CaCrO_4$ in Jordanien, *Geol. Jb.*, Vol. 83, pp. 717–724.

HELLER, L., 1952, The crystal structure of dicalcium silicate α–hydrate, *Acta Cryst.*, Vol. 5, pp. 724–728.

HELLER, L., and TAYLOR, H.F.W., 1951, Hydrated calcium silicates, Part II, hydrothermal reactions: Lime: silica ratio 1:1, *J. Chem. Soc.*, pp. 2397–2401.

HELLER, L., and TAYLOR, H.F.W., 1952a, Hydrated calcium silicates, Part IV, hydrothermal reactions: Lime: silica ratios 2:1 and 3:1, *J. Chem. Soc.*, pp. 2535–2541.

HELLER, L., and TAYLOR, H.F.W., 1952b, Hydrated calcium silicates, Part III, hydrothermal reactions of mixtures of lime: silica molar ration 3:2, *J. Chem. Soc.*, pp. 1018–1020.

HELLER, L., and TAYLOR, H.F.W., 1956, *Crystallographic data for the calcium silicates*, (H.M.S.O. London).

HELLER, L., FARMER, V.C., MACKENZIE, R.C., MITCHELL, B.D., and TAYLOR, H.F.W., 1962, The dehydroxylation and rehydroxylation of trimorphic dioctahedral clay minerals, *Clay Min. Bull.*, Vol. 5, pp. 56–72.

HENTSCHEL, G., 1961, Seltene Mineralneubildungen in einem Kalksteinenschlüssen der Lava des Ettringen Bellerberges, *Fortsch. Min.*, Vol. 39, p. 345.

HENTSCHEL, G., 1964, Mayenit, $12CaO.7Al_2O_3$, und Brownmillerit, $2CaO(Al, Fe)_2O_3$, zwei neue Minerale in den Kalksteinenschlüssen der Lava des Ettringen Bellerberges, *N.Jb. Min.* Mh., pp. 22–29.

HENTSCHEL, G., 1968, Ettringit vom Schelkopf bein Brank in der Eifel, *Aufschluss*, Vol. 19, pp. 198 200.

HOCHLEITNER, R., 1972, Cyclowollastonit von der Halden das Graphitabbaus bei Pfaffenreuth in der Nähe von Hauzenberg, *Aufschluss*, Vol. 23, pp. 340–341.

HOLDRIDGE, D.A., and WALKER, E.G., 1968, DTA curves of some Israeli clays and associated materials, *Trans. Brit. Ceram. Soc.*, Vol. 67, p. 243–269.

HOMME, F.C. and ROSENZWEIG, A., 1958, Spurrite and monticellite skarns in the Tres Hermas Mountains, Luna County, New Mexico, *Bull. Geol. Soc. Amer.*, Vol. 69, p. 1586.

HOSS, H., and ROY, R., 1960, Zeolite studies III, On natural phillipsite, gismondite, chabazite and gmelinite, *Beitr. Min. Petr.*, Vol. 7, pp. 389–408.

HUCKENHOLTZ, H.G., 1969, Synthesis and stability of Ti-andradite, *Amer. J. Sci.*, 267-A (Schairer vol.), pp. 209–232.

HUGHES, C.J., 1960, An occurrence of tilleyite-bearing limestones in the Isle Rhum, Inner Hebrides, *Geol. Mag.*, Vol. 97, pp. 384–388.

HURLBURT, C.S., and BAUM, J.L., 1960, Ettringite from Franklin, New Jersey, *Amer. Min.*, Vol. 45, pp. 1137–1143.

HUTTON, C.O., 1943, Hydroglossular, a new mineral of the garnet-hydrogarnet series, *Trans. Roy. Soc., New Zealand*, Vol. 73, pp. 174–180.

JAHANBAGLAO, C.I., and ZOLTAI, T., 1968, The crystal structure of a hexagonal Al-serpentine, *Amer. Min.*, Vol. 53, pp. 14–24.

JASMUND, K., and HENTSCHEL, G., 1964, Seltene Mineral paragenesen in Kalksteineinschlüssen der Lava des Ettringen bein Mayen (Eifel), *Beitr. Min. Petr.*, Vol. 10, pp. 296–313.

JEFFERY, J.W., 1952, The crystal structure of tricalcium silicate, *Acta. Cryst., Copenhagen*, Vol. 5, pp. 209–213.

JOESTEN, R., 1974, Pseudomorphic replacement of melilite by idocrase in a zoned calc-silicate skarn, Christmas Mountains, Big Bend Region, Texas *Amer. Min.*, Vol. 59, pp. 694–699.

JONES, F.E., 1938, The calcium aluminate complex salts, *Proc. 2nd Intern. Symp. Chem. Cements, Stockholm*, pp. 231–245.

JONES, F.E., 1960, Hydration of calcium aluminates

and ferrites, *4th Intern. Symp. Chem. Cements, Washington*, pp. 205–242.

KALOUSEK, G.L., 1952, Application of differential thermal analysis in a study of the system lime-silica-water, *Proc. 3rd Intern. Symp. Chem. Cements London*, pp. 296–311.

KALOUSEK, G.L., DAVIS, C.W., and SCHMERTZ, W.E., 1949, An investigation of hydrating cements and related hydrous solids by differential thermal analysis, *Amer. Concret Inst. Proceedings*, Vol. 45, pp. 693–712.

KALOUSEK, G.L., and ADAMS, M.; 1951, Hydration products formed in cement pastes at 25° to 175° , *Amer. Concret. Inst. Proceedings*, Vol. 48, pp. 77–90.

KALOUSEK, G.L., 1957, Crystal chemistry of hydrous calcium silicates, I, Substitution of aluminium in lattice of tobermorite, *J. Amer. Ceram. Soc.*, Vol. 40, pp. 74–80.

KALOUSEK, G.L., LOGIUDICE, J.S., and DODSON, V.H., 1954, Studies on the lime-rich crystalline solid phases in the system lime-silica-water, *J. Amer. Ceram. Soc.*, Vol. 37, pp. 7–13.

KALOUSEK, G.L., and ROY, R., 1957, Crystal chemistry of hydrous calcium silicates, II, Characterization of interlayer water, *J. Amer. Ceram. Soc.*, Vol. 40, pp. 236–239.

KALOUSEK, G.L., and PREBUS, A.F., 1958, Crystal chemistry of hydrous calcium silicates,III, Morphology and other properties of tobermorite and related phases, *J. Amer. Ceram. Soc.*, Vol. 41, pp. 124–132.

KARIAKIN, L.I., 1962, Mineral formation processes in blast-furnaces, *Min. Sbornik Geol. Soc. Lvov.*, No. 16, pp. 359–372.

KHOROSHEVA, D.P., 1968, The bayerite of the bauxite horizon of the Middle Pridneprovie, *Dokl. Akad. Nauk SSSR*, Vol. 182, pp. 434–436.

KIROV, G.N., and POULIEFF, C.N., 1968, On the infra-red spectrum and thermal decomposition products of thaumasite, *Min. Mag.*, Vol. 36, pp. 1003–1012.

KISELEV, A.I., 1938, The mineralogy of Chalilov deposits of chromspinelids, Mg-carbonates, and nickel-bearing ores of the south Ural, *Mem. Len. Mining Inst.*, Vol. II, pp. 1–59.

KLUG, H.P. and ALEXANDER, L.E., 1954, *X-ray diffraction procedures*, Wiley, New York.

KNILL, D.C., 1960, Thaumasite from County Down, North Ireland, *Min. Mag.*, Vol. 32, pp. 416–418.

KNOPF, A., and LEE, D.E., 1957, Fassaite from near Helena, Montana, *Amer. Min.*, Vol. 42, pp. 73–77.

KOIZUMI, M., 1953, The differential thermal analysis curves and dehydration curves of zeolites, *Min. J. Japan*, Vol 1, pp. 36–47.

KOLODNY, Y., BAR, M., and SASS, E., 1971, Fission track age of the "Mottled Zone Event" in Israel, *Earth and Planet Sci., Lett.*, pp. 269–272.

KOLODNY, Y., SCHULMAN, N., and GROSS, S., 1973, Hazeva Formation sediments affected by "Mottled Zone Event". *Israel J. Earth-Sci.*, Vol. 22, pp. 185–193.

KOLODNY, Y., and GROSS, S., 1974, Thermal metamorphism by combustion of organic matter: isotopic and petrological evidence, *J. Geol.* Vol. 82, pp. 489–506.

KOROLIUK, V.N., LAVRENTIEV, Y.G., PALCHYK, N.A., and REVERDATTO, V.V., 1974, The first occurrence of rankinite in SSSR. *Zap. Vses. Min. Obshch.* Vol. 103, pp. 136–139.

KOSTOV, I., 1962, Apophyllite from two occurrences in Bulgaria, *Bull. Geol. Inst. Bulgarian Acad.* Sci., Vol. 10, pp. 39–48.

KRAMM, T.P., and SUKHITSKAYA, N. YA., 1965, Melnikovite from the Kimmerian sediments of Kerch Peninsula, *Min. Sbornik. Geol. Soc. Lvov.*, Vol. 19, pp. 520–523.

KRAUSKOPF, K.B., 1956, Dissolution and precipitation of silica at lower temperatures, *Geochim. Cosmochim. Acta*, Vol. 10, pp. 1–26.

KUSACHI, J., NUMANO, T., and HENMI, K., 1971a, Mineraux de contact de Kushiro, prefecture d'Hiroshima. II. Spurrite and lilleite, *J. Min. Soc. Japan* Vol. 10, pp. 170–180. (Abstract. Bull. Signaletique 1972, Vol. 33–1173.

KUSACHI, J., NUMANO, T., and HENMI, K., 1971b, Mineraux de contact de Kushiro, Hiroshima prefecture III. Foshagite, hillebrandite et scawtite, *J. Min. Soc. Japan*, Vol. 10, pp. 296–304, (Abstract Bull. Signaletique 1972, vol. 33–2738).

LAPHAM, D.M., 1961, New data of deweylite, *Amer. Min.*, Vol. 46, pp. 168–188.

LAPIN, V.V., 1946, On the composition of minerals

of the melilite group and on a Na and Co bearing akermanite from slag, *Akad. Nauk. SSSR Belyankin Jubilee Volume*, pp. 585–597.

LARSEN, E.S., and FOSHAG, W.F., 1921, Merwinite, a new mineral from the contact zone at Crestmore, California, *Amer. Min.*, Vol. 6, pp. 143–148.

LEA, F.M., 1956, *The Chemistry of Cement and Concrete*, Revised edition of Lea and Desch, Edward Arnold, Publishers, London.

LEHMAN, J., 1874, Über den Ettringit, ein neues Mineral in Kalkeinschlüssen der lava von Ettringen (Laacher Gebiet) *N. Jb. Min. Geol.* pp. 273–275.

LEO, G.W., 1960, Autunite from Mt. Spokane, Washington, *Amer. Min.*, Vol. 45, pp. 99–128.

LEPP, H., 1957, The synthesis and probable geologic significance of melnikovite, *Econ. Geol.*, Vol. 52, pp. 528–535.

LISTER, D.H., and GLASSER, F.P., 1967, Phase relations in the system $CaO–Al_2O_3$–Iron oxide, *Trans. Brit. Ceram.* Soc., Vol. 66, pp. 293–305.

LUCE, R.W., 1971, Identification of serpentine varieties by infra-red absorption, *U.S. Geol. Surv. Prof. Paper*, 750B, pp. 199–201.

MACKAY, A.L., and TAYLOR, H.F.W., 1954, Truscottite, *Min. Mag.*, Vol. 30, pp. 450–457.

MAJUMDAR, A.J., 1965, The ferrite phase in cements, *Trans. Brit. Ceram. Soc.*, Vol. 64, pp. 105–119.

MAJUMDAR, A.J., and ROY, R., 1956, The system $CaO–Al_2O_3–H_2O$, *J. Amer. Ceram. Soc.*, Vol. 39, pp. 434–442.

MAJUMDAR, A.J., and REHSI, S.S., 1970, Mechanism of stabilization of high magnesia cements by reactive silica under autoclave conditions, *BRS current papers*, Vol. 9/70, pp. 141–150.

MAMEDOV, Kh. S., and BELOV, N.V., 1958, On the crystal structure of tobermorite, *Dokl. Akad. Nauk SSSR*, Vol. 123, pp. 163–165.

MASON, B., 1957, Larnite, scawtite and hydrogrossular from Tokatoka, New Zealand, *Amer. Min.*, Vol. 42, pp. 379–392.

McCONNELL, J.D.C., 1942, Griphite, a hydrophosphate garnetoid, *Amer. Min.*, Vol. 27, pp. 452–461.

McCONNELL, J.D.C., 1953, An American occurrence of volkonskoite, Clay and Clay Minerals, *Proc. of 2nd national conf. on clays, Univ. of Missouri*, publication 327.

McCONNELL, J.D.C., 1954, The hydrated calcium silicates riversideite, tobermorite and plombierite, *Min. Mag.*, Vol. 30, pp. 293–305.

McCONNELL, J.D.C., 1955, The hydration of larnite ($\beta–Ca_2SiO_4$) and bredgite ($\alpha–Ca_2SiO_4$) and the properties of the resulting gelatinous mineral plombierite, *Min. Mag.*, Vol. 30, pp. 672–680.

McCONNELL, J.D.C., 1960, Vaterite from Ballycraigy, Larne, Northern Ireland, *Min. Mag.*, Vol. 32, pp. 534–544.

McLINTOCK, H.F.P., 1932, On metamorphism produced by the combustion of hydrocarbons in the Tertiary sediments of southwest Persia, *Min. Mag.*, Vol. 23, pp. 207–226.

MACKENZIE, R.C., 1957, (editor), *The differential thermal investigation of clays*, Min. Soc. London.

METZGER, A., 1953, The presence of bredigite in portland cement clinkers, *Zement-Kalk-Gips*, Vol. 6, pp. 269–270.

MEYER, J.W., and JAUNARAJS, K.L., 1961, Synthesis and crystal chemistry of gyrolite and reyerite, *Amer. Min.*, Vol. 46, pp. 913–933.

MIDGLEY, H.G., 1951, A serpentine mineral from Kennack Cove, Lizard, Cornwall, *Min. Mag.*, Vol. 29, pp. 526–530.

MIDGLEY, H.G., 1957, A compilation of X-ray powder diffraction data of cement minerals, *Mag. Concr. Res.*, Vol. 9, pp. 17–24.

MIDGLEY, H.G., 1958, The composition of the ferrite phase in portland cement, *Mag. Concr. Res.*, Vol. 10, pp. 13–16.

MIKHEYEV, V.I., 1957, *Rentgenometricheskij opredelitel mineralov*, (X-ray determination of minerals), Moscow, 870 p.

MINATO, M., and KATO, A., 1967, Truscottite from Toi mine, Shiruoha prefecture, *Min. J. (Japan)*, Vol. 5, pp. 144–157.

MINGUZZI, C., 1937, Sulla presenza della portlandite fra i prodotti vesuviani, *Periodico Mineral.*, Vol. 8, pp. 5–13.

MITSUDA, T., 1970, Synthesis of tobermorite from zeolite, *Min. J. (Japan)*, Vol. 6, pp. 143–159.

MIYAKE, H.J., 1965, *In* Chukhrov F.W. and Bonshtedt-Kupletskaya M. (editors), 1972, *Mineraly*, Vol. III/I, p. 480.

MOEHLMAN, R.S., and GONYER, F.S., 1934, Monticellite from Crestmore, California, *Amer. Min.*, Vol. 19, pp. 474–479.

MUCKI, M., OJI, Y., and OGAWA, T., 1968, Mineralogical properties of lizardite from Kashii, Fukuoka City, *J. Geol. Soc., (Japan)*, Vol. 74, pp. 305–312.

MURDOCH, J., 1955, Bultfonteinite from Crestmore, California, *Amer. Min.*, Vol. 40, pp. 900–906.

MURDOCH, J., and CHALMERS, R.A., 1958, Ettringite (Woodfordite) from Crestmore, California, *Amer. Min.*, Vol. 45, pp. 1275–1278.

MURDOCH, J., 1961, Crestmore, past and present, *Amer. Min.*, Vol. 46, pp. 245–257.

NAGELSCHMIDT, G., 1937, A new calcium silicophosphate, *Journ. Chem. Soc.*, London, pp. 865–867.

NAIDU, M.G., and COVINDARAJULU, B.V., 1954, Occurrence of calciphyres near Mallarajanahundi, Nanjangud (Mysore State), *Current Science*, Vol. 23, N. 10.

NALIVKINA, E.B., 1969, Hibschite from near the Bug River, *Zap. Vses. Min. Obshch.*, Vol. 89, pp. 714–718.

NÁRAY–SZABÓ, I., and PETER, E., 1967, Nachweis von Nordstrandit und Bayerit in ungarischen Ziegeltonen, *Acta Geol. Acad. Sci. Hung.* Vol. II, pp. 375–377.

NELSON, B.W., and ROY, R., 1958, Synthesis of the chlorites and their structural and chemical constitution, *Amer. Min.*, Vol. 43, pp. 707–725.

NEWKIRK, T.F., and THWAITE, R.D., 1958, Pseudoternary system calcium oxide-monocalcium aluminate-dicalcium ferrite, *J. Res. Nat. Bur. Stand.*, Vol. 61, p. 233.

NOCKOLDS, S.R., and VINCENT, H.C.G., 1947, On tilleyite and its associated minerals from Carlingford, Ireland, *Min. Mag.*, Vol. 28, pp. 151–158.

NORTHWOOD, D.O., and LEWIS, D., 1969, Transformation of vaterite to calcite during grinding, *Amer. Min.*, Vol. 53, pp. 2089–2092.

NURSE, R.W., 1954, The dicalcium silicate phase, *Proceedings of the Third International Symposium on the chemistry of cement, London*, 1952, pp. 56–90.

NURSE, R.W., and MIDGLEY, H.G., 1955, Mineralogy of blast-furnace slags, *Silicates Ind.*, Vol. 16, pp. 211–217.

NURSE, R.W., WELCH, J.H., and GUTT, W., 1959, High-temperature phase equilibrium in the system dicalcium silicate-tricalcium phosphate, *J. Chem. Soc.*, Vol. 220, pp. 1077–1083.

NURSE, R.W., WELCH, J.H., and MAJUMDAR, A.J., 1965, The $12CaO.7Al_2O_3$ phase in the $CaO–Al_2O_3$ system, *Trans. Brit. Cer. Soc.*, Vol. 64, pp. 323–332.

OSBORNE, G.D., 1932a, The occurrence of custerite and a monticellite in metamorphosed limeston from Carlingford, *Geol. Mag.*, Vol. 69, pp. 61–62.

OSBORNE, G.D., 1932b, The metamorphosed limestones and associated contaminated igneous rocks of the Carlingford district, *Geol. Mag.*, Vol. 69, pp. 209–233.

PABST, A., 1937, The crystal structure of plazolite, *Amer. Min.*, Vol. 22, pp. 861–868.

PABST, A., 1942, Re-examination of hibschite, *Amer. Min.*, Vol. 27, pp. 783–792.

PAGE, J.N., 1968, Chemical differences among the serpentine "polymorphs". *Amer. Min.*, Vol. 53, pp. 201–215.

PALACHE, CH., BERMAN, H., and FRONDEL, C., *System of Mineralogy* of J.D. Dana and E.S. Dana, 7th edition, Wiley, New York; 1944, Vol. 1; 1951, Vol. 2; 1962, Vol. 3.

PARRY, J., and WRIGHT, F.E., 1925, Afwillite, a new hydrous calcium silicate from Dutoitspan mine, Kimberley, South Africa, *Min. Mag.*, Vol. 20, pp. 277–285.

PARRY, J., WILLIAMS, A.F., and WRIGHT, F.E., 1932, On bultfonteinite, a new fluorine-bearing hydrous calcium silicate from South Africa, *Min. Mag.*, Vol. 23, pp. 145–162.

PICARD, L., 1931, Geological researches in the Judean Desert, Jerusalem, Goldberg Press, 108 p.

POLUSHKINA, A.P., and SIDORENKO, G.A., 1963, Melnikovite as a mineral species, *Zap. Vses. Min. Obshch.*, Vol. 92, pp. 547–554.

POLUSHKINA, A.P., and SIDORENKO, G.A., 1968, Melnikovite ought to be considered a definite mineral species, *Zap. Vses. Min. Obshch.*, Vol. 97, pp. 321–324.

RADUSINOVIC, D.R., 1966, Greigite from the Lojane chromium deposit, Macedonia, *Amer. Min.*, Vol. 51, pp. 209–215.

RANKIN, G.A., and WRIGHT, F.E., 1915, The ternary system $CaO–Al_2O_3–SiO_2$, *Amer. J. Sci.*, Vol. 39, pp. 1–79.

REEUWIJK, L.P., 1971, The dehydration of gismondite, *Amer. Min.*, Vol. 56, pp. 1655–1659.

REISS, Z., 1966, Recent advances in marine Late Paleogene and Neogene stratigraphy of Israel, *Israel Earth-Sci.*, Vol. 15, pp. 8–26.

REVERDATTO, V.V., 1964, Metamorphism in the contacts of Anakit trappean Massif in the Low Tunguska River, Materials on genetic and experimental mineralogy, Vol. 2, pp. 97–169, *Akad. Nauk. SSSR, Novosibirsk.*

REVERDATTO, V.V., 1965, Paragenetic analysis of carbonate rocks of the spurrite-merwinite facies, *Geologiya i Geofizika, Akad. Nauk. SSSR, Sibirskoe otdelenie,* No. 2, pp. 3–20.

REVERDATTO, V.V., 1970, *The facies of contact metamorphism,* Translated from Russian 1973, Canberra, 263 p.

ROBERTS, M.H., 1957, New calcium aluminate hydrates, *J. Appl. Chem.*, London, Vol. 7, pp. 543–546.

ROSS, C.S., and KERR, P.F., 1934, Halloysite and allophane, *U.S. Geol. Surv. Prof. Paper* 185G, pp. 135–148.

ROWLANDS, D.L.G., and WEBSTER, R.K., 1971, Precipitation of vaterite in lake water, *Nature,* Phys. Sci., Vol. 229, p. 158.

ROY, D.M., 1958a, Studies in the system $CaO–Al_2O_3–SiO_2–H_2O$, III, New data on the polymorphism of Ca_2SiO_4 and its stability in the system $CaO–SiO_2–H_2O$, *Jour. Amer. Cer. Soc.*, Vol. 41, pp. 293–299.

ROY, D.M., 1958b, Studies in the system $CaO–Al_2O_3$-SiO_2-H_2O. IV. Phase equilibria in the high lime portion of the system. CaO-SiO_2-H_2O. *Amer. Min.* Vol. 43, pp. 1009–1028.

ROY, D.M., and ROY, R., 1954, An experimental study of the formation and properties of synthetic serpentines and related layer silicate minerals. *Amer. Min.* Vol. 39, pp. 957–975.

ROY, D.M., and ROY, R., 1957, System $CaO–Al_2O_3–Sio_2–H_2O$. VI. The grossularite–$3CaO–Al_2O_3–6H_2O$ join, *Bull. Geol. Soc. Amer.*, Vol. 68, p. 1788 (abstract).

ROY, D.M., and ROY, R., 1962, Crystalline solubility and zeolitic behavior in garnet phases in the system $CaO–Al_2O_3–SiO_2–H_2O$, *Proceedings of the IV Intern. Symp. of Chemistry of Cement, Washington,* 1960, Vol. I, pp. 307–314.

ROY, D.M., and HARKER, R.I., 1962, Discussion of M.F.W. Taylor's paper: Hydrothermal reactions in the system $CaO–SiO_2–H_2O$ and the steam curing of cement and cement-silica products, *Proceedings of the IV International Symposium of Chemistry of Cement, Washington,* 1960, Vol. I, pp. 196–201.

RUCKLIDGE, J.C., and ZUSSMAN, J., 1965, The crystal structure of the serpentine mineral lizardite $Mg_3Si_2O_2(OH)_4$, *Acta Cryst.*, Vol. 19, pp. 381–389.

SASVARI, K., and ZALAI, A., 1957, The crystal structure and thermal decomposition of alumina and alumina hydrates as regarded from the point of view of lattice geometry, *Acta Geol. Acad. Sci. Hug.*, Vol. 4, pp. 415–466, (Ab. *Am. Min.* (1958) Vol. 43, p. 626).

SCHALLER, W.T., 1935, Monticellite from San Bernardino County, California, and the monticellite series, *Amer. Min.*, Vol. 20, pp. 815–827.

SCHNEIDER, W.G., and THORVALDSON, T., 1943, The hydration of the aluminates of calcium: III, The hydration of the 5:3, 1:1 and 3:5 calcium aluminates, *Canad. J. Res.*, Vol. 31, pp. 34–42.

SCHOEN, R., and ROBERSON, CH., 1970, Structures of Al-hydroxides and geochemical implications, *Amer. Min.*, Vol. 55, pp. 43–77.

SEGNIT, E.R., 1950, New data on the slag minerals nagelschmidtite and steadite, *Min. Mag.*, Vol. 29, pp. 173–190.

SERDYUCHENKO, D.P., 1933, Chrome nontronites and their genetic relations with the serpentines in the Northern Caucasus, *Zap. Vses. Min. Obshch.*, ser. 2, Vol. 62, pp. 376–390.

SHAHAR, Y., and WURZBÜRGER, U., 1967, A new oil shale deposit in the Northern Negev, Israel, *Proc. 7th World Pet. Congr., Mexico,* Vol. 3, pp. 719–728.

SKINNER, B.J., ERD, R.C., and GRIMALDI, F.S., 1964, Greigite, the thiospinel of iron, a new mineral *Amer. Min.*, Vol. 49, pp. 543–555.

SMITH, D.K., 1962, Crystallographic changes with the substitution of aluminium for iron in dicalcium ferrite, *Acta Cryst.*, Vol. 15, pp. 1146–1152.

SMITH, D.K., MAJUMDAR, A.J., and ORDWAY, F., 1961, Polymorphism in the dicalcium silicate, *J. Amer. Cer. Soc.*, Vol. 44, pp. 405–411.

SOBOLEV, V., 1935, A rare type of contact metamorphism of limestones, *Zap. Vses. Min. Obshch.*, Vol. 64, pp. 162–165.

SPEAKMAN, K., 1968, The stability of tobermorite in the system $CaO–SiO_2–H_2O$ at elevated temperatures and pressures, *Min. Mag.*, Vol. 36, pp. 1090–1103.

SPEAKMAN, K., 1970, Reactions in the system $CaO–MgO–SiO_2H_2O$. Hydrothermal treatment of some compositions on the joins $Ca_3Si_2O_7–Mg_3Si_2O_7$ and $Ca_2SiO_4–Mg_2SiO_4$, *Min. Mag.*, Vol. 37, pp. 578–587.

SPEAKMAN, K., and MAJUMDAR, A.J., 1971, Synthetic "deweylite", *Min. Mag.*, Vol. 38, pp. 225–234.

STASCHUK, M.F., and KROPACHEVA, S.K., 1969, Die Sulfide der dreiwertigen Eisens rezenten Sedimenten und Sedimentgesteinen. *Deut. Ges. Geol. Wiss. Ber.* V. 14 B, pp. 139–144.

STEINOUR, H.H., 1951, Aqueous cementinous systems containing lime and alumina. Bulletin 34, *Research and Development Laboratories, Portland Cement Assoc.* (Chicago).

STERN, T.W., STIEFF, L.R., GIRHARD, M.N., and MEYROWITZ, R., 1956, The occurrence and properties of metatyuyamunite, $Ca(UO_2)_2(VO_4)_2 \cdot 3\text{-}5H_2O$, *Amer. Min.*, Vol. 41, pp. 187–201.

STOLKOWSKI, J., 1951, Essai sur le déterminisme des formes minéralogiques du calcaire chez les étres vivants *Inst. Oceanogr., Monaco, Ann.*, Vol. 26, pp. 1–113.

STRUNZ, M., 1970, *Mineralogische Tabellen*, 5-te Auflage, Akademische Verlagsgesellschaft, Leipzig.

SWEET, J.M., 1961, Tacharanite and other hydrated calcium silicates from Portree, Isle of Skye, *Min. Mag.*, Vol 32, pp. 745–753.

SWITZER, G., and BAILEY, E.H., 1953, Afwillite from Crestmore, California, *Amer Min.*, Vol. 38, pp. 629–633.

TATEKAVA, M., 1969, Apophyllite from Gobessho in Ôtsu City, *Min. J. (Japan)*, Vol. 6, pp. 1–7.

TAVASCI, B., 1935, Constitution of fused cements – the system $CaO–Al_2O_3–SiO_2$ and its application for the study of fused cements, *Chimica industria (Milan)*, Vol. 17, pp. 461–471.

TAYLOR, H.F.W., 1954, The identity of jurupaite and xonotlite, *Min. Mag.*, Vol. 30, pp. 338–341.

TAYLOR, H.F.W., 1961, The chemistry of cement hydration, *"Progress in Ceramic Science"*, Vol. 1, Pergamon Press, Oxford, pp. 89–145.

TAYLOR, H.F.W., 1962, Hydrothermal reactions in the system $CaO–SiO_2–H_2O$ and the steam curing of cement and cement-like silica products, *Fourth Intern. Symp. on Chem. of Cement, Washington*, 1960, Proc., pp. 167–190.

TAYLOR, H.F.W., 1964, (editor), *The chemistry of cements*, Vols. I, II, Academic Press.

TAYLOR, H.F.W., and HARRISON, J.W., 1956, Relationship between calcium silicates and clay minerals, *Clay. Min. Bull.*, 1956, Vol. 3, pp. 98–111

TAYLOR, J.H., 1935, A contact metamorphic zone from the Little Belt Mountains, Montana, *Amer. Min.*, Vol. 20, pp. 120–128.

TAYLOR, A.M., and ROY, R., 1964, Zeolite studies IV, Na-P zeolites and the ion exchanged derivates of tetragonal Na-P^1, *Amer. Min.*, Vol. 49, pp. 656–682.

TEMPLE, A.K., and HEINRICH, E.W., 1964, Spurrite from Northern Coahuila, Mexico, *Min. Mag.*, Vol. 33, pp. 841–852.

TERRIER, P., HORNAIN, H., and SOCROUN, G., 1968, Note sure des bélites naturelles, *Report of C.E.R.I.L.H. L-Pt.* 6B/2610, Paris, 3 p.

TERRIER, P., and HORNAIN, H., 1967, Sur l'application des méthodes mineralogiques à l'industrie des liants hydrauliques, *C.E.R.I.L.H. Publication Technique* No. 180, Paris, 55 p.

THORVALDSON, T., and SHELTON, G.R., 1929, Steam curing of portland cement mortars, *Canad. J. Res.* Vol. I., 148–154.

TILLEY, C.E., 1929, On larnite (calcium orthosilicate, a new mineral) and its associated minerals from the limestone contact zone of Scawt Hill, County Antrim, *Min. Mag.*, Vol. 22, pp. 77–86.

TILLEY, C.E., 1933, Portlandite, a new mineral from Scawt Hill, County Antrim, *Min. Mag.*, Vol. 23, pp. 419–420.

TILLEY, C.E., 1938, Aluminous pyroxenes in metamorphosed limestones, *Geol. Mag.*, Vol. 75, pp. 81–86.

TILLEY, C.E., 1942, Tricalcium disilicate (rankinite), a new mineral from Scawt Hill, *Min. Mag.*, Vol. 26, pp. 190–196.

TILLEY, C.E., 1947, The gabbro-limestone contact zone

of Camas Mor, Muck, Inverness-shire, *Bull. Comm. geol. Fin.*, Vol. 20, pp. 97–105.

TILLEY, C.E., 1951, A note on the progressive metamorphism of siliceous limestones and dolomites, *Geol. Mag.*, Vol. 88, pp. 175–178.

TILLEY, C.E., and ALDERMAN, A.R., 1934, Progressive metasomatism in the flint nodules of the Scawt Hill contact zone, *Min. Mag.*, Vol. 23, pp. 513–518.

TILLEY, C.E., and HARWOOD, H.F., 1931, The dolerite-chalk contact at Scawt Hill, County Antrim, *Min. Mag.*, Vol. 22, pp. 439–468.

TILLEY, C.E., MEGAW, H.D., and HEY, M.H., 1934, Hydrocalumite ($4CaO.Al_2O_3.12H_2O$), a new mineral from Scawt Hill, County Antrim, *Min. Mag.*, Vol. 23, pp. 607–615.

TILLEY, C.E., and VINCENT, H.C.G., 1948, The occurrence of an orthorhombic high-temperature form of Ca_2SiO_4 (bredigite) in Scawt Hill, *Min. Mag.*, Vol. 28, pp. 255–271.

TOROPOV, N.A., MERKOV, L.D., and SHISHAKOV, N.A., 1937, The binary system $5CaO.3Al_2O_3$–$4CaO.Al_2O_3.Fe_2O_3$, *Tsement* No. 1, 28.

TOROPOV, N.A., and BOIKOVA, A.I., 1956, Investigation of the system ferrite-calcium aluminate, *Zhur. Neorg. Khim.*, Vol. 1, pp. 2106–2109.

TOROPOV, N.A., VOLKONSKIY, B.V., and SADKOV, V.I., 1957, The problem of polymorphism of dicalcium silicate, *Dokl. Akad. Nauk. SSSR*, Vol. 112, pp. 467–469.

TRÖMEL, G., HARKORT, H.J., and HOTOP, W., 1948, Investigation of the system $CaO–P_2O_5–SiO_2$, *Zeitsch. für anorg. Chemie*, Vol. 256, pp. 253–272.

TRÖMEL, G., 1952, Use of the high temperature X-ray camera in ceramic problems, *Ber. Deut. Keram. Ges.*, Vol. 29, pp. 2–6.

TSAO–YUNG–LUNG, 1964, Hydrougrandite, a new variety of hydrogarnet from Hsiaosungshan, *Acta Geol. Sinica*, Vol. 44, No. 2, pp. 219–228, Abstract M.A., Vol. 17, p. 400.

TSCHERNICH, R.W., 1972, Zeolites from Skookumchuck Dam, Washington, *Min. Record*, Vol. 30, pp. 30–34.

TURNBULL, A.G., 1973, A thermochemical study of vaterite, *Geoch. Cosmochim. Acta*, Vol. 37, pp. 1593–1602.

USHAKOVA, E.N., 1959, On some hydrosilicates of Zavalia in the Middle Bug district, *Min. Sbornik Geol. Soc. Lvov* No. 13, pp. 328–337.

VAN BEMST, A., 1955, Contribution to the study of the hydration of pure calcium silicates, *Bull. Soc. Chim. Belges*, Vol. 64, pp. 333–351.

VAN VALKENBURG, A., and RYNDERS, G.F., 1958, Synthetic cuspidine, *Amer. Min.*, Vol. 43, pp. 1195–1202.

VENIALE, F., and VAN DER MAREL, H.W., 1963, An interstratified saponite-swelling chlorite mineral as a weathering product of lizardite from St. Margherita Staffora (Pavia Provina), Italy, *Beitr. Min. Petr.*, Vol. 9, pp. 198–245.

VERMAAS, F.H.S., 1953, A new occurrence of Ba-feldspar at Otjosundu, South-West Africa and an X-ray method for determining the composition of hyalophane, *Amer. Min.*, Vol. 38, pp. 845–857.

VORMA, A., 1961, A new apophyllite occurrence in the Viipuri Rapakivi area, *C.R. Soc. geol. Finlande*, Vol. 33, pp. 399–404; (M. A. Vol. 15, p. 456).

WALKER, G.P.L., 1951, The amygdale minerals in the tertiary lavas of Ireland, I. The distribution of chabazite habits and zeolites in the Garron plateau area, County Antrim. *Min. Mag.* Vol. 29, pp. 773–791.

WALKER, G.P.L., 1971, The distribution of amygdale minerals in Mull and Morvern (western Scotland), West Commem. Vol. (Univ. Saungar, India), pp. 181–184.

WELLS, L.S., CLARKE, W.F., and McMURDIE, H.F., 1943, Study of the system $CaO–Al_2O_3–H_2O$ at the temperatures of 21° C and 90° C, *J. Res. Nat. Bur., Stand.* Vol. 30, pp. 367–409.

WHITTAKER, E.J.W., and ZUSSMAN, J., 1956, The characterization of serpentine minerals by X-ray diffraction, *Min. Mag.*, Vol. 31, pp. 107–126.

WHITTAKER, E.J.W., and ZUSSMAN, J., 1958, The characterization of serpentine minerals, *Amer. Min.*, Vol. 43, pp. 917–920.

WILLIAMS, S.A., 1968, More data on greigite. *Amer. Min.*, Vol. 53, pp. 2087–2088.

WINCHELL, A.N., 1959, *Elements of optical mineralogy*, Part II, fourth ed., and Part III, second ed., New York.

WRAY, J.L., and DANIELS, F., 1957, Precipitation of calcite and aragonite, *J. Amer. Chem. Soc.*, Vol. 79,

pp. 2031–2034.

WRIGHT, F.E., 1908, On the contact minerals from Velardena, Durango, Mexico (gehlenite, spurrite, hillebrandite), *Amer. J. Sci.*, Vol. 26, No. 156.

WYATT, M., 1953, *The Camansury (Skye) gabbro-limestone contact*, Part II of PhD thesis, Cambridge University.

YAMAGUCHI, S., and KATSURAI, T., 1960, Zur Bildung des ferromagnetischen Fe_3S_4, *Kolloid. Zeit.* Vol. 170, pp. 147–148.

YAMAUCHI, T., 1937, A study on the celite, Part I. The system $CaO–Fe_2O_3$, *J. Japan Ceram. Assoc.*, Vol. 45, p. 279; brownmillerite pp. 361–375; III – the system $3CaO.Al_2O_3–2CaO.Fe_2O_3$, pp. 433–436; IV – the system $5CaO.3Al_2O_3–2CaO.Fe_2O_3$, pp. 614–631; V – the system $3CaO.Al_2O_3–5CaO.3Al_2O_3–2CaO.Fe_2O_3$. pp. 880–896.

ŽABINSKI, W., 1966, Hydrogarnets, *Polish Acad. Sci., Mineralogical Transactions*, No. 3, pp. 1–69.

ZELLER, E.J., and WRAY, J.L., 1956, Factors influencing precipitation of calcium carbonate, *Am. Assoc. Petrol. Geol. Bull.*, Vol. 40, pp. 140–152.

ZHARIKOV, U.A., and SHMULOVICH, K.I., 1969, High temperature mineral equilibrium in the system $CaO–SiO_2–CO_2$, *Geochem. International*, Vol. 6, pp. 853–869.

ZHUKOV, N.M., 1971, Al-serpentine in metasomatites of the 50 Let Oktyabrya chalcopyrite deposit, Zap. Vses. Min. Obshch., *Vol. 100, pp. 355–356.*

ZUR STRASSEN, H., 1958, The chemical reactions involved in the hardening of cement. Zement, Kalk, Gips, Vol. 11, pp. 137–143.

ZUSSMAN, J., and BRINDLEY, G.W., 1957, Serpentine with 6-layer orthohexagonal cells, *Amer. Min.*, Vol. 42, pp. 666–670.

★ ★ ★

EXPLANATION OF PLATE I

Scan-electromicrographs (SEM) showing:

1 Crystal of magnetite from a weathered calc-silicate rock.

2 Twinned crystals of hercynite, residual on the surface of autoclaved larnite rock.

3 Mayenite (spherical individual in the center) from the freshly fractured surface of a larnite rock.

4 Same specimen as shown in (3) after autoclaving at 110° C. The spherical holes are spaces previously occupied by mayenite.

5 Hexagonal plate of calcium-aluminate-hydrate from a jennite rock.

Thin-section photomicrographs showing:

6 Magnetite and andradite in a melilite matrix.

7 Minute octahedral crystals of spinel, disseminated in a melilite matrix.

8 Magnesioferrite crystals (dark) in gehlenite-larnite matrix.